Iodine Speciation in Atmospheric Aerosols in the Marine Boundary Layer

Dissertation

zur Erlangung des Grades

„Doktor der Naturwissenschaften“

im Promotionsfach Chemie

am Fachbereich Chemie, Pharmazie und Geowissenschaften

der Johannes Gutenberg-Universität Mainz

M.Sc. Senchao Lai

geb. in Chaozhou (Guangdong), V.R. China

Mainz, 2008

天行健，君子以自强不息；
地勢坤，君子以厚德載物。

《易經》

As Heaven's movement is ever vigorous, so must a gentleman ceaselessly strive along. As Earth is vast and grand, so a gentleman must embrace everything with virtue and tolerance.

Classic of Changes

Abstract

Iodine chemistry plays an important role in the tropospheric ozone depletion and the new particle formation in the Marine Boundary Layer (MBL). The sources, reaction pathways, and the sinks of iodine are investigated using lab experiments and field observations. The aims of this work are, firstly, to develop analytical methods for iodine measurements of marine aerosol samples especially for iodine speciation in the soluble iodine; secondly, to apply the analytical methods in field collected aerosol samples, and to estimate the characteristics of aerosol iodine in the MBL.

Inductively Coupled Plasma – Mass Spectrometry (ICP-MS) was the technique used for iodine measurements. Offline methods using water extraction and Tetra-methyl-ammonium-hydroxide (TMAH) extraction were applied to measure total soluble iodine (TSI) and total insoluble iodine (TII) in the marine aerosol samples. External standard calibration and isotope dilution analysis (IDA) were both conducted for iodine quantification and the limits of detection (LODs) were both 0.1 μg L^{-1} for TSI and TII measurements. Online couplings of Ion Chromatography (IC)-ICP-MS and Gel electrophoresis (GE)-ICP-MS were both developed for soluble iodine speciation. Anion exchange columns were adopted for IC-ICP-MS systems. Iodide, iodate, and unknown signal(s) were observed in these methods. Iodide and iodate were separated successfully and the LODs were 0.1 and 0.5 μg L^{-1}, respectively. Unknown signals were soluble organic iodine species (SOI) and quantified by the calibration curve of iodide, but not clearly identified and quantified yet. These analytical methods were all applied to the iodine measurements of marine aerosol samples from the worldwide filed campaigns.

The TSI and TII concentrations (medians) in $PM_{2.5}$ were found to be 240.87 pmol m^{-3} and 105.37 pmol m^{-3} at Mace Head, west coast of Ireland, as well as 119.10 pmol m^{-3} and 97.88 pmol m^{-3} in the cruise campaign over the North Atlantic Ocean, during June – July 2006. Inorganic iodine, namely iodide and iodate, was the minor iodine fraction in both campaigns, accounting for 7.3% (median) and 5.8% (median) in $PM_{2.5}$ iodine at Mace Head and over the North Atlantic Ocean, respectively. Iodide concentrations were higher than iodate in most of the samples. In the contrast, more than 90% of TSI was SOI and the SOI concentration was correlated significantly with the iodide concentration. The correlation coefficients (R^2) were both higher than 0.5 at Mace Head and in the first leg of the cruise. Size fractionated aerosol samples collected by 5 stage Berner impactor cascade sampler showed similar proportions of inorganic and organic iodine. Significant correlations were obtained in the particle size ranges of 0.25 – 0.71 μm and 0.71 – 2.0 μm between SOI and iodide, and better correlations were found in sunny days. TSI and iodide existed mainly in fine particle size range (< 2.0 μm) and iodate resided in coarse range (2.0 – 10 μm). Aerosol iodine was suggested to be related to the primary iodine release in the tidal zone. Natural meteorological conditions such

as solar radiation, raining etc were observed to have influence on the aerosol iodine.

During the ship campaign over the North Atlantic Ocean (January – February 2007), the TSI concentrations (medians) ranged 35.14 – 60.63 pmol m^{-3} among the 5 stages. Likewise, SOI was found to be the most abundant iodine fraction in TSI with a median of 98.6%. Significant correlation also presented between SOI and iodide in the size range of 2.0 – 5.9 μm. Higher iodate concentration was again found in the higher particle size range, similar to that at Mace Head. Airmass transport from the biogenic bloom region and the Antarctic ice front sector was observed to play an important role in aerosol iodine enhancement.

The TSI concentrations observed along the 30,000 km long cruise round trip from East Asia to Antarctica during November 2005 – March 2006 were much lower than in the other campaigns, with a median of 6.51 pmol m^{-3}. Approximately 70% of the TSI was SOI on average. The abundances of inorganic iodine including iodine and iodide were less than 30% of TSI. The median value of iodide was 1.49 pmol m^{-3}, which was more than four fold higher than that of iodate (median, 0.28 pmol m^{-3}). Spatial variation indicated highest aerosol iodine appearing in the tropical area. Iodine level was considerably lower in coastal Antarctica with the TSI median of 3.22 pmol m^{-3}. However, airmass transport from the ice front sector was correlated with the enhance TSI level, suggesting the unrevealed source of iodine in the polar region. In addition, significant correlation between SOI and iodide was also shown in this campaign.

A global distribution in aerosol was shown in the field campaigns in this work. SOI was verified globally ubiquitous due to the presence in the different sampling locations and its high proportion in TSI in the marine aerosols. The correlations between SOI and iodide were obtained not only in different locations but also in different seasons, implying the possible mechanism of iodide production through SOI decomposition. Nevertheless, future studies are needed for improving the current understanding of iodine chemistry in the MBL (e.g. SOI identification and quantification as well as the update modeling involving organic matters).

TABLE OF CONTENTS

1. Introduction

The significance of iodine chemistry in the Marine boundary layer (MBL) has been highlighted by many studies (Davis et al., 1996; Vogt, 1999; O'Dowd et al., 2002b; Carpenter, 2003; O'Dowd and Hoffmann, 2005). Marine organisms such as macroalgae and microalgae are thought to be the main source of volatile iodine compounds (Carpenter, 2003; McFiggans et al., 2004; O'Dowd and Hoffmann, 2005). The ensuing photochemical iodine reactions provide significant impacts in the MBL atmosphere; in particular, tropospheric ozone depletion and new particle formation (Davis et al., 1996; O'Dowd et al., 2002b). However, the mechanisms and the cycle of iodine in the MBL are still not fully understood and thus more research is necessary.

1.1 Source of Iodine in the MBL

The exchange of iodine between atmosphere, ocean and land were initially suggested in the late 1950's (Bolin, 1959). Interest on atmospheric iodine chemistry then followed with the observation of iodine species in the gas phase and aerosol phase in the marine environment (Duce et al., 1965; Winchest and Duce, 1967; Moyers et al., 1970). Early laboratory studies indicated that iodine emissions were from the ocean (Miyake and Tsunogai, 1963) and that organically bound iodine probably accounted for iodine enrichment in the particles (Seto and Duce, 1971). These early results gave the first evidence that iodine was strongly related to oceanic sources.

1.1.1 Volatile Organic Iodine

To date natural sources are regarded as the dominant iodine sources on the global scale rather than anthropogenic source (Carpenter, 2003). Volatile halogen species such as I_2, CH_3I, CH_2I_2, CH_3ClI, C_3H_7I, and CH_2IBr etc are thought to be precursors for iodine atmospheric reactions, which are emitted to the atmosphere and trigger iodine cycling in the atmosphere (Carpenter, 2003). Marine organisms including macroalgae (seaweeds) and microalgae (phytoplankton) are the main sources of these compounds, though the exact mechanisms of synthesis and release are still unclear (Lovelock, 1975; Vogt et al., 1999; Laturnus et al., 2000; Küpper et al., 2002; Moore, 2003; Kupper et al., 2008). The mechanism for production of monohalogenate compounds involves a halide ion methyl transferase enzyme (Wever et al., 1991). Strong evidence is also shown that abiological production of CH_3I related to photolytic processes or Fe-catalyzed cycles (Moore and Zafiriou, 1994; Richter and Wallace, 2004; Williams et al., 2007). CH_2I_2 was monitored as the main form of organic iodine release (Collen et al., 1994; Mtolera et al., 1996; Carpenter et al., 2000). Di- or tri- halogenated hydrocarbon production involves haloperoxidase enzyme, present in a wide range of terrestrial and marine

organisms (Wever et al., 1991). Halo-peroxidases catalyze the oxidation of halides by hydrogen peroxide, which is released as part of normal cell metabolism and during defense reactions (Küpper et al., 2002). The resulting reactive electrophilic halogenating species can react with available organic material within the cell apolast via the iodoform reaction to form volatile organohalogens that are released to the surrounding seawater or air (Theiler et al., 1978). Modeling work on elucidicating the location of CH_2I_2 found that CH_2I_2 was emitted not only from the tidal zone but also from the further offshore (Carpenter et al., 2001), which suggested that macroalgae are not the only source of halocarbons due to its limited distribution in the inshore area. CH_2I_2 relating to the temperate microalgal production were observed from shipboard measurement (Klick and Abrahamsson, 1992; Moore and Tokarczyk, 1993; Schall and Heumann, 1993). Polar microalgae have been found to be capable of C_2H_5I, CH_2ICl, CH_2I_2, CH_3I production (Moore et al., 1996).

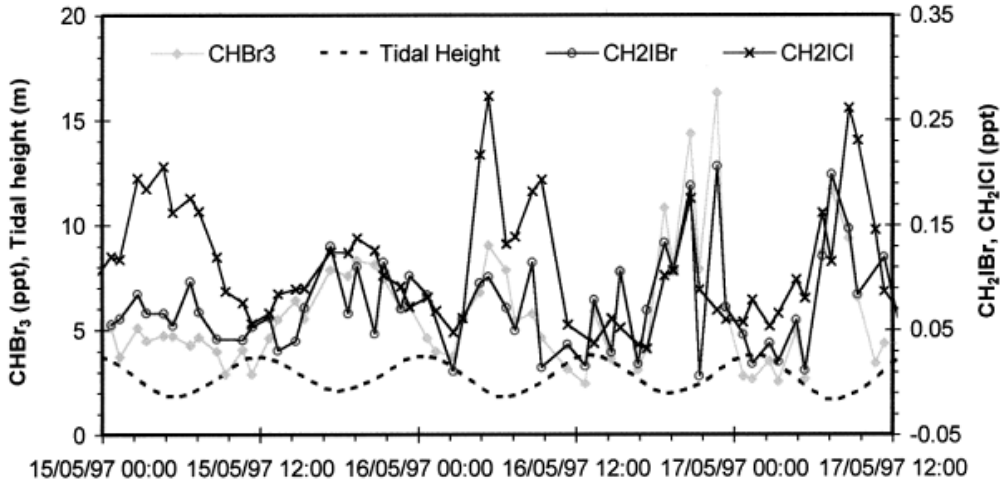

Figure 1- 1 Organohalogen mixing ratios and tidal height at Mace Head, Ireland.(Carpenter et al., 1999)

Volatile halocarbons in coastal sites are anti-correlated with the tidal height (Carpenter et al., 1999). This is consistent to the finding that macroalgae is the main source of iodocarbons due to more exposure of seaweed at the coast with low tide. However, the relative contribution of macroalgae and microalgae are not clear yet, given uncertainties of in emission rates and algal biomass (Carpenter, 2003). Volatile iodocarbons are present globally and have been observed in different coastal areas, open ocean as well as the polar regions (Schall and Heumann, 1993; Yokouchi et al., 1997; Bassford et al., 1999; Carpenter et al., 1999; Carpenter et al., 2000; Carpenter and Lewis, 2002; Carpenter, 2003; Carpenter et al., 2003; Williams et al., 2007).

1.1.2 Elemental Iodine

Elemental iodine (I_2) has been suggested as the main precursor for new particle formation at Mace Head, rather than volatile iodocarbons (McFiggans et al., 2004;

Saiz-Lopez and Plane, 2004; McFiggans, 2005). The source of I_2 was also found to be macroalgae species such as Laminaria sp. during oxidative stress (Palmer et al., 2005). In chamber experiment conducted in Mace Head, a linear correlation was found between I_2 concentrations and biomass and between particle concentration and I_2 concentrations (O'Dowd and Hoffmann, 2005). The flux values derived from the chamber experiments were in excellent agreement from the direct measurement of new particle flux using eddy covariance techniques (Flanagan et al., 2005). Molecular iodine concentrations were measured at Mace Head and nearby hot spots by different techniques (Saiz-Lopez and Plane, 2004; Chen, 2005; Sellegri et al., 2005; Saiz-Lopez et al., 2006a). I_2 concentration showed a diurnal variation with maximum level of 93 pptv at night and 25 ppt during daytime (Saiz-Lopez and Plane, 2004). The I_2 concentrations measured by DOAS (differential optical absorption spectroscopy), BBCRDS (broadband cavity ring-down spectroscopy), and denuder technique were consistent with a range of 30 – 115 pptv (Saiz-Lopez et al., 2006a) at Mace Head.

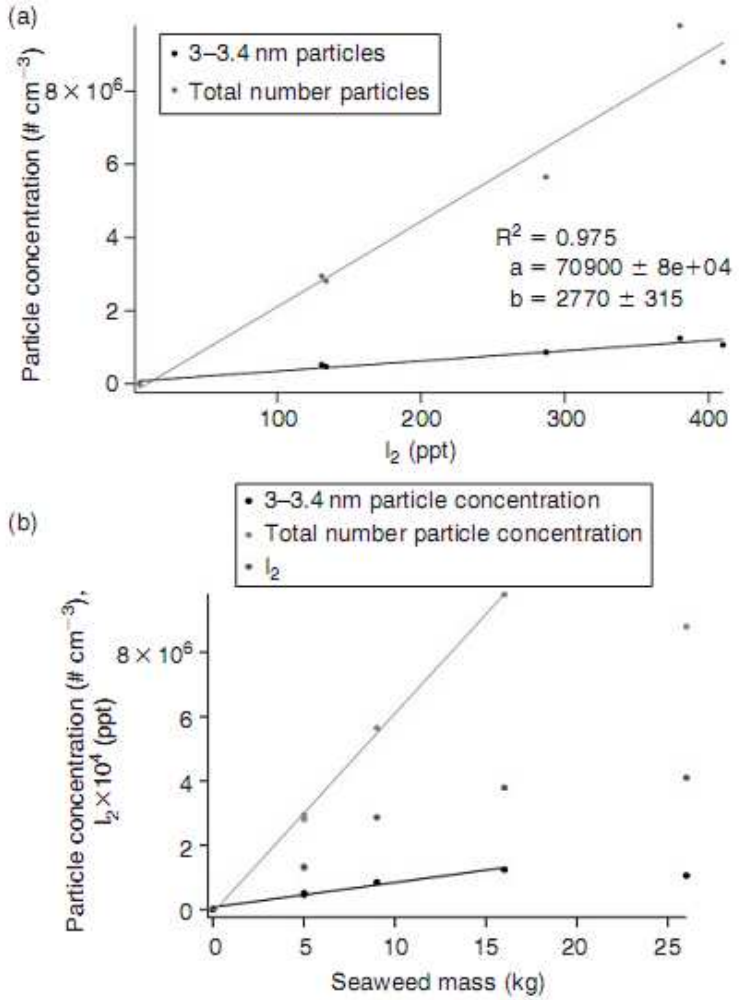

Figure 1- 2 Relationship between seaweed mass, molecular iodine and particle concentration for the chamber experiments. Regression lines on upper plot refer to (a) relationship between total particle concentration and I_2 and (b) relationship between 3 – 3.4 nm particle concentration and I_2 concentration

Recently a biological formation mechanism was proposed for I_2. Iodide, which was most accumulated form of iodine in algae, detoxified ozone on the thallus surface and in the apoplast, releasing high levels of I_2 (Kupper et al., 2008). Irradiated iodide solution is found to produce free iodine escaping to the gas phase according to Reaction 1-1, which is shown to be a possible abiological process in the seawater (Miyake and Tsunogai, 1963). A reaction of iodide with ozone at the sea-surface may also produce I_2 (Reaction 1-2) (Garland and Curtis, 1981; Thompson and Zafiriou, 1983). In addition, sufficient concentrations of I radical from oxidation of iodide or photolysis of organic iodides, which increase the possibility of I_2 production.

$$2I^- + 0.5O_2 + H_2O + h\nu \rightarrow I_2 + 2OH^- \qquad \text{(Reaction 1- 1)}$$

$$2I^- + O_3 + 2H^+ \rightarrow I_2 \uparrow + O_2 + H_2O \qquad \text{(Reaction 1- 2)}$$

Sea-air boundary is an important layer for the release volatile iodine into the atmosphere. The sea surface contains the iodocarbons such as CH_3I, CH_2I_2, CH_2ClI etc with typical I concentration in the order of 10^{-10} mol L^{-1} (Chen, 2005). I_2 can be produced by biological and abiological processes and then enriched in this layer. As a result, the sea water near the interface becomes locally super-saturated, thus causing a flux from the aqueous phase into the atmosphere (Singh et al., 1983). The Sea-air flux of non-soluble or sparingly soluble gas is affected by wave type, wind driven turbulence, bubbles, temperature gradients, and surface films (Liss and Slater, 1974; Phillips, 1991; Carpenter, 2003). Recently the enriched dissolved (non-volatile) organically bound iodine was suspected to transfer to the atmosphere within the sea surface micro layer by bubble busting process and may be responsible for the organic iodine in aerosols (Baker, 2005) though no solid proof has yet been found.

1.2 Iodine Chemistry in the Atmosphere

The current knowledge of iodine chemistry in the atmosphere is shown in Figure 1-3 (von Glasow and Crutzen, 2003). The cycle is initiated by photolysis of volatile iodine species, such as iodocarbons and molecular iodine, following their release from the ocean (Carpenter, 2003; Saiz-Lopez and Plane, 2004). Under UV-vis exposure, a series of gas phase reactions and the aerosol recycling processes occur, resulting in ozone destruction as well as the new particle formation, which could have strong impact on climate if it occurs on a global scale (Carpenter, 2003; von Glasow and Crutzen, 2003).

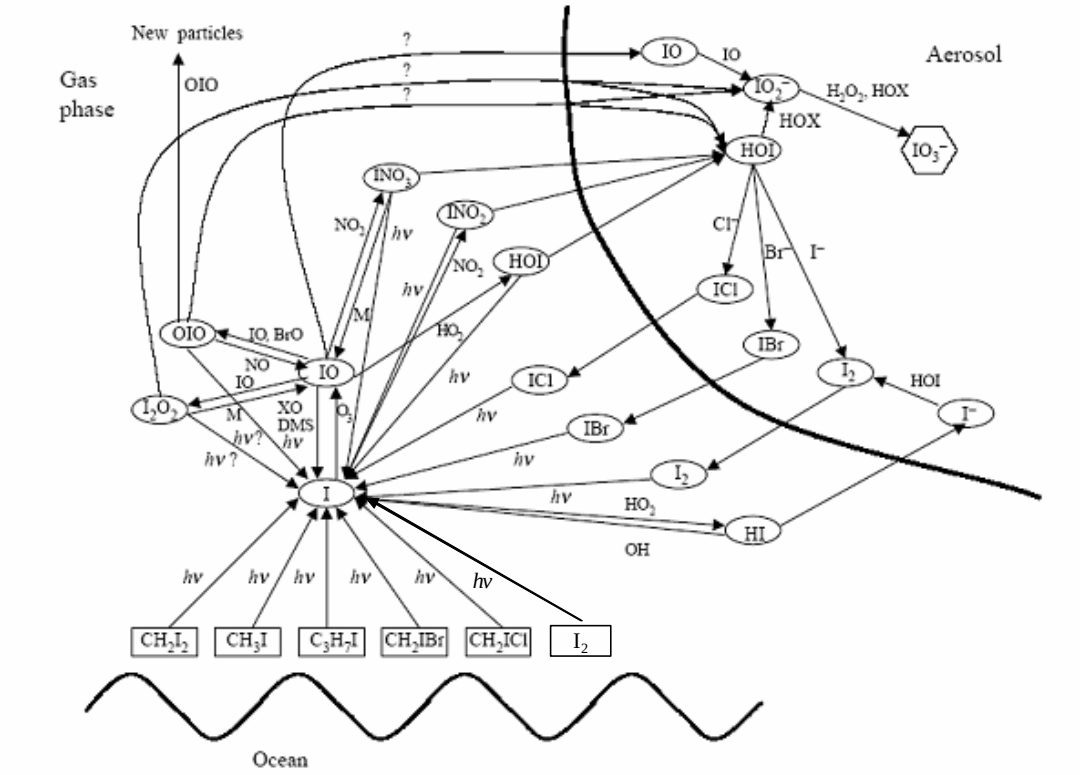

Figure 1- 3 Schematic of iodine reactions in the marine boundary layer (cited from von Glasow and Crutzen, 2003 with modification)

1.2.1 Gaseous Processes and Tropospheric Ozone Depletion

Once released to the atmosphere photolytic decomposition is the predominant fate of organic iodine compound or molecular iodine (Reaction 1-2 and 1-3). Alternatively, gas phase oxidation by OH radicals is of less importance because of the relatively slow OH reaction rate (Vogt, 1999). The lifetime of iodocarbons ranges from several days e.g. CH_3I, several hours to several minutes e.g. CH_2I_2, I_2 (Vogt, 1999; Carpenter, 2003). Iodocarbons with two chromophores, e.g., CH_2I_2, CH_2ICl, and CH_2IBr, have shown to be the most important iodine atom precursors in some environments (Carpenter et al., 1999). However, the main source of I atoms in coastal environments is the molecular iodine flux from the seaweed instead of CH_2I_2 as reported (McFiggans et al., 2004; Saiz-Lopez et al., 2006a). I_2 is rapidly photolyzed releasing I atom with a photo-dissociation rate constant (J) of 0.12 ± 0.03 s^{-1} (Saiz-Lopez et al., 2004).

$$R-I+h\nu \rightarrow R+I \qquad \text{(Reaction 1- 3)}$$

$$I_2+h\nu \rightarrow 2I \qquad \text{(Reaction 1- 4)}$$

It is thought that the predominant fate of I atoms is reaction with ozone to produce monoxide (IO) radicals. The time scale of this reaction is about 2 s at an ozone mixing

ratio of 20 nmol mol^{-1} (Jenkin, 1992). At low NO_x levels, which are typically observed in the unpolluted MBL, the major fate of IO is photodissociation to regenerate I atom. This cycle has no net effect on IO_x or O_3 chemistry.

$$I + O_3 \rightarrow IO + O_2 \qquad \text{(Reaction 1- 5)}$$

$$IO + h\nu \rightarrow I + O \qquad \text{(Reaction 1- 6)}$$

Although this reaction cycle is the predominant pathway for I-to-IO inter-conversion, a number of temporary inorganic reservoir products are formed via IO_x radical termination reactions with HO_2, NO_x, and IO. The photodissociated I atoms consequently cause the O_3 depletion via Reaction 1-5.

$$IO + HO_2 \rightarrow HOI + O_2 \qquad \text{(Reaction 1- 7)}$$

$$HOI(gas) \rightarrow HOI(aerosol) \qquad \text{(Reaction 1- 8)}$$

$$HOI(gas) + h\nu \rightarrow OH + I \qquad \text{(Reaction 1- 9)}$$

$$HOI(aq) + X^- + H^+ \rightarrow IX(gas) + H_2O \qquad \text{(Reaction 1- 10)}$$

$$IX + h\nu \rightarrow I + X \qquad \text{(Reaction 1- 11)}$$

$$IO + NO \rightarrow I + NO_2 \qquad \text{(Reaction 1- 12)}$$

$$IO + NO_2(+M) \rightarrow IONO_2(+M) \qquad \text{(Reaction 1- 13)}$$

$$IONO_2 + h\nu \rightarrow I + NO_3 \quad \text{or} \quad \rightarrow IO + NO_2 \qquad \text{(Reaction 1- 14)}$$

According to Reaction 1-7, hypoiodous acid (HOI) is formed by the reaction of IO with HO_2. HOI is believed to be the major component of gas phase inorganic iodine and an important route to the aerosol phase (Jenkin, 1992; Davis et al., 1996; Holmes et al., 2001). HOI is believed to react with halide ions (Reaction 1-10 and 1-11, X^- = I^-, Br^- and Cl^-) in seasalt aerosols to produce volatile dihalogens (I_2, IBr, ICl) which enter the gas phase in a process known as halogen activation(Vogt et al., 1999; McFiggans et al., 2000). The HOI-participating cycle is thought to be the dominant O_3 loss cycle at NO_x lower than 500 pptv (Stutz et al., 1999).

The dimmerisation to produce I_2O_2 and the formation of OIO are suggested as self-reactions of IO radicals (Vogt et al., 1999; Hoffmann et al., 2001). I atoms released

via Reaction 1-16 can continue to destruct ozone in the air. Also, OIO has a high photochemical stability in the atmosphere and is capable of self-reaction for new particle formation (Misra and Marshall, 1998; Hoffmann et al., 2001).

$$IO + IO \rightarrow I_2O_2 \qquad \text{(Reaction 1- 15)}$$

$$IO + IO \rightarrow I + OIO \qquad \text{(Reaction 1- 16)}$$

$$OIO + h\nu \rightarrow I + O_2 \quad \text{or} \quad \rightarrow IO + O(^3P) \qquad \text{(Reaction 1- 17)}$$

$$OIO + OIO \rightarrow I_2O_4 \quad \text{or} \quad \rightarrow [IO]^+[IO_3^-] \qquad \text{(Reaction 1- 18)}$$

$$I_2O_4 + nOIO \rightarrow [-I-O-IO_2-]_{1+n/2} \qquad \text{(Reaction 1- 19)}$$

Gaseous reactions leading to ozone depletion in the MBL were proved by the measurement of iodine oxides from both the lab studies and the field observations (Hoffmann et al., 2001; Jimenez et al., 2003; Saiz-Lopez et al., 2006b; Saiz-Lopez et al., 2007; Read et al., 2008; Schonhardt et al., 2008).

1.2.2 New Particle Formation

In addition to ozone depletion caused by iodine chemistry in the MBL, new particle formation recently became a new focus for atmospheric iodine research (O'Dowd et al., 2002b; O'Dowd and Hoffmann, 2005). Atmospheric aerosols interact both directly and indirectly with the Earth's radiation budget and global climate change (Kolb, 2002). Aerosols have a direct effect on the global radiative balance by scattering (or absorbing) incoming solar radiation, leading to cooling (or warming). As an indirect effect, aerosols in the lower atmosphere can modify the size of cloud particles, changing how the clouds reflect and absorb sunlight, thereby affecting the Earth's energy budget. If the iodine-containing new particle formation processes occur on a large scale, it could have a significant effect on climate (Kolb, 2002).

The typical case of nucleation events driven by iodine chemistry was first observed at Mace Head, shown in Figure 1- 4 (O'Dowd and Hoffmann, 2005). The peak in particle concentrations occurs a number hours before the peak in sulphuric acid concentration, suggesting the new particle formation process was not due to the ternary nucleation of H_2SO_4-H_2O-NO_3. The particle concentration increased (more than 10^6 cm^{-3}) when low tide occurred, and decreased back to the background levels as the tidal height increased again. This nucleation is thought to be driven by biogenic emissions of iodine vapors that undergo rapid chemical reactions to produce condensable iodine oxides leading to nucleation and growth of new particles (O'Dowd and Hoffmann, 2005). Chamber

experiments to investigate the new particle formation by macroalgae (Laminaria digitata), after release of CH_2I_2, and I_2 and reaction with O_3 were conducted (McFiggans et al., 2004). Similar mass spectra were observed in natural and laboratory experiments, indicating the evidence of ultrafine iodine-containing particles produced by intertidal macroalgae exposed to ambient levels of ozone (Figure 1-5). In addition, the I_2 photolysis rate at Mace Head was reported to be three orders of magnitude larger that the flux of CH_2I_2 (McFiggans et al., 2004), suggesting I_2 might be the missing additional source of condensable iodine vapors responsible for new particle formation.

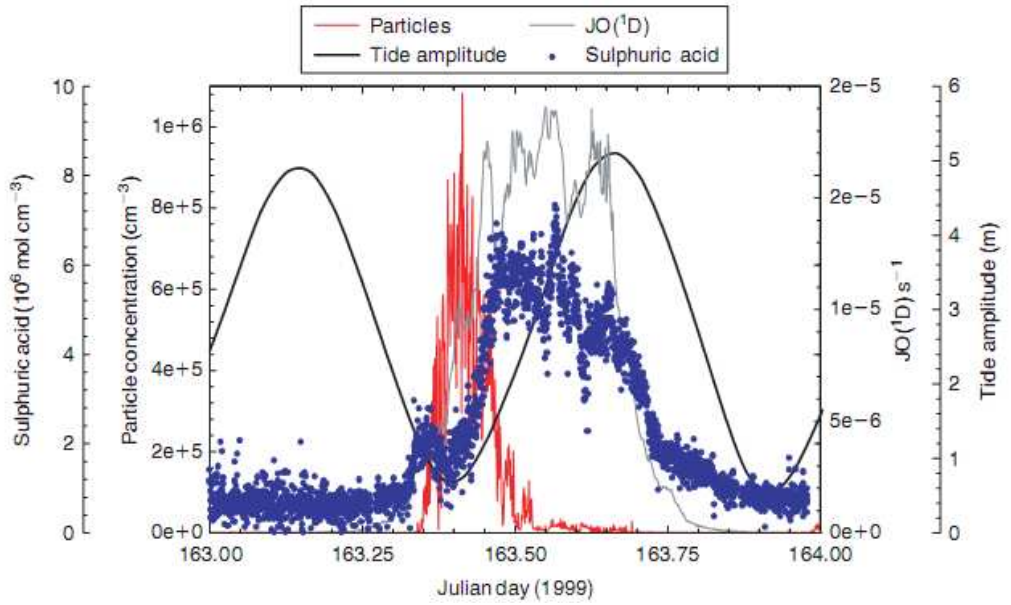

Figure 1- 4 Typical new particle formation event driven by iodine chemistry at Mace Head in 1999. JO(^{1}D) is a measure of photochemical activity. (O'Dowd et al., 2002a)

The net transfer of iodine from the gas to the condensed phase is reflected by the factor of 100- to 1000-fold enrichment of I in fine fraction marine aerosol by comparison to the I/Na ratio in seawater (Duce and Hoffman, 1976; Sturges and Barrie, 1988; Baker et al., 2000). The formation of OIO (Reaction 1-16) and the self reactions of OIO (Reaction 1-18 and 1-19) are regarded as the nucleation mechanisms for new particle formation (Hoffmann et al., 2001). OIO was measured in a filed campaign at Cape Grim by DOAS and the concentration was found to vary between lower than detection limit (0.5 ppt) and about 3 ppt (after sunset) (Allan et al., 2001). Day time OIO was first observed in the coastal North America (Stutz et al., 2007). Furthermore, although I_2O_5, formed through the accumulated oxidation of IO, was once supposed as the end iodine oxides for aerosol nucleation(Saunders and Plane, 2005), the low solubility of nucleated aerosols found by growth factor measurements supports the polymerization of I_2O_4 in nucleation due to its low solubility in many solvents including water (Vakeva et al., 2002; O'Dowd and Hoffmann, 2005). The aerosols induced from CH_2I_2 photolysis chamber experiment was measured by aerosol mass spectrometry (AMS) for composition analysis (Jimenez et al., 2003). The main fractions were indicative of

iodine oxides and/or oxy-acids, showing more potentially that iodide oxides result in particle formation.

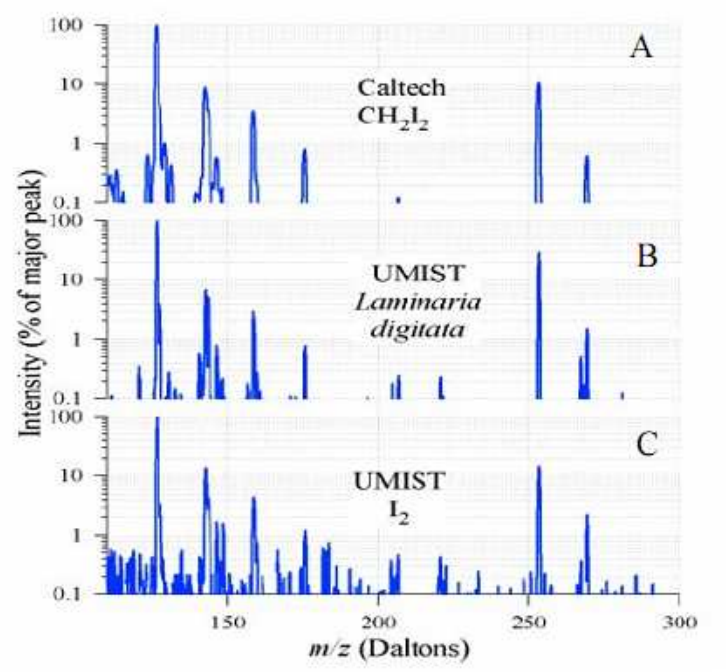

Figure 1- 5 Mass spectra from each of the three systems (A) CH_2I_2 exposed to ozone; (B) Laminaria digitata; and (C) iodine vapor exposed to ozone (McFiggans et al., 2004)

Condensed iodine is partly recycled back to the gas phase but some is taken up into the aerosol phase. The exact rates and mechanisms involved are key parameters for the prediction of iodine's impaction on the atmosphere. To date, although a large amount of studies concentrated on gaseous iodine reactions in the atmosphere, field data on the chemical speciation of iodine in aerosols are scarce. Early observations of iodine in aerosols can be dated back to the early 1970s (Moyers and Duce, 1972; Brauer et al., 1974; Rahn et al., 1977). Later, more measurements were obtained from both continental and coastal environments (Gaebler and Heumann, 1993; Wimschneider and Heumann, 1995; Murphy et al., 1997; Baker et al., 2000; Baker et al., 2001; Baker, 2004, , 2005; Chen, 2006). Unfortunately, most of the existing measurements of iodine in marine aerosols are based on bulk measurement of total iodine, i.e. the individual chemical iodine species that contribute to particulate iodine and that might give insight into the aerosol formation pathways have rarely been measured (e.g. differentiation between I^-, IO_3^-, I_xO_y) (O'Dowd and Hoffmann, 2005).

The iodine species measured in the previous work were mainly inorganic (water-soluble) iodine species: iodide and iodate (e.g. Baker, 2004). Surprisingly, higher iodide concentrations were found than iodate concentration in the aerosols from the Atlantic Ocean (Baker, 2004, , 2005). This is in the contrast to the current knowledge that iodate is the main stable iodine sink species in aerosols. Iodate is

theoretically removed from reactive iodine and not recycle back the gas phase (Vogt et al., 1999). The current models (Vogt et al., 1999; McFiggans et al., 2000) may therefore misrepresent iodine cycling, halogen activation resulting from iodine chemistry and the removal of iodine from ozone destructions reactions (Baker, 2004).

In addition, the total soluble iodine (TSI) concentrations are higher than the soluble inorganic iodine in marine aerosols. The difference between both fractions is defined as soluble organic iodine (SOI = TSI – iodide – iodate) (Baker, 2005). Analysis of marine aerosols from ship campaigns over the Atlantic Ocean found that SOI composed of 65% and 24% of TSI (Baker, 2005). This finding is supported by the correlation between iodine and organic matter in individual MBL aerosol (Murphy et al., 1997). SOI was dominant in fine particle size ranges, suggesting its formation via gas-to-particle conversion/gas-phase uptake processes (Baker, 2005). Total insoluble iodine (TII) in marine aerosols was determined by Inductively Coupled Plasma – Mass Spectrometry (ICP-MS) through a tetra-methyl-ammonium-hydroxide (TMAH) extraction, which may also direct to the organic iodine in aerosol phase (Chen, 2005). An early work in the 1960s reported the iodine dissociated from AgI in the atmosphere could react with volatile iodine to produce new aerosols. These may then act as the ice nuclei (Rosinski, 1966). The HOI-organic matter reaction is a potentially significant source of aerosol SOI, as HOI is known to be an active iodine species reacting with organic matter at seawater (Truesdale et al., 1995). Alternatively, soluble organic matter in fine mode aerosol produced by ejection directly from the sea surface microlayer (SSM) during bubble bursting may be another pathway for SOI uptake. However, such mechanisms are still unknown, and atmospheric iodine chemistry models currently do not include any aerosol phase reactions with organic substances. Recent modeling work tried to fill the gap between theoretical knowledge and the field observations (Pechtl et al., 2007). Pechtl et al investigated iodine formation via the reaction of HOI with dissolved organic matter (DOM). Iodate could be reduced in acidic media by inorganic reactions with iodide and H^+. The results showed better agreement between modeled and observed iodide and iodate concentrations. However, the modeled aerosol iodide concentrations were still significantly lower than observed values in field samples, suggesting more efforts need to be put into the aerosol iodine to improve the current understanding of iodine cycling in the MBL.

1.3 Iodine Sink

1.3.1 Wet Deposition of Atmospheric Iodine

Aerosol iodine is removed by precipitation (rain, snow etc) and recycles back to the ocean. Wet deposition of iodine was estimated as 2.7 μmol m^{-2} yr^{-1} at Weybourne, the English coastal site (Baker et al., 2001). A significant correlation was found between total monthly wet deposition of iodine and rainfall (Figure 1-6), demonstrating

substantial removal of iodine by precipitation (Baker et al., 2001). This is consistent with later work on iodine speciation in precipitation, that indicates aqueous iodine is most likely transferred directly from the aerosol to the droplet during aerosol activation (Gilfedder et al., 2008).

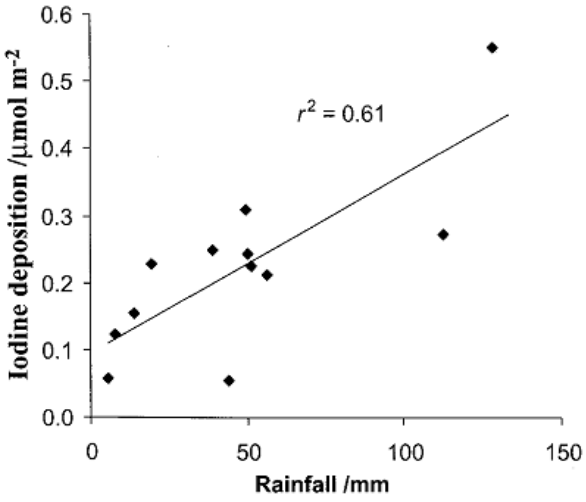

Figure 1- 6 Relationship between total monthly wet deposition of iodine and rainfall at Weybourne (Baker et al., 2001).

Iodine distributes globally in rain and snow, generally ranging between 1.6 – 78 nmol L^{-1} (Truesdale and Jones, 1996; Baker et al., 2001; Gilfedder et al., 2007a; Gilfedder et al., 2008). In addition to total iodine measurement, the iodine speciation in precipitation showed the existence of inorganic iodine (iodide and iodate), as well as SOI (Baker et al., 2001; Gilfedder et al., 2007a, 2007b; Gilfedder et al., 2008). Similar to the iodine speciation in marine aerosol, SOI was found to account for a significant fraction in the rainfall samples (Baker et al., 2001; Gilfedder et al., 2007b). Iodine speciation using Ion Chromatography (IC)-ICP-MS with an anion exchange column was applied for rain and snow speciation lately and several unidentified peaks were observed in the chromatograms, which gave the first report of separated SOI species in environmental samples (Gilfedder et al., 2007b). However, no structural information has been obtained and these peaks are not identified yet.

1.3.1 Ocean

The ocean covers over 70% of the Earth's surface, which is the source as well as the largest sink of iodine. In the sea water, iodine exited mainly as iodide, iodate, as well as volatile and non-volatile organic iodine with a total concentration of around 0.45 μmol (Wong, 1991). Concentrations of iodide and iodate in sea water are in the order of 0.7×10^{-7} mol L^{-1} and 3×10^{-7} mol L^{-1}, respectively (Tsunogai, 1971; Ullman et al., 1990). However, iodide and iodate levels vary with the sea water depth. Iodate is found to be

predominate in deep sea (> 250 m) while iodide increases with a decrease in the iodate levels near the surface (Waite and Truesdale, 2003). The biological reduction of iodate is thought to occur in the near-surface sea water (Waite and Truesdale, 2003; Chance et al., 2007). Also, iodide can also be formed by the decomposition of dissolved organic iodine in sea water (Wong and Cheng, 1998). Volatile organic iodine, which is suggested as the source of atmospheric iodine chemistry, is usually lower than 1 nmol (Lovelock, 1975; Singh et al., 1983; Klick and Abrahamsson, 1992; Moore and Tokarczyk, 1993). The contribution of non-volatile organic iodine is also small in the open oceans, usually < 5% of total dissolved iodine (Truesdale, 1978; Ullman et al., 1990; Tian and Nicolas, 1995). Its concentration decreases with depth and increases towards the coast (Wong and Cheng, 1998). It can become a major or even the predominant species in coastal marine waters (Wong and Cheng, 1998, , 2001).

1.3.3 Terrestrial Aqueous Environment

Precipitation may also transport iodine to continental aqueous environments. However, the proportion of iodine in the terrestrial aqueous environment derived from marine iodine source is still unclear. In addition, the cycling between terrestrial and oceanic environments is also not clear. The iodine speciation results from aerosols and precipitation (rain and snow) seems highly correlated due to the same unidentified signals are eluted from the same IC-ICP-MS system (Gilfedder et al., 2007b, 2007a; Gilfedder et al., 2008). The distribution of continental precipitation does not present a relation with the distance to the ocean, but decreases rapidly with increasing elevation (Gilfedder et al., 2007a). This is indicates terrestrial emissions such as anthropogenic sources (Muller, 2003), rock weathering (Muramatsu and Wedepohl, 1998), volcanic plumes (von Glasow and Crutzen, 2007)and so on may play their roles in terrestrial iodine cycling. Iodide, iodate and SOI are the main iodine fractions measured so far in terrestrial aqueous environments, and existence of SOI has been found by chromatography coupled to ICP-MS (Heumann et al., 1998; Rädlinger and Heumann, 1998; Gilfedder et al., 2007b). In brief, the terrestrial aqueous environment is thought a less important sink for the iodine cycling compared to the ocean.

1.4 Objectives of this Work

The main objectives of this work are to develop analytical methods for iodine speciation in marine aerosols and to gain an in-depth understanding of iodine chemistry in the MBL.

1.4.1 Method development

ICP-MS is a sensitive, accurate and reliable technique for iodine measurements in

environmental samples (Edmonds and Morita, 1998; Wuilloud and Altamirano, 2005). Therefore, analytical methods using ICP-MS for total iodine measurement in different matrixes were developed to measure TSI and TII in the marine aerosol samples. Also, experiment pretreatments were developed including ultrasonic assisted water extraction for soluble iodine and TMAH extraction for insoluble iodine in marine aerosol filter samples.

Measurement of individual iodine species is still an analytical challenge, especially at the relatively low natural concentration levels (μg/L) (O'Dowd and Hoffmann, 2005). Separation techniques (i.e. chromatography and electrophoresis) and ICP-MS were developed for soluble iodine speciation. IC with two anion exchange columns and gel electrophoresis (GE) were used for iodine separation, and ICP-MS was performed as the iodine specific detector. Inorganic iodine, namely iodide and iodate, was separated successfully and measured by both methods. SOI peaks were observed in the chromatograms and electropherograms.

1.4.2 Iodine Speciation in Marine Aerosols

To gain a holistic view of the iodine in marine aerosols, four field campaigns were conducted in this work and the developed methods for total iodine and iodine speciation were applied to iodine measurement of the collected aerosol samples.

MAP Campaigns at Mace Head

There were two parallelly intensive campaigns conducted during June – July 2006 in the Marine Aerosol Production (MAP) project. The Mace Head Campaign (MHC) took place at Mace Head Atmospheric Research Station (MHARS), west coast of Ireland. $PM_{2.5}$, PM_{10} and 5 stage Berner impactor cascade sampler (size range: 0.085 – 0.25 μm, 0.25 – 0.71 μm, 0.71 – 2.0 μm, 2.0 – 5.9 μm and 5.9 – 10 μm) were collected for iodine speciation. Simultaneously, Celtic Explorer ship Campaign (CEC) was performed over the North Atlantic Ocean to investigate the influence of biological activity on iodine chemistry in the open ocean. $PM_{2.5}$ was sampled onboard during the sampling period.

OOMPH Campaign over South Atlantic Ocean

The cruise campaign of the project “Organics over the Ocean Modifying Particles in both Hemispheres (OOMPH)” was conducted in the southern semisphere during January – February 2007. The scientific ship Marion Dufresne traveled a round trip between the South Africa and the South America, crossing the South Atlantic Ocean. 5 stage Berner impactor size fractionated samples (size range: 0.085 – 0.25 μm, 0.25 – 0.71 μm, 0.71 – 2.0 μm, 2.0 – 5.9 μm and 5.9 – 10 μm) was used to collect marine aerosol samples mainly over the open ocean.

Xue Long Ice Breaker Campaign from East Asia to Antarctica

During November 2005 – March 2006, a sampling campaign was conducted on the Chinese Ice braker *Xue Long* along a 30,000 km round-trip cruise from Shanghai, China to Prydz Bay, Antarctica, over the West Pacific Ocean, East and South Indian Ocean, and the coastal Antarctica. Total Suspended Particle (TSP) samples were collected during the campaign.

TSI, TII, iodide, iodate and unidentified organic iodine (UOIs) were obtained from the marine aerosol samples from the four campaigns. A characterization of the aerosol iodine in each individual campaign as well as on a global scale was estimated. The observations from these field campaigns will enhance the global atmospheric iodine database and the conclusions drawn based on these results add more evidence to the importance of iodine chemistry in atmosphere.

2. Development of Analytical Methods for Iodine Speciation in Marine Aerosols

Iodine speciation in aerosols is important for understanding the roles and the pathways of iodine chemistry in the MBL. Efficient sampling techniques for accurate collection of aerosols for speciation analysis are needed. Several aerosol collection techniques, including the principles and available samplers, are introduced in this chapter. Moreover, reliable analytical methods are another important aspect for the analysis of target species, e.g. iodine species. Although the inorganic iodine species including iodide and iodate have been measured in various research campaigns, the challenge of iodine speciation in marine aerosols remains due to the importance of organic iodine compounds were revealed. To date in marine aerosol samples the insoluble iodine species has seldom been reported and the soluble organically bound iodine is not fully understood yet. In this chapter, the analytical methods for total soluble iodine (TSI), total insoluble iodine (TII) and inorganic iodine (iodide and iodate) as well as soluble organic iodine in marine aerosol samples are presented. Inductively Coupled Plasma - Mass Spectrometry (ICP-MS) is used as the analytical technique for TSI and TII after appropriate extractions. Newly developed coupling techniques of Ion Chromatography coupled to ICP-MS (IC-ICP-MS) system with different anion exchange columns are described here and their performance is discussed. In addition, another coupling technique, Gel Electrophoresis coupled to ICP-MS (GE-ICP-MS), also shows its applicability for soluble iodine speciation.

2.1 Sampling

In atmospheric aerosol research it is vital to apply a suitable sampling technique for aerosol collection depending on the different analytical purposes. Filtration is probably the most widely utilized technique for aerosol measurement, owing to its flexibility, simplicity and economy. The basic idea for filtration sampling is to draw an aimed air stream through a suitable porous medium or filter which allows the gas penetration and particle collection in certain size ranges on its surface. Therefore, the properties of the filter medium, the preparation, transfer and pretreatment of the filter medium as well as the size selection mechanisms of sampling system need to be thoroughly considered.

2.1.1 Sampling Objectives

There are many sampling systems available for aerosol collection with different principles, sampling flows and also tailored to different environments. The challenge of designing, installing, operating, and using the data from a sampling work depends

mainly on the specific purpose. Hence, the sampling objective is always the primary consideration for searching a sampling device.

The main objective in this work is to perform iodine speciation in aerosols in the MBL. The sampling systems selected for the campaign takes the following criteria into account: (a) storage ability for future chemical analysis; (b) suitable sampling flow conditions to ensure enough mass collected; (c) ability to collect fine particle sizes (studies of new particle formation); (d) ability to collect different particle sizes in parallel for in-depth study; (e) suitability for different sampling environments in the MBL. Four samplers were selected according to these considerations. A self-built virtual impactor $PM_{2.5}$ sampler and a commercial hi-volume PM_{10} sampler were used to collect marine aerosols at Mace Head, located on the west coast of Ireland during the Marine Aerosol Production (MAP) campaign during June and July 2006. For size distribution investigation, a self-built Berner impactor cascade sampling system was settled at Mace Head and on a scientific vessel over the Indian Ocean. During the scientific cruise from Shanghai, China to Prydz Bay, Antarctica, a total suspended particle (TSP) sampler was fixed on the vessel during the cruising which was planed to investigate coarser size particles in order to avoid inadequate loading during sampling because no previous measurements have been concentrated on this sampling path. Sampling brace and water proof devices were self-designed and self-made to settle the sampling systems and allow them work properly under bad weather conditions such as rainy and windy circumstances.

2.1.2 Sampling Techniques

Methods for particle size separation include impaction, virtual impaction, elutriation, cyclonic flow etc (Hinds, 1999). In this section, the samplers and sampling media (filters) used in this work, as well as their principles are introduced.

1) Virtual Impactor $PM_{2.5}$ Sampler

A virtual impactor is a particle inertial classification device that is very similar to the conventional inertial impactor. Compared to direct impaction, a virtual impaction surface was placed in the virtual impactor inlet to direct the larger particles elsewhere (Watson and Chow, 2001). When a jet of particle-laden air is accelerated toward a collection probe, a small gap exists between the acceleration nozzle and the probe. A vacuum is applied to deflect a major portion of the airstream away from the collection probe. Particles larger than a certain size cross the deflected streamlines, whereas smaller particles follow the deflected streamlines (Loo and Cork, 1988). These two gas streams can then be directed to the collection filters, into another inertial classification devices, into and another impactor stage etc (see Figure 2-1 a). The particle collection efficiency curve for virtual impactor is quite sharp and suitable for aerosol collection in ambient environment. Virtual impactors have usually only one stage. The benefit of a

virtual impactor is the use of conventional fibre filters that do not suffer from bounce off like the substrates for impaction in the normal impactors or interferences of chemical analysis from substrate coating (Hoffmann and Warnke, 2007).

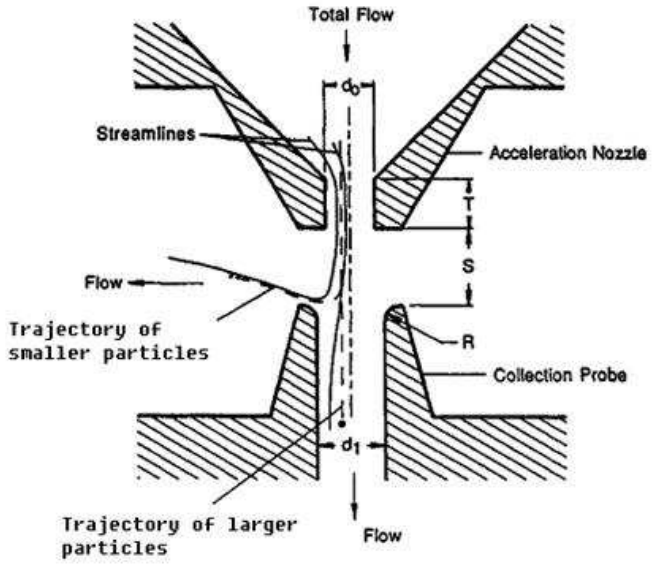

(a)

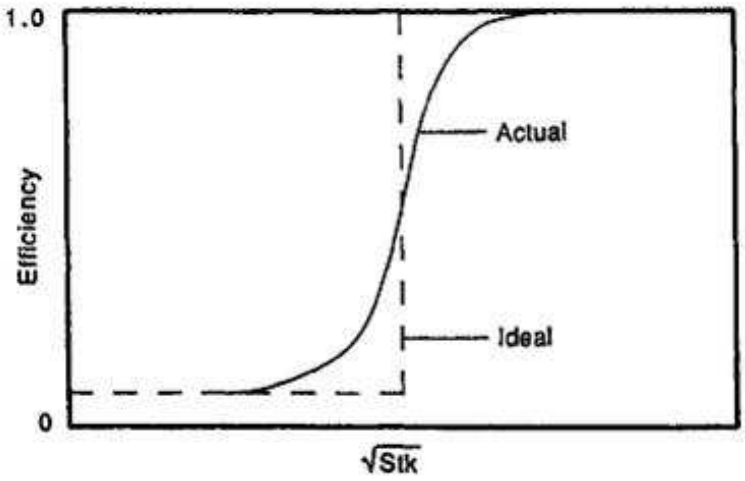

(b)

Figure 2- 1 Schematic diagram of virtual impactor (a) and its corresponding collection efficiency (b) (Marple et al., 2001)

A virtual impactor $PM_{2.5}$ sampler was self-built consisting of a commercial virtual impactor inlet, stainless steel filter holder, and a vacuum pump (VT4.8, Becker, Wuppertal, Germany). The virtual impactor inlet and sampling holder were cleaned with HNO_3 (5 %) - ethanol (5 %) -water solution in an ultrasonic bath before field sampling. The sampling filter was Φ43 mm cellulose nitrate membrane filter (self-cut

from the original filter Φ70 mm, Sartorius AG, Göttingen, Germany)

Figure 2- 2 Picture of virtual impactor inlet and the filter holder

2) Berner Impactor Cascade Sampler

Direct impaction is the widely applied in particle size separation because it is simple to construct and is well understood theoretically. Direct impaction systems consist of one or more jets positioned above an impaction plate. The impactor dimensions are selected to allow particles with diameters exceeding the desired cut point to strike and adhere to the plate.

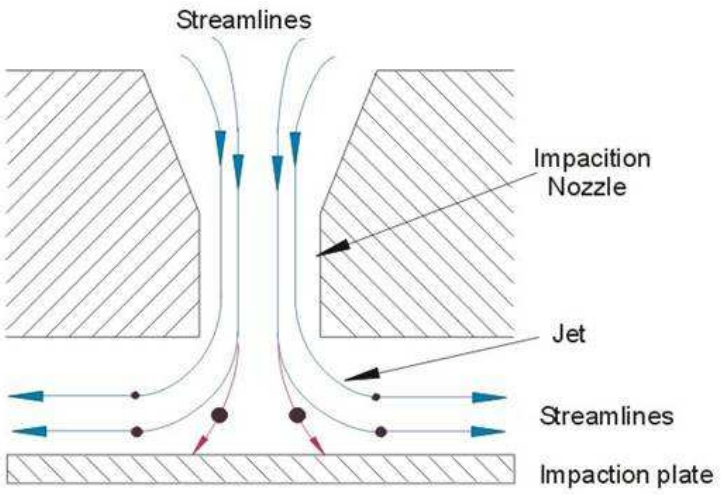

(a)

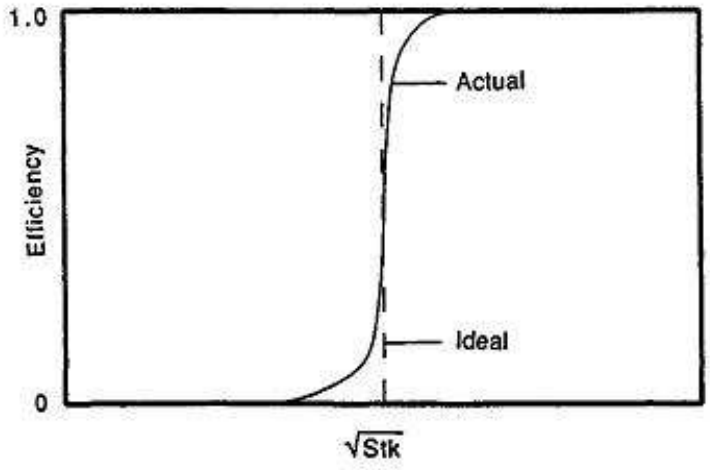

(b)

Figure 2- 3 Schematic diagram of a impactor (a) and the corresponding particle collection efficiency (b) (Marple et al., 2001)

As is shown in Figure 2-3, the gas streamlines pass through a nozzle and the output streamlines are directed against the impaction plate which deflects the flow to form an abrupt 90˚ bend. Particles larger than a certain size are unable to follow the streamlines and adhere to the plate. Smaller particles can avoid hitting the plate and follow the streamlines to the probe. Impaction inlets require frequent cleaning and oiling or greasing to prevent impacted particles from disaggregating or becoming re-entrained in the air flow (Watson and Chow, 2001; Chen, 2005). The collection efficiency curve is also shown in Figure 2-3 (b). The collection efficiency (as a function of particle size) is defined as the fraction of particles passing through the nozzle that are collected on the impaction plate. The ideal impactor has a perfectly sharp efficiency curve, that is, all particles larger than the cut size of the impactor are collected on the plate, while all smaller particles follow the gas flow out of the impaction region.

The Berner cascade impactor is designed for determining size distribution of aerosols (Berner and Lurzer, 1980). In this case, a series of impactor stages are installed in a cascade fashion such that the gas passes from one stage to the next. Each stage is fitted with a removable plate and the cutoff size is reduced at each stage by decreasing the nozzle size. A cascade impactor makes use of the fact that particle collection is governed by the Stokes number which is the ratio of the particle's stopping distance to the physical dimension of the body collector. The velocity of the particle-laden gas stream is increased in successive stages, resulting in the collection of successively smaller particles in the subsequent stages.

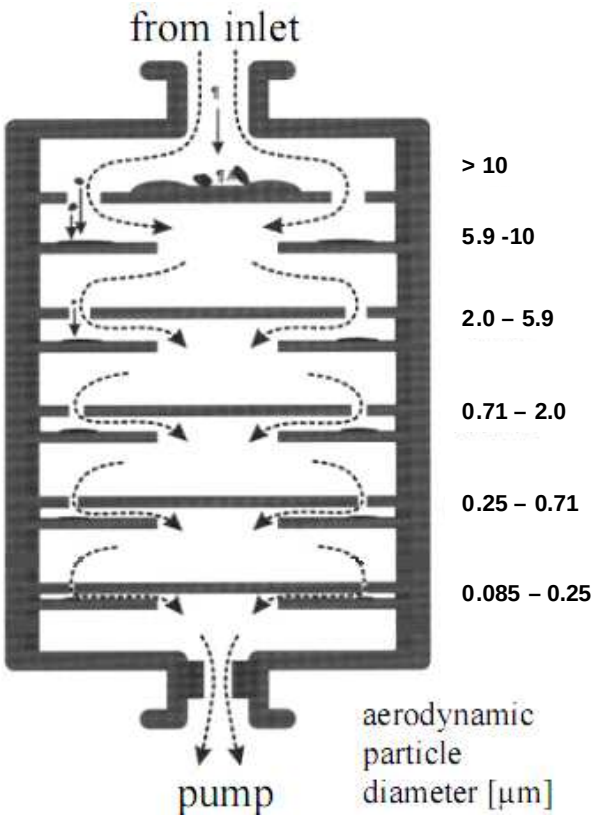

Figure 2- 4 Schematic diagram of cascade impactor

A 5-stage cascade impactor, namely Berner impactor (Firma Dr. Eberhard Steinweg, Grebenhain, Germany), with fractionated sizes: 0.085 – 0.25, 0.25 – 0.71, 0.71 – 2.0, 2.0 – 5.9, 5.9 – 10.0 μm was used for the size fractionated particle sample collection in the field campaign of this work (see Figure 2-4 and Figure 2-5). The sampling flow rate of is fixed to 4.5 m^3 h^{-1} by using the vacuum pump (AEG, Type AM 90 LX4, 1.25 kW, Busch GmbH, Germany).

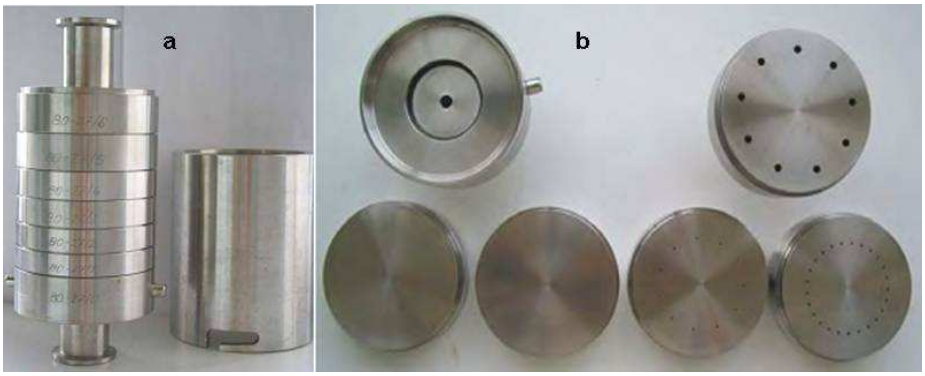

Figure 2- 5 Picture of Berner Impactor (a. side view; b. impaction plates)

Cellulose nitrate filter (self-cut from the original filter Φ120 mm, Sartorius AG, Göttingen, Germany) which is cut as annular filters (size: Φ_o=78mm, Φ_i=40mm) were placed in each impaction stage to collect aerosols of different size ranges.

All subassemblies of the impactor were cleaned by HNO_3 (5 %) - ethanol (5 %) -water solution in an ultrasonic bath before field sampling.

3) Hi-volume PM_{10} Sampler

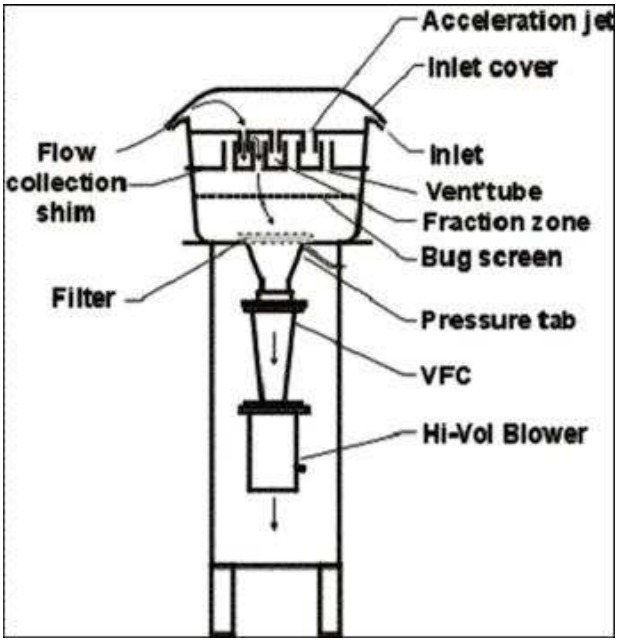

Figure 2- 6 Schematic diagram of Sierra-Andersen/GMW Model 12000

GMW Model 12000 Hi-volume PM_{10} Sampler (Sierra-Andersen, Rockland, MA, USA) was designated as the Federal Reference Method (FRM, USA) for ambient PM_{10} sampling. Figure 2-6 shows the structure of this sampler. It is designed to collect particles equal to or lower than a defined size (PM_{10}). When ambient air is drawn into the inlet, the acceleration nozzles fractionate particles larger than 10μm, which are impacted onto a greased collection shim. The air containing the PM_{10} particle fraction is channeled through to the filter holder. The flow rate is critical to maintain the PM_{10} cut point and when using the standard impactor dimension, a constant flow rate of 68 $m^3 h^{-1}$ (1133 L min^{-1}) is controlled by a volumetric flow controller (VFC) for a high volume sampler.

For PM_{10} sampling, it is necessary to use filter material with low flow resistance in order to maintain the prescribed flow rate. Quartz fiber filters (Whatman, Maidstone, UK) was therefore chosen for high-volume sampling for its good filtration characteristics with high flow and low pressure-drop and the excellent collection efficiency for small particles. All filters were preheated at 900℃ for 3 h to remove the carbonaceous contamination. All subassemblies were cleaned with HNO_3 (5 %) - ethanol (5 %) -water solution before field sampling.

4) TSP Sampler

Total suspended particle (TSP) is a used as a regulatory measure of the mass concentration of particulate matter (PM) in ambient air. It was defined by the size-selectivity of the inlet to the filter that collected the particles. Normally it refers to the aerosol sized less than 100 μm.

Figure 2- 7 Picture of Tianhong TH-1000 TSP sampler

A TH-1000 TSP sampler (Tianhong, Wuhan, China) was settled on the scientific icebreaker Xue-Long during the 23th China Antarctic Campaign. The sampler is developed for TSP collection with a sampling flow of 68 m^3 h^{-1}. Cellulose fiber filter (Grade 41, Whatman, Maidstone, UK) was chosen for sample collection.

2.2 Sample Pretreatment

The sample pretreatment procedure is schematically shown in Figure 2-8. After sampling, the samples were soaked with 10 mL ultra pure water (18mΩ, Milli-Q Water Purification System, Millipore, Bedford, MA, USA) and extracted with an ultrasonic bath for 20 min to remove soluble iodine species from the filter. The filters with insoluble iodine species were kept for further measurements. The extracts were measured, firstly, using ICP-MS for total soluble iodine (TSI). Then several ICP-MS coupling techniques such as IC-ICP-MS (with two different systems) and GE-ICP-MS measurements were applied for soluble iodine speciation. Iodide, iodate and other unidentified organic iodine (UOI) species were found during these speciation measurements. The filters with insoluble iodine were further extracted with

Tetra-methyl-ammonium-hydroxide (TMAH). TMAH is a strong aqueous alkaline regent and very effective for extraction of trace elements. During the pretreatment, 2 mL 10% TMAH (diluted from 25%, 99.9999%, Alfa, Karlsruhe, Germany) solution was added to the water-extracted filter and put into an oven at 90 ℃ for 3 h (Chen, 2005). The cellulose nitrate filters decompose in TMAH solution, which avoids any loss of iodine species during the extraction step. Then the total insoluble iodine (TII) was determined by ICP-MS. Before injected into any analytical system, filtration was necessary to remove the particles in samples which would cause clogging of, for example, IC column, the gel of GE, nebulizer, sampler, and skimmer of ICP-MS. Membrane filters (pore size 0.45μm, Φ 26 mm, poly-propylene membrane, VWR, Darmstadt, Germany) were used for particle filtration.

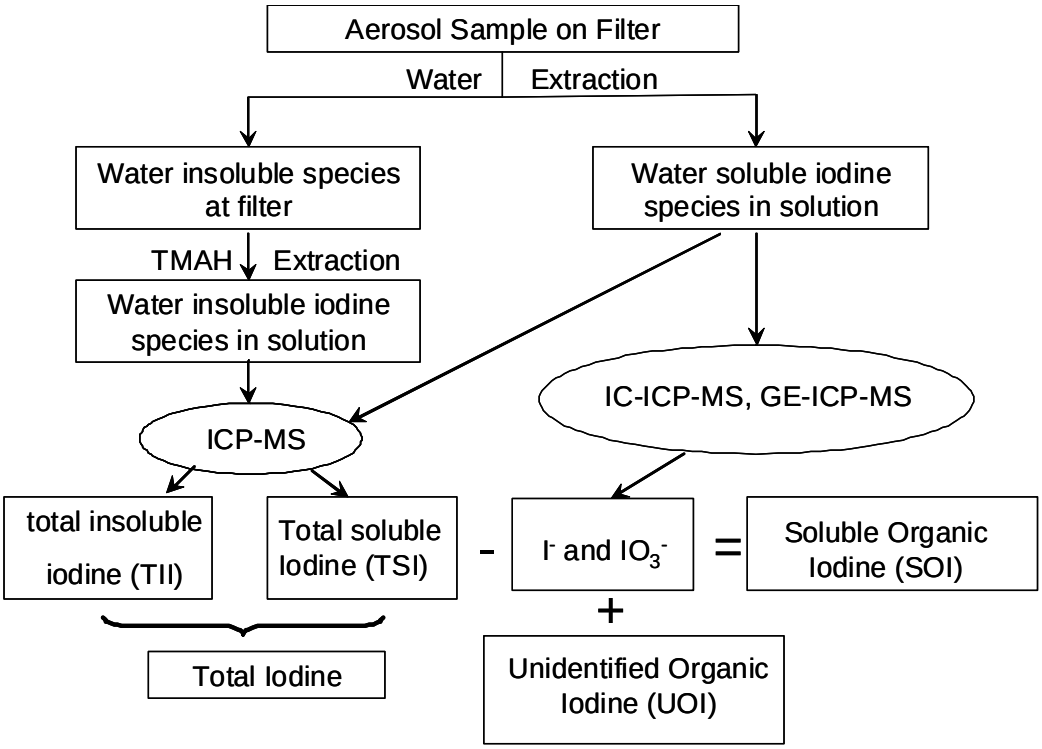

Figure 2- 8 Procedure of sample pretreatment in iodine speciation

2.3 Total Soluble Iodine and Total Insoluble Iodine Measurement in Marine Aerosols

ICP-MS is a fast, precise and accurate multi-element technique for trace element determination. An ICP-MS can be thought of as four main processes, including sample introduction and aerosol generation, ionization by an argon (Ar) plasma source, mass

discrimination, and the detection system. The sample introduction system transports the sample (solid or liquid) into the centre of Ar plasma. For solid samples, a laser ablation (LA) device is normally used to produce sample aerosol into the plasma. Aqueous samples are introduced by a nebulizer, which aspirates the sample with high velocity Ar, forming a fine mist. Aerosols then pass into a spray chamber where larger droplets are removed via a drain and smaller droplets transferred into the plasma torch. An Ar plasma flame which is generated and maintained by a high radiofrequency (RF), is used as an efficient ionisation source. The temperature can reach the order of 6000 – 10000 K. The hot plasma removes any remaining solvent and causes sample atomization followed by ionization. Subsequently, sample ions are introduced through a pumped vacuum interface into the Mass Spectrometry (MS). The interface solves the incompatible working pressures between plasma (atmospheric pressure) and extracts with ions with two cones with small orifice. Then the sample ions pass into the high vacuum region of the MS. When a quadrupole is used as a mass analyzer, it acts as a mass filter that separates ions according to their mass/charge ratio (m/z). Finally, the detector is located at the far end of the mass spectrometer in the high vacuum (10-5 torr) part of the mass spectrometer chamber. Its purpose is to detect, amplify and measure the analyte ions passing through the mass spectrometer. The most commonly used type of detector in ICP-MS is an electron multiplier.

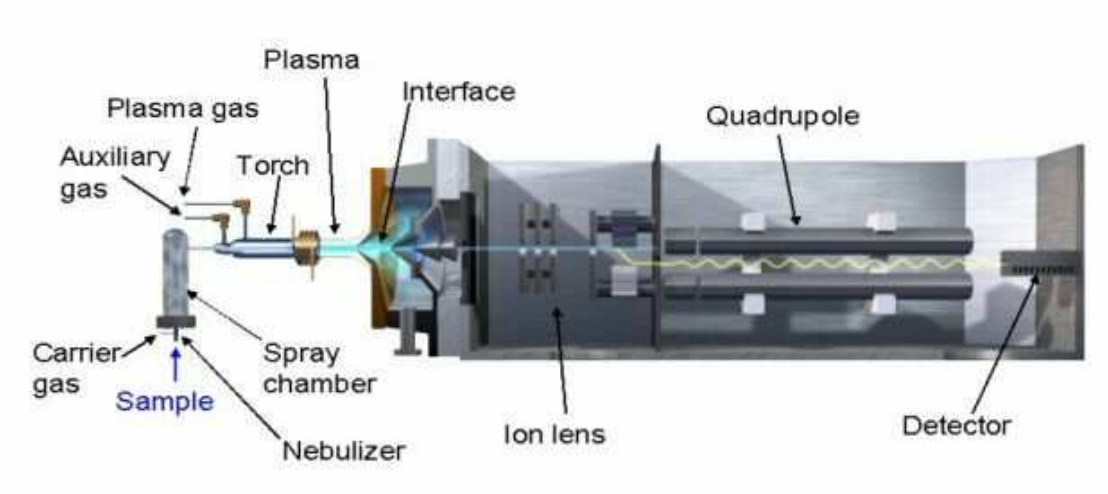

Figure 2- 9 Schematic diagram of quadrupole ICP-MS

The analytical methodologies developed to determine iodine species in environmental samples have involved almost exclusively ICP-MS (Wuilloud and Altamirano, 2005). ICP-MS is especially advantaged for iodine measurement in marine aerosol samples due to several reasons. Firstly, ICP-MS has excellent detection capability for elemental analysis. Concentrations of total iodine and iodine species in marine aerosols are as low as pmol per m^3. High sensitivity and low detection limit are always necessary for such low concentration measurements. Secondly, ICP-MS is designed for element selective measurement, which makes it possible to be used as an element specific detector. Hence,

it has the potential to be involved in the hyphenation techniques e.g. GC-ICP-MS, High Performance Liquid Chromatography (HPLC)-ICP-MS, IC-ICP-MS, GE-ICP-MS and Capillary Electrophoresis (CE)-ICP-MS. Isotope ratio measurement is also possible so that isotope dilution analysis can be successfully achieved.

In this section, analytical methods for measuring TSI and TII are introduced. External calibration analysis and isotope dilution analysis (IDA) are both applied in the quantification of total iodine and iodine species.

2.3.1 Experimentation

1) Reagent

Iodine standard:

Iodide standard for IC (1000 mg L^{-1} Fluka, Deisenhofen, Germany) were used to prepare different concentrations of standard for an external calibration curve. Tellurium (^{126}Te) (ICP-Standard, 1000 $\mu g mL^{-1}$, Merck, Darmstadt, Hessen, Germany) was used as an internal standard.

For IDA, potassium iodate standard (Fluka, Deisenhofen, Germany) is used for method development. Long-lived $^{129}IO_3^-$ standard (NEN Chemicals, Boston, MA, USA) enriched in ^{129}I by about 86 % was used for isotope dilution. (**Safety note:** As ^{129}I is a long-lived radioactive isotope solutions containing enriched iodine were used in concentrations lower than 100 $\mu g\, L^{-1}$, which refers to an activity lower than 0.66 $Bq{\cdot}g^{-1}$).

Milli-Q water (Milli-Q Water Purification System, Millipore, Bedford, MA, USA) and TMAH (25%, 99.9999%, Alfa, Karlsruhe, Germany) were used for water extraction and TMAH extraction, respectively.

Gas: argon for the ICP was 99.996 Vol-% (Westfalen AG, Münster, Germany).

2) Instrument

HP4500 quadrupole ICP-MS (Agilent, Waldbronn, Germany) equipped with a micro-flow nebulizer and a cooled double-pass spray chamber (both AHF, Feuerbacher, Tübingen, Germany) was applied for iodine measurement. The ICP-MS parameters were daily optimized for optimal detection by continuous injection of 10 $\mu g\, L^{-1}$ IO_3^- and 200 $\mu g\, L^{-1}$ Te. Details of the operating conditions used throughout this work are given in Table 2-1.

Table 2- 1 Instrumental parameters for HP4500 ICP-MS system.

System	HP4500	
Plasma	RF power	1250 W
	Cool Gas Flow	20 L min^{-1}
	Auxiliary Gas Flow	1.0 L min^{-1}
Sample Introduction	Nebulizer Gas Flow	1.0 L min^{-1}
	Nebulizer	Micro-flow (Quartz)
	Spray Chamber	Cooled Double-pass Spray Chamber
	Sampler cone	Ni, 1.0 mm orifice
	Skimmer cone	Ni, 0.7 mm orifice
Acquisition	Mode	Spectrum
	Replicates	5
	Isotopes monitored	^{126}Te, ^{127}I
		^{126}Te, ^{127}I, ^{129}I, ^{131}Xe (IDA)

3) Sample pretreatment

The pretreatment of TSI and TII collections were both described in detail in Section 2.2.

2.3.2 Results and Discussion

1) External Calibration Analysis

With this method, an excellent linear calibration curve was obtained (Figure 2-10) in the analytical range between 1 to 50 μg L^{-1}. The aerosol samples extracted with 10 mL water were generally within this range. Samples with higher concentrations were diluted to keep the measurement within the working range.

Calibration curves were made daily with daily prepared iodide standards. The limits of detection (LOD) were both 0.10 μg L^{-1} for TSI and TII measurements, calculated from the standard deviations of the blank samples (n = 7) with the 3s criterion. As is mentioned in section 2.2, the measurements of TSI and TII were performed in different matrices, TSI in water extracted matrix and TII in TMAH solution. The recoveries in both matrices were studied using a standard addition technique (see Table 2-2). The recoveries ranged from 97.8 - 105.7% for TSI measurement and 96.7 – 101.2% for TII

measurement. The reproducibilities (n = 7) for 10 μg L^{-1} addition in a real sample matrix were 3.03% and 2.19 % for TSI measurement and TII measurements, respectively.

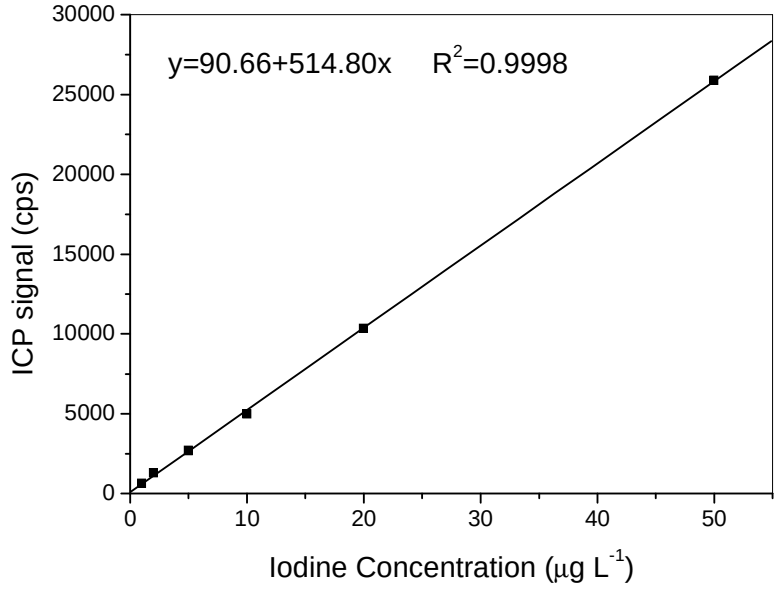

Figure 2- 10 Example of calibration curve in iodine measurement by ICP-MS

Table 2- 2 Investigation on recovery of iodine measurement in different matrix

Added iodine (μg L^{-1})	Measured (μg L^{-1}) Matrix 1[a]	Recovery (%)	Measured (μg L^{-1}) Matrix 2[b]	Recovery (%)
5	4.89	97.8	5.05	101.0
10	10.09	100.9	10.12	101.2
20	21.04	105.7	19.80	99.0
50	51.13	102.3	49.30	96.7

a. Matrix from aerosol water extraction; b. Matrix from TMAH extraction.

2) Isotope Dilution Analysis (IDA)

ICP-MS has the unique capability of using an enriched isotope of the element of interest as the internal standard. This technique, which is known as isotope dilution mass spectrometry (IDMS), has been known for nearly 50 years. IDMS is made possible through the availability of enriched stable isotopes of most of the elements. The IDMS technique involves the addition of a known amount of an enriched isotope of the element of interest to the sample. This addition is made prior to sample preparation

during which the spiked addition of the enhanced isotope is “equilibrated” with the sample. By measuring the isotope ratio of the sample and sample + spike isotope addition and knowing the isotopic ratio of the enhanced addition, the sample concentration can be calculated. The entire measurement is based upon ratio measurements of one isotope of the element to another. Drift, quenching and other related matrix effects do not present an interference with IDMS. This technique is considered as a definitive method and is well suited and established method for the certification of reference materials. IDMS is free from matrix effects (physical interference) but it is not interference-free in that mass interference must still be dealt with (isobaric, MO^+, M^{++}, etc.) in addition to correction of the signal intensity for detector dead time and mass bias interference.

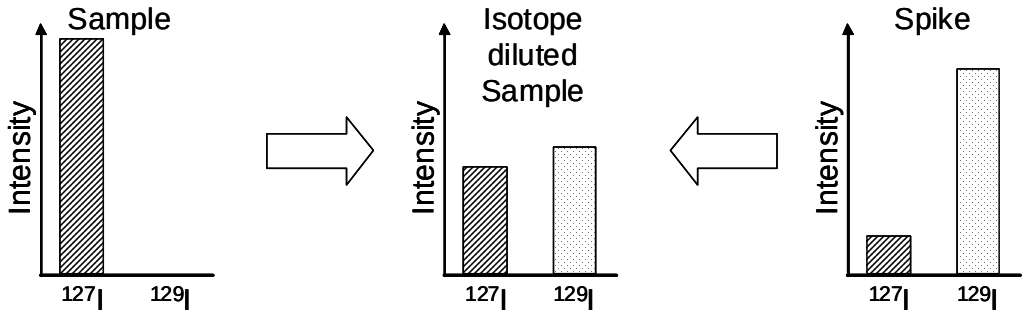

Figure 2- 11 Schematic diagram of iodine isotope dilution analysis

$$m_{Sample} = m_{Spike} \cdot cS_{pike} \cdot (R \cdot {}^{129}a_{Spike} - {}^{127}a_{Spike}) \qquad \text{(Equation 2- 1)}$$

m_{Sample}: amount of I in the sample [g]

m_{Spike}: amount of I in the spike [g]

c_{Spike}: concentration of I in the spike [g g-1]

R: measured isotope ratios in the sample

${}^{127}a_{Spike}$: isotope abundance in the spike [%]

IDMS is therefore not applicable to monoisotopic elements. Although iodine is naturally monoisotopic element, iodine-129 is produced by the fission of uranium atoms during operation of nuclear reactors and by plutonium (or uranium) in the detonation of nuclear weapons. The half life of I-129 is 15.7 million years. During the iodine IDA, spiked iodine standard with I-127 and I-129 was used to dilute the sample (see Figure 2-11). The isotopic ratio of I-127 to I129 was measured with ICP-MS to calculate the mass of iodine in sample. Iodine mass calculation is based on Reaction 2-1. As natural iodine is monoisotopic and within this work no naturally occurring ^{129}I could be detected, mass bias effects do not need to be considered, because the isotope ratio $^{127}I/^{129}I$ for both, the spike standard and the sample after isotope equilibration, was treated identically. Nevertheless, mass bias was determined to be about 1.5 % for $^{129}Xe/^{131}Xe$, which originates as contaminant from Ar gas. For ^{127}I and ^{129}I

measurements only ^{129}Xe has to be considered as spectral interference, since it cannot be separated within the mass spectrometer even in the high resolution mode. Within this work the background for m/z = 129 was constant and a possible time-dependent contribution of Xe was further controlled by monitoring ^{131}Xe. This ensured that obtained signals at m/z = 129 appeared uniquely from spiked ^{129}I.

3) Results

Before the sampling campaign, the filter blanks were investigated with IDA by ICP-MS. Cellulose nitrate filters (n = 11, Φ = 70 mm) were chosen randomly and extracted with TMAH (90℃, 3h) and analyzed for total iodine. The blanks ranged from 0.56 – 5.31 ng per filter with an average of 1.62 ng. Water extraction was applied to another 11 randomly selected filters to check the blank of TSI. The results showed that TSI blank in cellulose in the range of N.D.-3.74 ng per filter with an average of 1.38 ng in one filter. The blanks of cellulose fibre and quartz filter were both checked with TMAH and water extractions. Total iodine and TSI were both lower than 2.0 ng in each cellulose fibre filter (Φ = 70 mm). For the quartz filter (20 cm × 25 cm), less than 10 ng of iodine was found in each filter both in water extraction and in TMAH extraction. This indicates that the blanks of all these filters are satisfactory for iodine aerosol sampling.

The methods mentioned above were applied for iodine measurement in several field campaigns. The results are presented in the following chapters.

2.3.3 Summary

Methods for iodine analysis have been successfully achieved by an ICP-MS technique with external calibration analysis and IDA. Both methods are found to be sensitive, accurate, and reliable for iodine measurement in marine aerosol samples. The methods were applied to measure the blanks of total iodine and TSI in different sampling materials. The results show that cellulose nitrate filter, cellulose fibre filter and quartz filter are all suitable for iodine aerosol sampling. Real samples from field campaigns were also measured with the methods to study the iodine chemistry in MBL.

2.4 Measurement of Soluble Iodine Species using IC-ICP-MS

Element speciation can be achieved by coupling two powerful techniques: one providing excellent separation of element species and the other giving high sensitivity for element detection. The use of ICP-MS coupled with separation techniques for element speciation has attracted more and more attention. Chromatographic techniques, such as HPLC, gas chromatography (GC), and CE are commonly used ones for ICP-MS coupling. Ion chromatography (IC) is one of the LC techniques using an ion exchange column for the separation of ions and polar molecules. It is based on the

interactions of charged analytes (anions or cations) with the charged (positively or negatively) functional groups of the stationary phase. When positively charged analytes react with negatively charged sites in the column, it is referred to as cation-exchange, and when negatively charged analytes interact with positively charged sites, it is anion-exchange. Both mechanisms are highly controlled by the pH of the mobile phases because it affects the dissociation of weakly acidic or basic compounds. Packing materials are beads of crosslinked styrene and divinylbenzene. The mobile phases employed normally consist of an aqueous salt buffer solution, sometimes mixed with a certain amount of organic modifier. When IC is coupled to ICP-MS, the salt contents in the mobile phase must be kept to a minimum (<2% total dissolved solid) to prevent clogging of the nebulizer and erosion of sampler and skimmer. Organic contents in mobile phase may affect the stability of the plasma even extinguish it so the use of organic content in mobile phase must also be controlled. If there are higher organic contents in mobile phase, oxygen should be added to assist the burning of organics. Then the system must be modified and Platinum (Pt) sampler and skimmer should be used.

The measurement of iodide and iodate has been studied with different separation techniques with ICP-MS and Neutron Activation Analysis (NAA) as detectors. Separation of iodide and iodate is always the challenge of analysis. An offline technique of ion exchange preparation was reported to separate iodide and iodate using AG2-X8 resin(Hou et al., 1999; Chen, 2005). Self-made columns were prepared with the resin, then iodide and iodate were sequentially washed out by changing the washing eluent. The collected iodide and iodate were finally measured by ICP-MS or NAA. Although this method provided good performance for iodide and iodate separation, the disadvantages are obvious. The preparation process is complicated, time-consuming, and difficult to control. A similar performance of the separation is hard to achieved evenly in the different columns (normally the column was used only once for one sample) and by different operators. Recently, more effort was put into the online techniques for iodide and iodate separation and measurement. Reversed Phase (RP) LC, IC, GE and CE were reported to separate iodide and iodate successfully and then measure online with ICP-MS (Heumann et al., 1998; Michalke and Schramel, 1999; Saionz et al., 2006; Bruchert et al., 2007; Gilfedder et al., 2007b; Yang et al., 2007).

Here two online IC-ICP-MS systems are introduced. These systems are both anion exchange IC coupled to quadrupole ICP-MS but they are located in different labs and with different analytical column producers. The methods are described to show their performance for the speciation of water soluble iodine in marine aerosol samples.

2.4.1 Experimentation

1) Chemical

Iodine Standard: Iodide standard for IC (1000 mg/L, Fluka, Deisenhofen, Germany) and Potassium iodate standard (0.1 N, Alfa, Karlsruhe, Germany) were used to prepare different concentrations of standard for external calibration curves.

Mobile phase: 0.06 mol L^{-1} $(NH_4)_2CO_3$ (Acros, Nidderau, Germany) for G3286A IC column; 0.035 mol L^{-1} NaOH for AS16 IC column.

Gas: argon for the ICP and helium for eluent degassing were in the purity of 99.996 Vol-% (both Westfalen AG, Münster, Germany).

2) Instrument

IC-ICP-MS system 1(in Uni-Mainz)

IC system consists of a Serial 200 LC pump (Perkin Elmer, Waltham, USA), a Serial 200 autosampler (Perkin Elmer, Waltham, USA), and a DG1310 degaser (Uniflow, Tokyo, Japan). An anion exchange column (G3268A, Agilent, Waldbronn, Germany) is equipped in the system.

ICP-MS system: HP4500 (Agilent, Waldbronn, Germany) was applied as the element specific detector for iodine measurement. The ICP-MS parameters were daily optimized for optimal detection by continuous injection of 10 µgL^{-1} IO_3^-. Details of the operating conditions used throughout this work are given in Table 2-3.

Table 2- 3 Instrumental parameters for HP4500 ICP-MS system.

System	HP4500	
Plasma	RF power	1250 W
	Cool Gas Flow	20 L min^{-1}
	Auxiliary Gas Flow	1.0 L min^{-1}
Sample Introduction	Nebulizer Gas Flow	1.0 L min^{-1}
	Nebulizer	Cross-flow nebulizer(Quartz)
	Spray Chamber	Cooled Double-pass Spray Chamber
	Sampler cone	Ni, 1.0 mm orifice
	Skimmer cone	Ni, 0.7 mm orifice
Acquisition	Mode	Time resolve
	Measuring time	350 s
	Isotopes monitored	^{127}I

IC-ICP-MS system 2 (in Sipplingen Laboratory Germany)

IC system consists of a Serial 200 LC pump (Perkin Elmer, Waltham, USA) and a Serial 200 autosampler (Perkin Elmer, Waltham, USA). An anion exchange column (AS16) and its guard column (AG16) (both Dionex, Überlingen, Germany) are equipped in the system.

ICP-MS system: Elan 6100 (Perkin Elmer, Waltham, USA) was applied as the element specific detector for iodine measurement. The ICP-MS parameters were daily optimized for optimal detection of a selection of masses. A Meinhard nebulizer and cyclone spray chamber were used to gain larger signal from ICP-MS (Gilfedder, 2007).

2.4.2 Results and Discussion

1) Results from System 1

The retention times of iodide and iodate were optimized by changing the concentration of $(NH_4)_2CO_3$ in the mobile phase. Figure 2-12 shows the influence of $(NH_4)_2CO_3$ concentration in the mobile phase on the retention time of iodide and iodate.

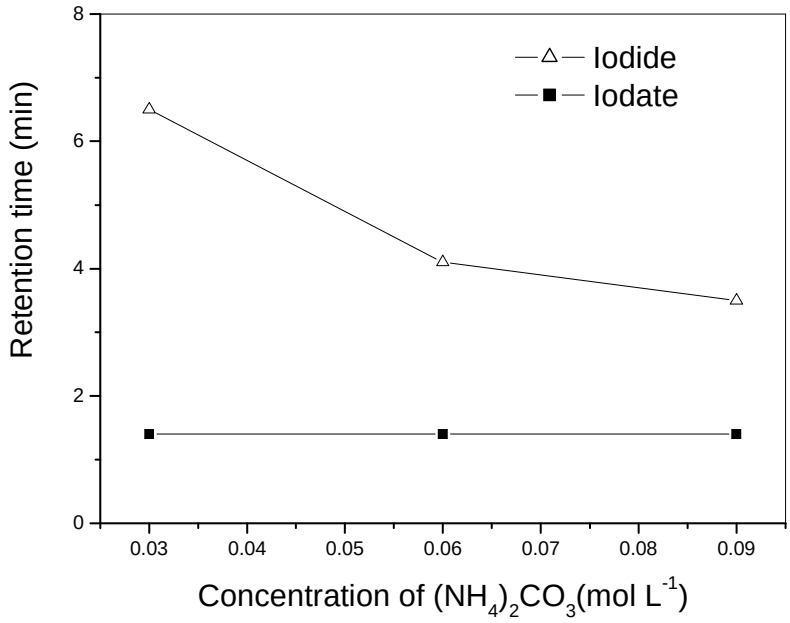

Figure 2- 12 Retention time of iodide and iodate in different mobile phase concentrations

For the tested conditions, iodide and iodate were separated successfully. The retention time of iodate did not change under different concentrations of $(NH_4)_2CO_3$. Iodide had a

shorter retention at higher $(NH_4)_2CO_3$ concentrations. Finally, 0.06 mol L^{-1} $(NH_4)_2CO_3$ (pH 9.4) was selected as the mobile due to the good separation, the lower salt content for ICP-MS, and the shorter running time for the whole measurement.

The flow rate and connection tubing were also optimized. Flow rate of 1.0 mL min^{-1} and PEEK (Polyetheretherketone) connection tubing with an inner diameter (i.d.) of 125 μm (Upchurch, Oak Harbor, USA) were chosen due to better peak shapes for both peaks. The injection volume was 20 μL. A chromatogram of 50 μg L^{-1} iodide and iodate standards is shown in Figure 2-13. The retention times of iodide and iodate were 4.0 min and 1.4 min.

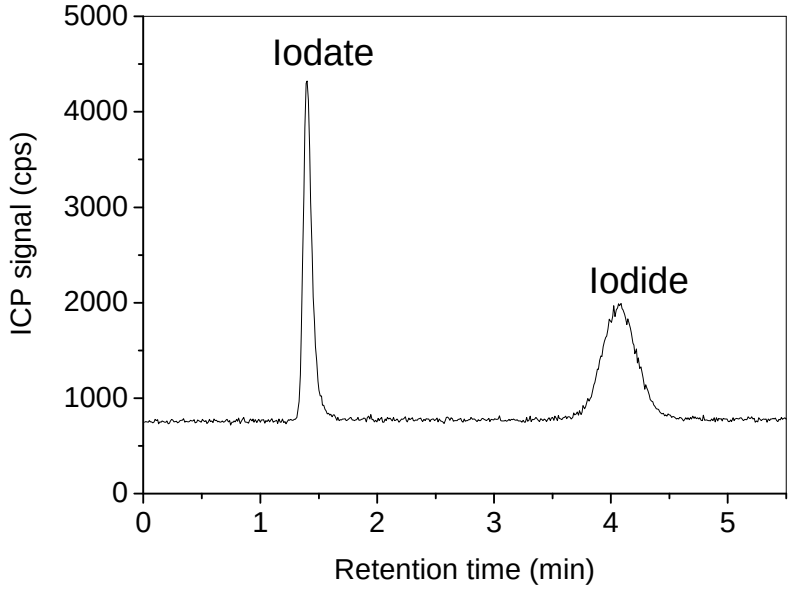

Figure 2- 13 Iodide and iodate (both 50 μg L^{-1}) separation by IC-ICP-MS

Figure 2-14 gives an example of calibration curves for iodide and iodate, respectively. Excellent linear regressions were found in both calibrations of iodide and iodate. The linear ranges are less than 50 μg L^{-1} and less than 100 μg L^{-1} for iodide and iodate, respectively. The calibrations were run daily for quantifications, providing the R^2 values better than 0.9. The LODs were respectively 0.5 μg L^{-1} and 0.1μg L^{-1} for iodide and iodate. The reproducibilities for 5 μg L^{-1} iodide and iodate (n = 7) were 3.03% and 1.74%, respectively.

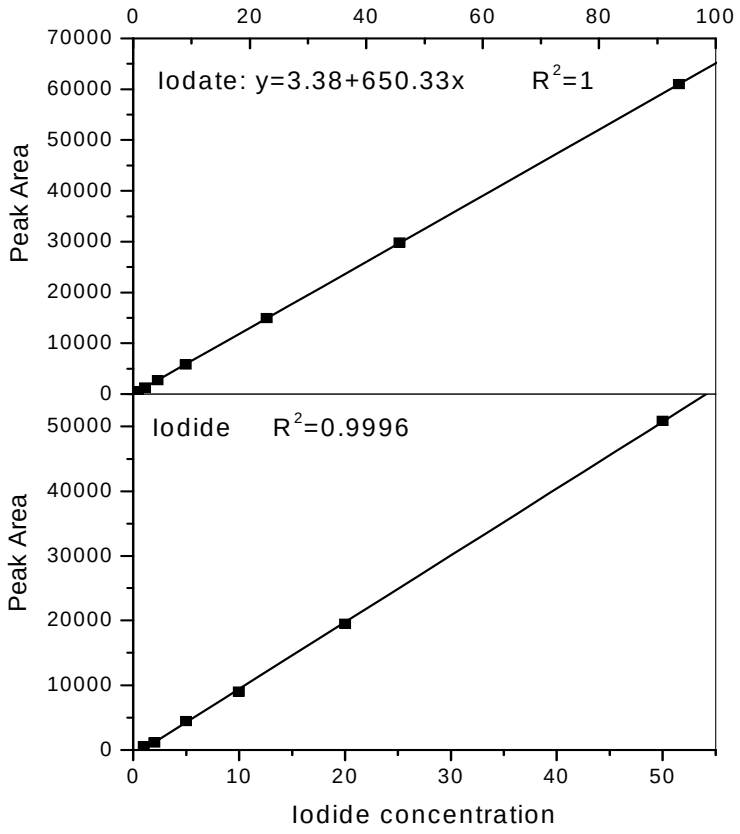

Figure 2- 14 Calibration curves of iodide and iodate

Recoveries of iodide and iodate in the matrix of marine aerosol sample were investigated and the results are shown in the Table 2-4. Recoveries of iodide and iodate ranged from 97.3 – 103.4% and 97.4 – 103.4%, respectively.

Table 2- 4 Recovery of iodine measurement in different matrix

Added ($\mu g\ L^{-1}$)	Measured ($\mu g\ L^{-1}$)	Recovery (%)	Added ($\mu g\ L^{-1}$)	Measured ($\mu g\ L^{-1}$)	Recovery (%)
Iodide			Iodate		
1	0.99	99.0	0.5	0.49	97.4
2	1.97	98.7	1.0	1.00	100.5
5	4.98	99.6	2.5	2.52	100.9
10	9.73	97.3	5.0	5.00	100
20	20.67	103.4	10	9.83	103.4
50	50.12	100.2	25	24.36	100.2

The blanks of iodide and iodate in the sampling materials including cellulose nitrate, cellulose fibre and quartz filter were all measured in their water extracts and were both lower than the LODs, indicating they are all "clean" enough for aerosol sampling measurements.

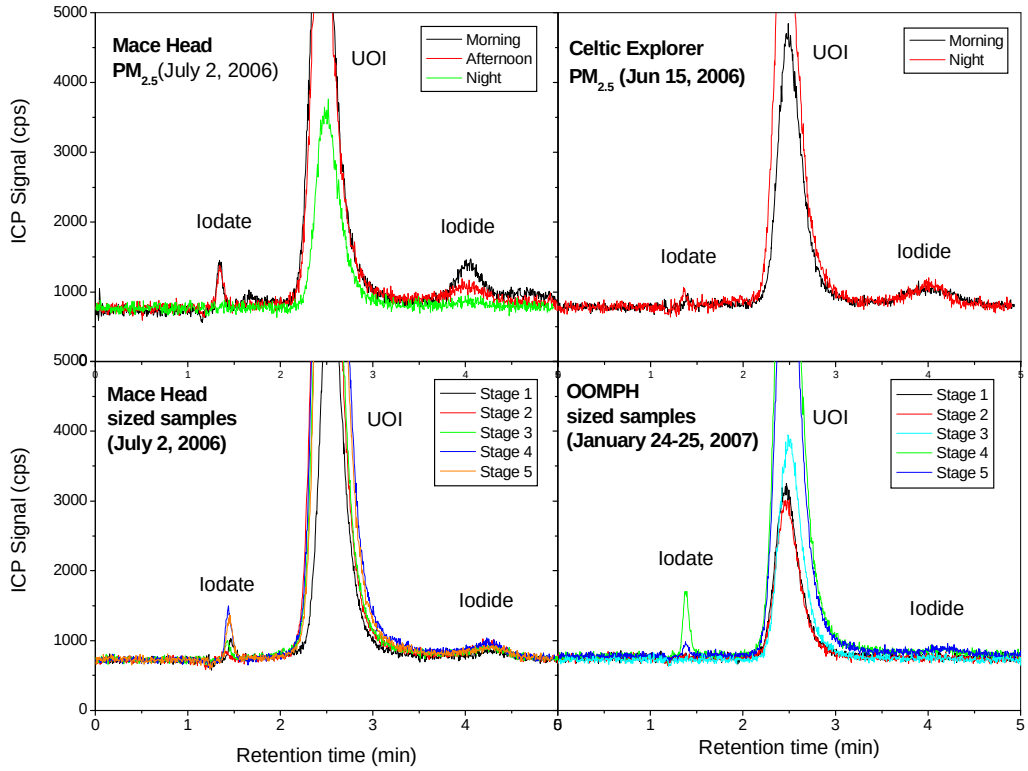

Figure 2- 15 Typical chromatograms showing iodide, iodate, and UOI in aerosol samples from different sampling campaigns: upper left, $PM_{2.5}$ from Mace Head, Ireland; upper right, $PM_{2.5}$ from North Atlantic; lower left, size fractionated samples from Mace Head, Ireland; and lower right, size fractionated samples from South Atlantic.

During the measurements, one organic iodine peak was frequently observed in the chromatograms of real samples (see Figure 2-15). Several commercial organic iodine compounds were tested for comparison but no similar retention time was found. The peak was thus called unidentified organic iodine (UOI). Without the available standards, accurate quantification can be difficult. However, the peak was quantified with the iodide calibration curve because iodine atoms are converted to I^+ in the plasma prior to quantification with mass spectrometer.

The IC-ICP-MS method was applied for the measurements of aerosol samples from the field campaigns. The results are listed and discussed in the following chapters.

2) Results from system 2

The IC-ICP-MS system 2 was setup in Sipplingen Laboratory (Überlingen, Germany),

with which the method for iodine speciation in aqueous solution was developed (Gilfedder et al., 2007b). A Meinhhard nebulizer, a cyclone spray chamber as well as the AS16 anion exchange column were the key parts in this coupling system. They together provide an enhanced signal and good peak shapes during separation. The mobile phase was 0.035 mol L^{-1} NaOH for IC column with a flow rate of 0.9 mL min^{-1}. The LODs were both 0.03 μg L^{-1} for iodide and iodate. The accuracy was checked by running standard reference material BCR-611, which is a groundwater sample with iodide levels of about 9.4 μg L^{-1}. Concentrations were always within the standard deviation given in the certificate and deviated from the average value by less than 10%. Typical chromatograms of rain and aerosol samples are shown in Figure 2-16. Several UOIs (up to five peaks) also presented using this method and the first UOI peak was suggested to be iodoaecetic acid due to the similar retention time, but without further confirmation is needed. Description of the related samples and detail discussion please see Chapter 3.

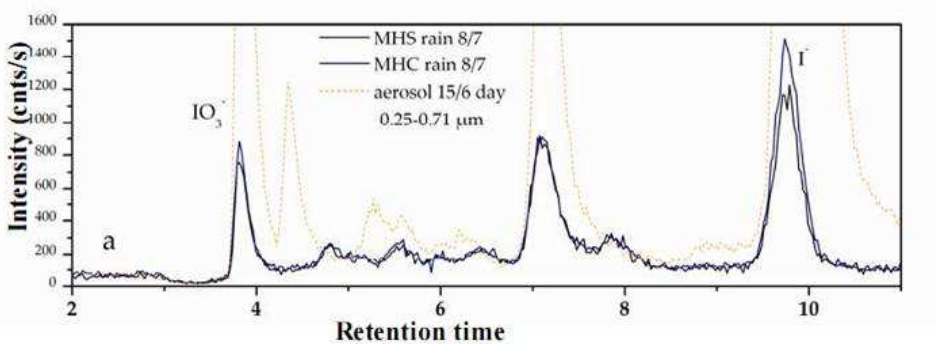

Figure 2- 16 Typical chromatograms of rain and aerosol samples from system 2 ((Gilfedder, 2007))

2.4.3 Summary

Two IC-ICP-MS methods were developed and found to be successful for iodine speciation in the aqueous phase. Both were accurate, sensitive and fast methods for iodine speciation in aerosol and rain samples. Iodide and iodate, and UOI(s) were observed and quantified with both methods. The system 1 is faster in measurement time but the LODs were lower with the system 2. The chromatograms from the two methods indicate UOIs measured were not comparable. Less UOI peaks, but with higher amount was measured in system 1 while more peaks (4-5 peaks) and lower peak heights of UOI were found in system 2. Because these peaks are still not identified, UOIs in real samples should be investigated more thoroughly in the future.

2.5 Measurement of iodide and iodate using GE-ICP-MS

Gel Electrophoresis (GE) is normally used for separation of large molecules such as

peptidess, proteins, DNA etc which differ in size, charge and conformation. The gel has a porous, sponge-like structure allowing the molecules to pass through it in an electric field. Agarose is a commonly used material for GE in many applications. Agarose is a polysaccharide extracted from seaweed. It is typically used at concentrations of 0.5 to 2%. Agarose gels are non-toxic and easy to prepare by mixing agarose powder with buffer solution, melt it by heating, and pour the gel. The gel is immersed within an electrophoresis buffer that provides ions to carry a current and some type of buffer to maintain the pH at a relatively constant value. When the electric field is applied, molecules migrate toward either the positive or negative pole according to their charge. Identically, charged molecules are separated based on their size. Smaller molecules move more easily through the gel pores than larger molecules.

Although GE is seldom applied for small-molecules, an online coupling of GE and ICP-MS was developed for the separation and detection of low-molecular weight iodine species. The experimental setup of coupling is described in detail and is applied in combination with species-specific isotope dilution analysis to analyze iodide and iodate in aerosol samples.

2.5.1 Experimentation

1) Reagents

Gel for GE separation was prepared by dissolving SeaKam LE and MetaPhor agarose (both Cambrex, Rockland, MA, USA) in electrode buffer of 0.05 mol L^{-1} boric acid eluent and then loaded into a glass column. The prepared column was subsequently placed in oven at 80℃ to remove bubbles which block the electron transfer during the measurement.

Electrode buffer and elution buffer were both 0.05 mol L^{-1} boric acid (Suprapur®, Merck, Darmstadt, Germany) at a pH value of 8.0, by adding sodium hydroxide solution (30 %, Suprapur®, Merck). The elution buffer contained an internal standard of 10 µgL^{-1} Te (Tellurium ICP-Standard, 1000 µgmL^{-1}, Merck, Darmstadt, Germany).

Iodine standard: Potassium iodide and potassium iodate standards (both Fluka, Deisenhofen, Germany) were dissolved in Milli-Q water to prepare the different concentrations of standard. ^{129}I enriched iodide and iodate standards (^{129}I ~86 %) (NEN Chemicals, Boston, MA, USA) were used for species-specific isotope dilution. In order to prevent an isotope exchange between I^- and IO_3^- the solutions were kept at pH > 6 during storage and analysis. (**Safety note:** As ^{129}I is a long-lived radioactive isotope solutions containing enriched iodine were used in concentrations lower than 100 µgL^{-1}, which refers to an activity lower than 0.66 Bq·g^{-1}).

Gas: argon for the ICP and helium for eluent solution degassing were both in the purity

of 99.996 Vol-% (both Westfalen AG, Münster, Germany).

All solutions were prepared using Milli-Q ultra pure water.

2) Instrumentation

ICP-MS system

HP4500 quadrupole ICP-MS (Agilent, Waldbronn, Germany) was equipped with a µ-flow nebulizer and a cooled double pass spray chamber (both AHF, Feuerbacher, Tübingen, Germany). The ICP-MS parameters were daily optimized for optimal detection by continuous injection of 10 $\mu g L^{-1}$ IO_3^- and Te in 50 $mmol \cdot L^{-1}$ borate buffer (pH = 8.0). Details of the operating conditions used throughout this work are given in Table 2-5.

Species-specific isotope dilution was used for quantification. Isotope ^{126}I, ^{127}I, ^{129}I, and ^{131}Xe were monitored during the measurement. $^{127}I^-$ and $^{127}IO_3^-$ were both quantified by measuring the ratio of $^{127}I/^{129}I$. For the principle and the calculation of measured ^{127}I mass, refer to section 2.3.2.

Table 2- 5 Instrumental parameters for the ICP-MS system.

System	HP4500	
Plasma	RF power	1250 W
	Cool Gas Flow	20 L min^{-1}
	Auxiliary Gas Flow	1.0 L min^{-1}
Sample Introduction	Nebulizer Gas Flow	1.0 L min^{-1}
	Nebulizer	Micro-flow (Quartz)
	Spray Chamber	Cooled Double-pass Spray Chamber
	Sampler cone	Ni, 1.0 mm orifice
	Skimmer cone	Ni, 0.7 mm orifice
Acquisition	Mode	Time resolve
	Measuring time	1000 s
	Isotopes monitored	^{126}Te, ^{127}I, ^{129}I, ^{131}Xe

GE system

GE system (Mini Prep Cell with high-voltage supply PowerPac 3000, Bio-Rad Laboratories, Munich, Germany) was coupled to the ICP-MS for iodine speciation. The

setup of GE and ICP-MS coupling and the gel elution region are shown in the Figure 2-17. The separated compounds eluting from the gel are directly released into the elution buffer within the elution frit. This buffer is continuously pumped (100 µL·min^{-1}) through an outlet (1.5 mm diameter) in the dialysis membrane into a tube, which is directly connected to the membrane. The membrane has a molecular weight cut-off of 3.5 kDa and ensures the electrical connection to the lower electrode buffer. The dialysis membrane is fixed by a support frit for practical reasons (Bruchert et al., 2007).

Table 2- 6 Optimized operating parameters of the GE system.

Parameter	
Voltage	250 – 300 V
Electrode buffers	0.05 mol·L^{-1} boric acid, pH = 8.0
Eluent	0.05 mol·L^{-1} boric acid, pH = 8.0, 10 µg L^{-1} Te
Injection volume	10 µL
Gel length	5 cm
Gel i.d.	2.2 mm
Gel materials	Agarose

The injection volume was 10 µL with normal pipette (Eppendorf AG, Hamburg, Germany). Prior to analysis all analyzed solutions were diluted with ^{129}I enriched iodide and iodate mixed solution and glycerol (85 % (w/w) aqueous solution, Acros, Geel, Belgium).

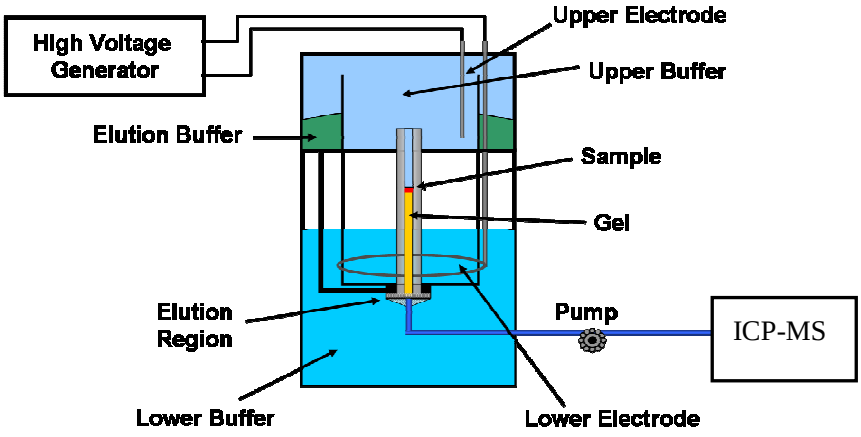

a

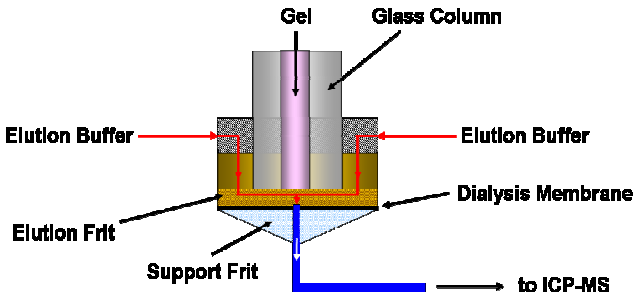

b

Figure 2- 17 Experimental set-up: (a)GE-ICP-MS coupling; (b) Gel elution region.

2.5.2 Results and Discussion

Operating parameters, such as gel concentration and length, voltage, etc. were systematically investigated for the optimization of iodide and iodate separation. The optimized conditions are summarized in Table 2-6. Under these conditions the precision of migration times was lower than 2 % (N = 5) for both species in the same separation gel. The gel made at different time could lead to the retention time differing lightly. The shorter gel lengths could also reduce the total analysis time without reduction of the electrophoretic resolution. However, stronger matrix effects on the electrophoretic behavior of iodide resulted in an unsatisfying separation, which made the use of longer gels necessary (Bruchert et al., 2007).

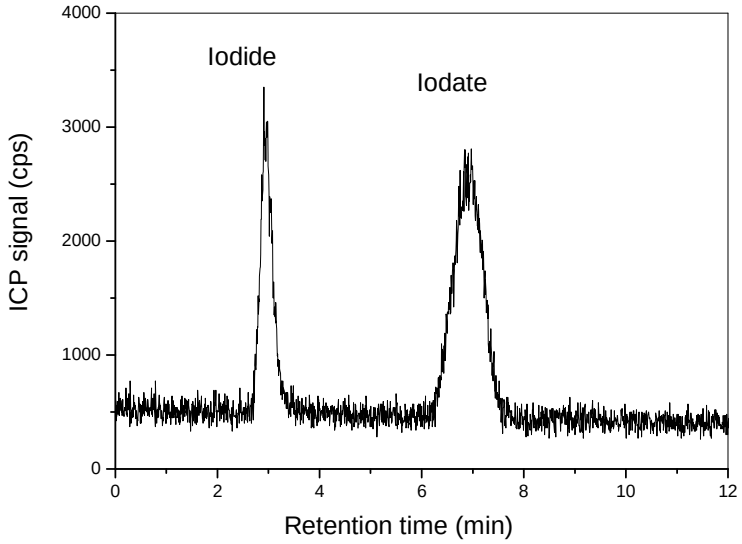

Figure 2- 18 Eletropherogram of 10 µg L^{-1} iodide and iodate standard

The LODs were both 0.5 μg L^{-1} for iodide and iodate in this system. Replicated injections (n = 7) showed a precision below 5% at 10 μg L^{-1} level for both species. The recoveries were both 100 ± 5%. As is shown in the Eletropherogram of iodide and iodate mixed standards (Figure 2-18), iodide and iodate were successfully separated.

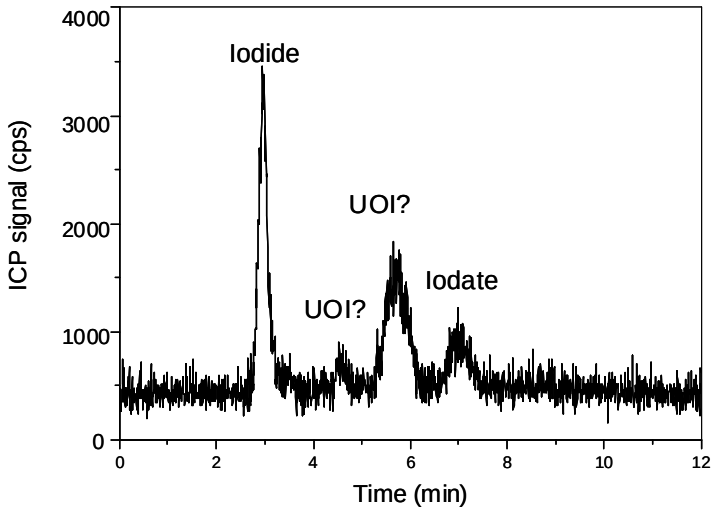

Figure 2- 19 Unknown peaks shown in the aerosol sample collected by Berner impactor cascade sampler from Mace Head, Ireland.

The method was also applied to the water soluble iodine speciation in marine aerosol samples. The data are presented and discussed in chapter 3. During the measurement, unknown peaks (UOIs) were observed in the eletropherograms. Normally two unknown peaks were found in addition to iodide and iodate peaks in the real samples (Figure 2-19). The two peaks are still unidentified as the gel was not stable and it needs to be re-prepared after days of using. With the slight difference of preparation every time, it seems hard to obtain the unknown peaks from the real samples. Therefore, more investigations are worth performing on the unknown iodine species in marine aerosol samples.

2.5.3 Summary

An online GE-ICP-MS technique was developed for iodide and iodate measurement in marine aerosols in the μg L^{-1} range. ^{129}I enriched iodide and iodate standards were used for the quantification of species-specific isotope dilution. The method applied in real aerosol sample measurements was found to be sensitive and reliable. Unidentified peaks were also observed with this method in marine aerosol samples from Mace Head, Ireland. The method also demonstrated that GE has a good potential for low-molecular ion separation. With coupling to ICP-MS, it could become a promising technique for element speciation.

3. Field Measurement during MAP Campaigns

Iodine chemistry has attracted attention recently due to its role in the new particle formation in the MBL (O'Dowd et al., 2002b). Volatile iodine species such as I_2 and iodocarbons are emitted from marine macroalgae. After a series of atmospheric reactions under UV radiation, iodine species are taken up into aerosols in the marine atmosphere. If this phenomenon occurs on a large scale, it could have significant effects on climate(Kolb, 2002). The finding has encouraged the research on iodine chemistry at Mace Head, Ireland, a hotspot for the study on new particle formation from natural sources. Here the sampling campaigns in EU-project "MAP" (Marine Aerosol Production from Natural Sources) are introduced. The results of iodine speciation in marine aerosols from the ship cruise over the North Atlantic Ocean and at Mace Head are shown and the characterizations of iodine species are discussed.

MAP is a European Union integrated project involving 16 different institutions. One of the key objectives is to focus on new aerosol formation mechanisms, including the iodine-related nucleation in the MBL. The investigation of various iodine species in the gas phase and particle phase as well as the relationship between iodine and marine organisms such as macro and micro algae are the vital parts of the project. The parallel campaigns were conducted at Mace Head Atmospheric Research Station (MHARS), Ireland and on the *Celtic Explorer* scientific vessel over the North Atlantic Ocean in the summer of 2006. Different sized aerosols such as $PM_{2.5}$, PM_{10}, and size fractionated aerosols (5 stages, smaller than 10 μm) were collected for iodine speciation. The characteristics of different iodine species were studied in both campaigns to enlarge the database of iodine investigation in the MBL.

3.1 Methodology

3.1.1 Sampling

1) Mace Head Campaign (MHC)

MHARS is located on the west coast of Ireland at 53.3° N, 9.9° W (see Figure 3-1). The atmosphere there is not strongly polluted as the dominant wind direction is from the west, with a long fetch over the North Atlantic Ocean (Huang et al., 2001). Aerosols collected at MHARS are regarded as the background natural aerosols mainly influenced by the marine environment.

The MHC was conducted from June 13 – July 5, 2006. The sampling point was set about 100 m from the tidal zone where there are high densities of macroalgae. A

virtual impactor $PM_{2.5}$ sampler, hi-vol PM_{10} sampler, and Berner impactor cascade sampler (5 stages with fractionated size ranges: 0.085 – 0.25 μm, 0.25 – 0.71 μm, 0.71 – 2.0 μm, 2.0 – 5.9 μm, 5.9 – 10 μm) were all applied during this intensive sampling campaign. The working flow rates were 1.5 m^3 h^{-1} and 4.5 m^3 h^{-1}, for virtual impactor and Berner impactor, respectively. No sampling air interference happened between them due to the relatively low sampling flow. Therefore, the virtual impactor and Berner impactor were fixed on a supporting bracket with a self-conducted water-proof roof. The pumps were housed inside the station. The PM_{10} sampler was placed about 100 m away from the other samplers due to its relatively high flow of 68 m^3 h^{-1}. Cellulose nitrate filters were used for the virtual impactor and Berner impactor while the PM_{10} sampler was equipped with quartz filters. For the specifications of selected filters please see section 2.1.2. During the sampling period, PM_{10} sampler had fatal pump failure causing only limited samples collection. Therefore, PM_{10} samples are mainly used for the comparison of SOI measurement especially for verifying the existence of UOIs.

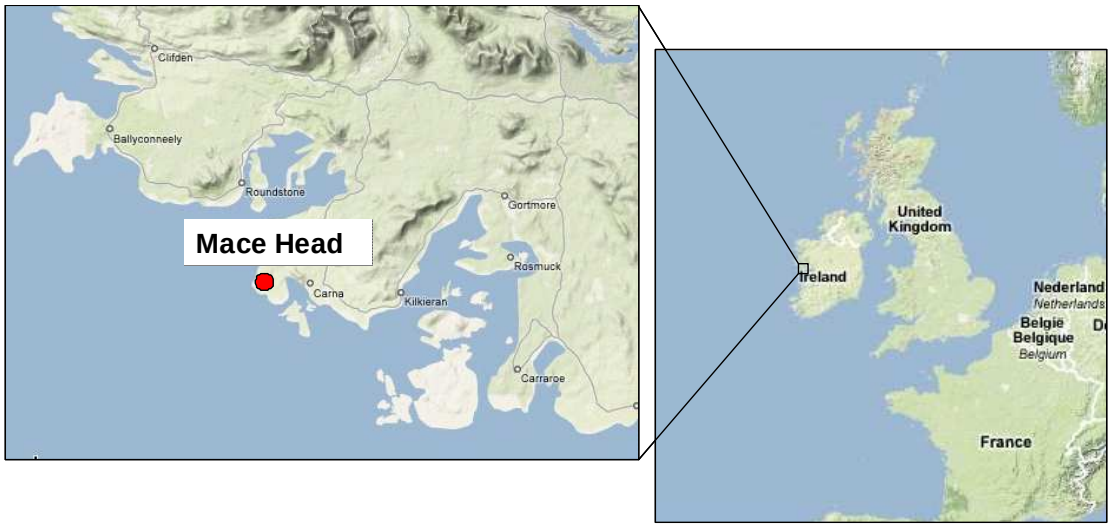

Figure 3- 1 Location of Mace Head Atmospheric Research Station, Galway, Ireland.

During the sampling, morning (8:00 – 14:00), afternoon (14:00 – 18:00), and night (18:00 – 8:00) $PM_{2.5}$ samples were collected on every sampling day to investigate the diurnal variation. For PM_{10} and fractionated size aerosol sampling, day (8:00 – 18:00) and night (18:00 – 8:00, +1 day) samples were taken daily.

After sampling, $PM_{2.5}$ and size fractionated samples were stored in 50 mL Poly-propylene vials (GREINER BIO ONE, Frickenhausen, Germany). PM_{10} filters were folded then covered with aluminum foil and stored in separate sealed plastic bags. All of the samples were stored in a freezer at less than 20℃ to prevent any unexpected loss of volatile compounds.

Rain samples were collected at two locations during the period of MHC: firstly from the MHARS and secondly from a small cottage about 200 m inland from the MHARS. The samples were collected directly with a polypropylene funnel (pre-cleaned with

Milli-Q water) draining into the sample bottles.

2) Celtic Explorer Campaign (CEC)

To investigate the iodine species in marine aerosols in open ocean area, the CEC was conducted during June to July 2006. There were two legs of the campaign: one from June 12 to June 22 and the other from June 25 to July 5. During the campaign, the activities of plankton were monitored by the fluorometer.

For aerosol collection, one virtual impactor $PM_{2.5}$ sampler was placed on the deck of the vessel to sample $PM_{2.5}$ particles. The $PM_{2.5}$ sampler was the same as that used at MHARS, operating with a flow rate of 1.5 m^3 h^{-1}. Cellulose nitrate filters were also used. During the campaign, day (8:00 – 18:00) and night (18:00 – 8:00) samples were taken on every sampling day. The samples were stored in a freezer at less than 20℃.

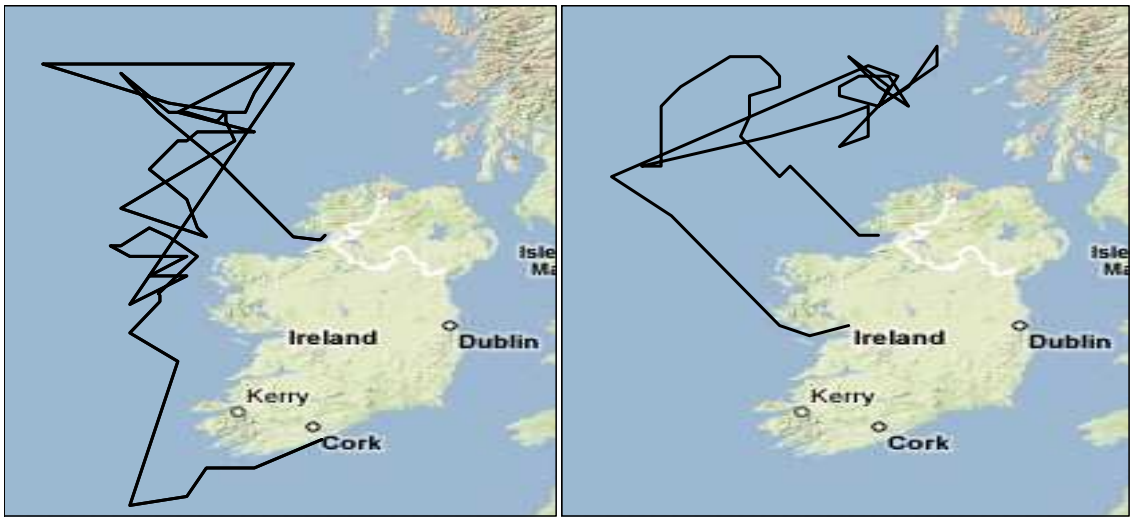

a b

Figure 3- 2 Sketch map of the path of Celtic Explore over the North Atlantic Ocean (a) the first leg, June 12 – 21, 2006; (b) the second leg, June 25 – July 5, 2006

3.1.1 Chemical Analysis

The chemical analysis consisted of the measurements of total water soluble iodine (TSI), total insoluble iodine (TII), and the speciation of water soluble iodine in aerosol samples. TSI and water soluble iodine speciation were made in the rain samples. The pretreatments and analytical methods are all thoroughly introduced and discussed above (see Chapter 2).

The aerosol samples were firstly extracted with an ultrasonic assisted water extraction process. The TSI was measured either by the HP4500 quadrupole ICP-MS (Agilent, Waldbronn, Germany) or by the Elan 6100 ICP-MS (Perkin Elmer, Waltham, USA).

The water soluble iodine species were measured either by IC-ICP-MS system 1 equipped with G3268A IC column (Agilent, Waldbronn, Germany) or by the IC-ICP-MS system 2 with AS 16 IC column (Dionex, Überlingen, Germany). A detailed description of these two analytical systems are presented in section 2.4. The TII was pretreated with an TMAH extraction at 90℃ for 3 hours and then measured with the HP4500 quadrupole ICP-MS.

Rain samples were measured by Elan 6100 ICP-MS to obtain TSI amount and by IC-IC-MS system 2 for water soluble iodine speciation.

Iodide and iodate could be successfully separated and measured with the two IC-ICP-MS system. The soluble organic iodine (SOI) was calculated as the difference of TSI and the inorganic iodine species (iodide and iodate). Meanwhile, unknown peaks were found in almost all of the aerosol chromatograms and rain samples. One big unknown peak was detected with G3268A IC column and 4-5 small unknown peaks were found with AS 16 IC column. Different commercial iodo-compounds were used to check the unknown peaks. Only the first unknown peak eluting out of the AS 16 column was found to have similar retention time of iodo-acetate. Other unknown peaks in both columns remain unidentified so far. They are named as unidentified organic iodine compounds (UOIs). The UOI concentrations were quantified by using the iodide calibration curve because iodine atom is converted to I^+ in the plasma prior to quantification with mass spectrometer. Nevertheless, a large of TSI was not eluted from the both IC columns and this part remains unknown until now.

3.1.3 Additional Information

Meteorological data have been simultaneously obtained from both campaigns including temperature, pressure, wind strength, wind direction etc. Tidal Height data were obtained from website of Easy Tide (http://easytide.ukho.gov.uk). The fluorescence data were collected to show the activities of phytoplankton along the path of CEC. Airmass back trajectory were calculated using HYSPLIT model (FNL data set) from NOAA Air Resources Laboratory.

3.2 Results and Discussion

3.2.1 $PM_{2.5}$ during the MHC and CEC

There were two virtual impactor $PM_{2.5}$ samplers placed parallel in the MHC and CEC. The results of the different iodine species in $PM_{2.5}$ from both campaigns were listed in the table 3-1 and 3-2.

Table 3- 1 Concentrations of iodine species in $PM_{2.5}$ marine aerosols during the MHC (n = 57)

Iodine species	Range (pmol/m^3)	Median (pmol/m^3)	Average (pmol/m^3)
Total soluble iodine (TSI)	47.25 – 1533.00	240.87	335.69 ± 279.27[a]
Total insoluble iodine (TII)	3.39 –573.74	105.37	140.70 ±117.96
Soluble organic Iodine (SOI)	26.33 – 1262.72	213.77	297.36 ± 234.32
Iodide	1.55 – 323.03	11.44	32.89 ± 62.61
Iodate	0.22 – 45.83	2.28	5.44 ± 8.16

a. standard deviation

All iodine species were found to be considerably variable in $PM_{2.5}$ during both campaigns. The TSI concentration was higher than TII in $PM_{2.5}$ during the MHC. It ranged from 47.25 to 1533.00 pmol m^{-3} with a median of 240.87 pmol m^{-3}, higher than TII ranging from 3.39 to 573.74 pmol m^{-3} with a median of 105.37 pmol m^{-3}. However, TSI in $PM_{2.5}$ from the CEC was much lower than that at Mace Head ranging from 16.71 to 561.01 pmol m^{-3} with a median of 119.10 pmol m^{-3}. The TII level was similar to those observed during the MHC with a median of 97.88 pmol m^{-3}. Comparable levels of TSI and TII were found in the samples from CEC. It suggested that the sources of insoluble iodine may widely spread and contribute more to the samples from the open ocean.

Table 3- 2 Concentrations of iodine species in $PM_{2.5}$ marine aerosols during the CEC (n = 32)

Iodine species	Range (pmol/m^3)	Median (pmol/m^3)	Average (pmol/m^3)
Total soluble iodine (TSI)	16.71 – 561.01	119.10	160.83 ± 147.82[a]
Total insoluble iodine (TII)	18.54 – 592.96	97.88	135.94 ± 152.47
Soluble organic Iodine (SOI)	9.04 – 509.88	113.93	151.46 ± 142.49
Iodide	N.D.[b] – 49.55	2.87	5.93 ± 9.67
Iodate	N.D. – 29.88	1.21	3.44 ± 6.46

a. standard deviation; b. not detectable

The $PM_{2.5}$ samples were taken during the morning, afternoon and night at Mace Head.

In the most cases, TSI in the morning and the afternoon samples (medians, 337.37 pmol m^{-3} and 302.31 pmol m^{-3}, respectively) were both higher than observed in the night samples (median, 148.67 pmol m^{-3}). The temporal variation of TSI in $PM_{2.5}$ during the MHC was displayed in the Figure 3-3.

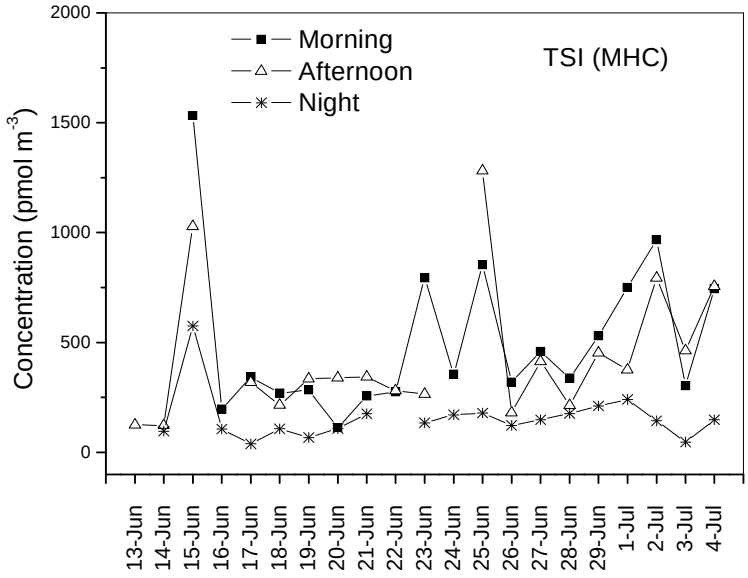

Figure 3- 3 Temporal variations of the TSI during the MHC sampling period.

There were three peak values of TSI found during the sampling period, which were on June 15, June 23 and July 2. The CPC (Condensation Particle Counter) data (including D > 3 nm, D > 5 nm, and D > 10 nm) during this time period are shown in Figure 3-4. The relations can be found between the CPC data and the levels of TSI in $PM_{2.5}$. Nucleation can be seen from the CPC data on the days with higher TSI concentrations, indicating the relationship between the particle phase iodine and the new particle formation. However, the nucleation seems quite weak on June 15 and July 1, and is probably insufficient to clarify the reason for the high TSI on June 15.

Meteorological data including temperature, wind direction and speed, tidal height, rain fall and so on were collected and analyzed to determine their influence on the iodine species variations. The three enhanced concentrations periods are found all located during or near the periods of low tidal height. During the sampling period, there were two low tidal height periods which were from June 13 to June 17 and from June 23 to July 1 (see Figure 3-5). Low tide is considered as positive factor for the release of volatile organic iodine (VOI) such as I_2 and iodinate hydrocarbon from the macroalgae in the coastal area due to the exposure of macro algae during low tide periods (O'Dowd et al., 2002b; Chen, 2005). Nevertheless, the correlation between the TSI and the tidal height is not strictly correlated.

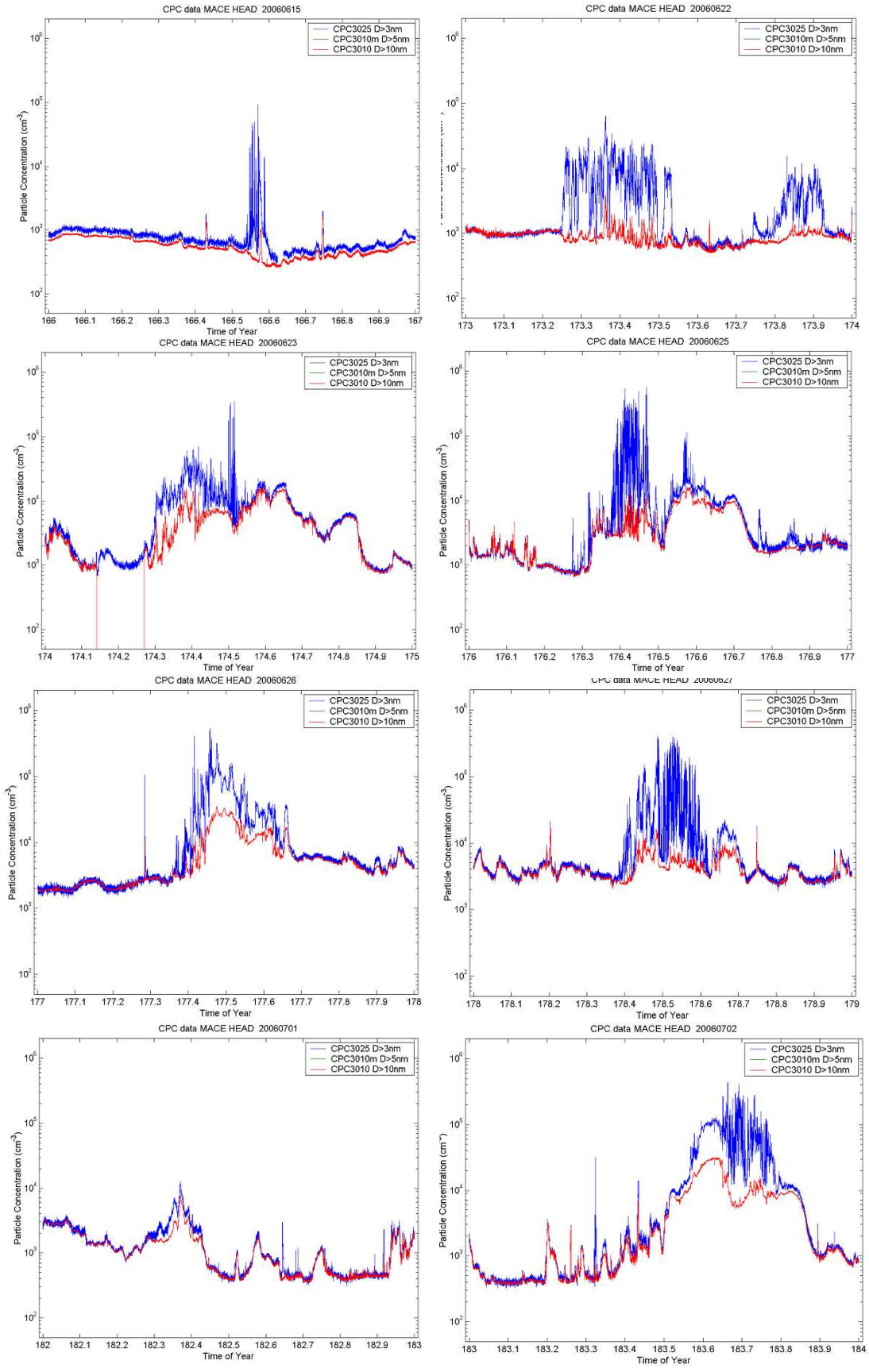

Figure 3- 4 CPC data in several selected days in the MHC

Rainfall was found to be another important factor affecting the variation of TSI. Heavy raining took place during June 17 – 20, June 25 – 26 and June 29. Low TSI concentrations were observed on these days. Obviously, wet deposition played an important role on the TSI variation. It also explains why the highest TSI concentrations were not observed on the days with lowest tide. Interestingly, the TSI concentrations on June 15 especially in the morning and the afternoon are extremely high, suggesting something unknown should happen on that day contributing to the high iodine loading. This peak also observed in the size fractionated samples which are discussed as follows.

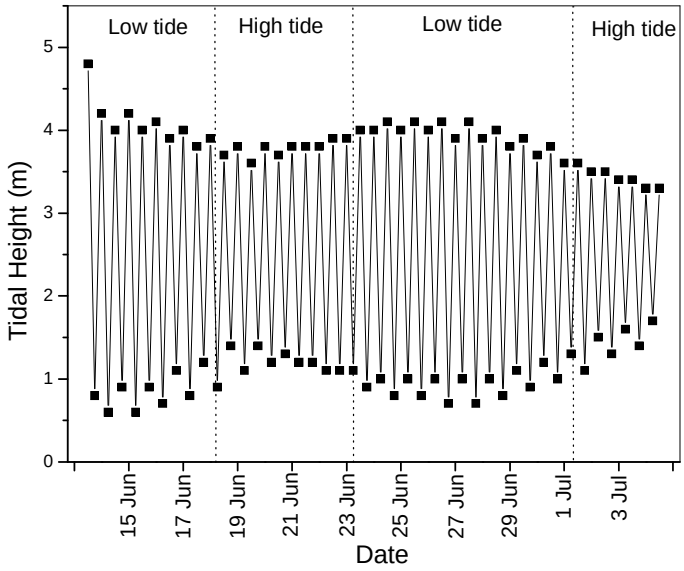

Figure 3- 5 Variation of tidal height during the MHC sampling period (June 13, 2006 – July 4, 2006)

As is shown in Figure 3-6, the TSI concentration during the CHC was variable. The ranges during leg 1 and leg 2 were comparable. Night samples contained higher TSI concentrations than the day samples. Because the vessel encountered a heavy, the sampling was halted after June 19, leading to less samples being collected on the first leg of CEC. The TSI concentrations were still enhanced collected on June 13 and June 15, which is difficult to interpret as variable weather conditions occurred during these days. However, the influence of rain on TSI was again found. For example, after a heavy shower on June 17 and continuously light raining on the following days, it led to low levels of TSI being observed. During the second leg of CEC, a clearer trend could be found in the TSI. The enhanced TSI levels are found to be related to the activity of the marine phytoplankton which was onboard monitored by a fluorometer. The peak values measured on June 29 and July 2 match highly active phytoplankton activities, whereas low values of TSI on June 27, June 30 and July 3 also correlate with the low phytoplankton activity period. Although the mechanisms are still not clear, the relationship between TSI and the phytoplankton activity hint at a very important

possible source of the oceanic iodine emissions.

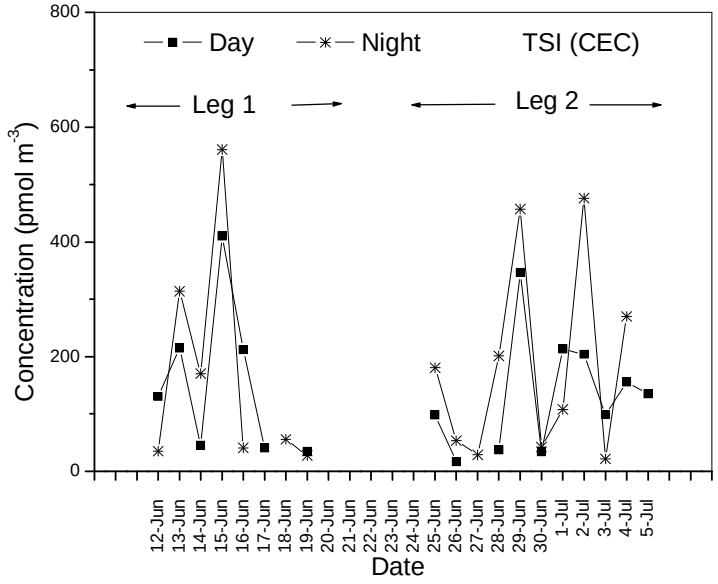

Figure 3- 6 Temporal variation of TSI in $PM_{2.5}$ in the CEC

The morning and afternoon TII concentrations during the MHC were also higher than nighttime samples, which is similar to the trend of TSI. Median morning, afternoon and night concentrations were 141.17 pmol m^{-3}, 109.77 pmol m^{-3}, and 60.50 pmol m^{-3}, respectively. The TII variation during the MHC was inconsistent to the TSI variation, indicating the controlling factors may be different from those for TSI. No evident correlation was observed between TII and the meteorological data during the MHC. During the CEC, the diurnal variation of TII were different with higher nighttime TII levels (median, 99.46 pmol m^{-3}) than daytime TII levels (median, 59.20 pmol m^{-3}). Also, no clear trend or correlation could be found in the TII variation during the CEC. TII has been seldom investigated in the previous research and the formation mechanism of insoluble iodine in the MBL is still an open question. More effort should be put into TII characterization as well as its formation mechanisms to clarify its contribution to the iodine chemistry in the MBL.

During both campaigns, inorganic iodine, namely iodide and iodate, were less abundant. Iodide and iodate ranged from 1.55 – 323.03 pmol m^{-3} and 0.22 – 45.83 pmol m^{-3}, respectively, accounting for 0.9 – 30.9% with a median of 5.8% for iodide and 0.1 – 20.2% for iodate with a median of 0.9% in TSI in $PM_{2.5}$ from the MHC. Even lower levels of iodide and iodate were observed during the CEC. Indeed iodide and iodate were not detectable (N.D.) in some of the samples from the CEC. Iodide was in the range of N.D.– 49.55 pmol m^{-3} while iodate ranged from N.D. to 29.88 pmol m^{-3}. They accounted for 0 – 57.5% with a median of 1.9% for iodide and 0 – 23.4 with a median of 1.0% for iodate. The low enrichment of inorganic iodine in marine aerosols was in

accord with the previous studies (Baker et al., 2000; Baker et al., 2001; Baker, 2004, , 2005).

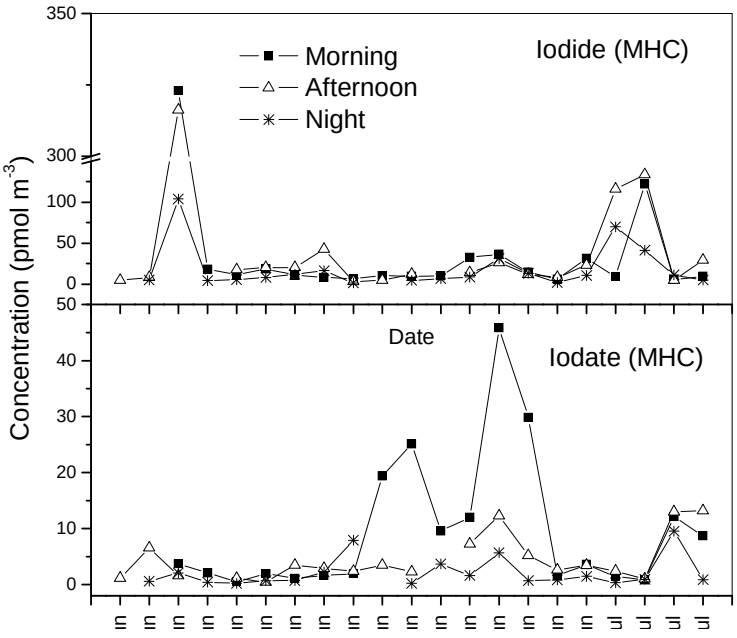

Figure 3- 7 Temporal variations of iodide and iodate in $PM_{2.5}$ during the MHC.

The temporal variations of iodide and iodate during the MHC are shown in Figure 3-6. The variation of iodide is similar to that of TSI, indicating the release mechanisms may be coupled. Again the tidal height and the rainfall at the site might influence on the variation. Iodate showed an increase between June 22 – 27 and also during July 3 – 4 especially for the morning samples (8.71 – 29.88 pmol m^{-3}). The back trajectories arrived at Mace Head during June 24 – 27 and July 3 – 4 show the airmass passed through the terrestrial area instead of ocean in most cases. The influence of terrestrial sources may be potentially favorable for the formation of iodate. Figure 3-8 shows a statistic box chart showing the iodate/iodide ratio in $PM_{2.5}$ during the MHC and CEC. Only with a few exceptions (most of them were in the morning), the iodate/iodide ratios were lower than 1 with medians of 0.25, 0.24, and 0.12, for the morning, afternoon, and night samples, respectively. Day samples obviously had more iodate while more variable ratios were found in the morning. Variable iodate/iodide ratios were also observed in the day and night samples during the CEC. The medians of day and night iodate/iodide ratios were 0.33 and 0.32, respectively. Iodide in both campaigns was shown to be the more dominant inorganic iodine species in $PM_{2.5}$. This phenomenon has been frequently reported in aerosol samples in the MBL (Baker et al., 2001; Baker, 2004, , 2005; Chen, 2005; Gilfedder et al., 2008). It raises a serious question about the current understanding of iodine chemistry in the atmosphere. According to the modeling simulations, iodate is more dominant iodine species because it is more stable and can accumulate when aerosol ages (McFiggans et al., 2000; von Glasow et al., 2002; O'Dowd and Hoffmann, 2005). To date the gap between theoretical simulation and the

filed observation is not clear yet though more efforts were put in to fill in it(Pechtl et al., 2007; Gilfedder et al., 2008).

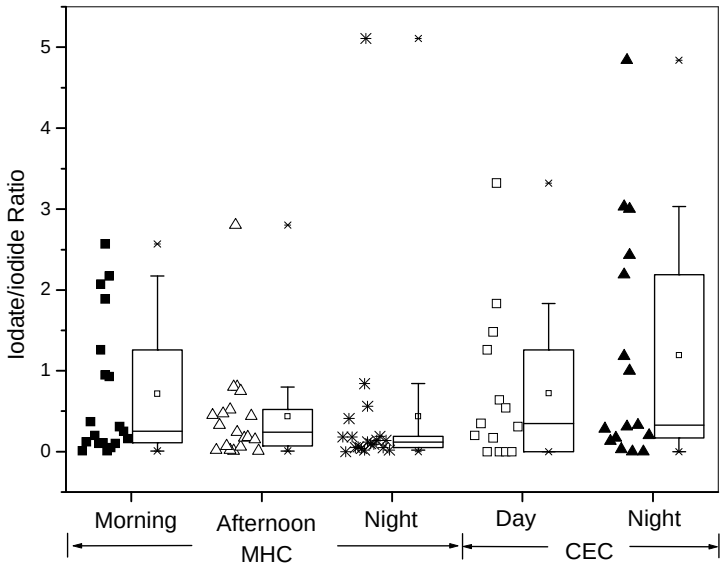

Figure 3- 8 Iodate/iodide ratios in $PM_{2.5}$ in the MHC and CEC.

SOI, which is termed as the difference of TSI and inorganic iodine (iodide and iodate), was the most abundant iodine fraction in the data. The percentages of SOI in TSI from Mace Head were 55.7 – 98.6% (median, 93.0%) and 33.0 – 100.0% (median, 95.9%) during the CEC, respectively. The high percentage of SOI in TSI in both campaigns suggests a large role for organic iodine in the aerosol uptake mechanisms of iodine compounds in the MBL, which was also emphasized by previous research (Baker, 2005). The SOI percentage in TSI was considerably higher than other campaigns in the Atlantic Ocean (Baker, 2005). However, the investigation and estimation of organic iodine were made not only in the aerosol samples but also in the hydrosphere and precipitation such as rain and snow (Wong and Cheng, 2001; Gilfedder et al., 2007b; Gilfedder et al., 2008). The ubiquitous existence of organically bound iodine in the different iodine sinks shows its important contribution to iodine chemistry. However, not many studies have determined the organic iodine species as well as their formation, pathway and fate in the MBL. There is a growing realization that participation of organic matter in the iodine chemistry is of importance for improving the current understanding to a large extent (Baker, 2005; Pechtl et al., 2007; Gilfedder et al., 2008).

Correlations between SOI and iodide were observed in $PM_{2.5}$ during the MHC (see Figure 3-9). The regression coefficients (R^2) were all higher than 0.5 ($P < 0.0001$) in the morning, afternoon, and night datasets, suggesting that iodide formation is related to the organic iodine decomposition (Baker, 2005; Gilfedder et al., 2008). Iodinated marine gels or colloids can be ejected into the atmosphere by bubble busting processes

from the ocean surface (Leck and Bigg, 2005; Bigg, 2007; Leck and Bigg, 2008) Under sunlight exposure, they may be photolysed to form smaller iodinated compounds and iodide. This is further suggested by the number of observations of iodide enrichment being significantly higher during the day compared to the night. It is shown here that lower slope of regression was found in the afternoon dataset due to the stronger solar radiation.

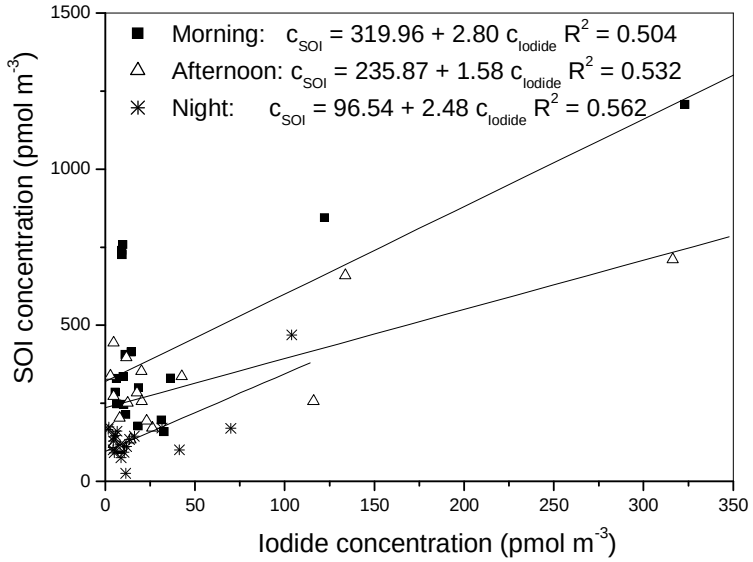

Figure 3- 9 Correlation between SOI and iodide in $PM_{2.5}$ during the MHC

During the CEC, an R^2 of 0.568 was found between SOI and iodide during the first leg (0.718 and 0.545 for the day and night dataset, respectively), while no correlation was shown during the second leg data. The difference between the two cruise legs shows the complexity of the relationship between organic iodine formation and iodide, especially over the open ocean area.

As is mentioned at Section 2.4, IC-ICP-MS was used for iodine speciation in the soluble iodine fraction in $PM_{2.5}$. Two IC columns, G3268A and AS16, were chosen for the separation of iodide and iodate. Several organic iodine peaks (UOIs) were also found in the chromatograms (see Figure 2-15 and Figure 2-16). One UOI was eluted between iodide and iodate peaks with G3268A IC column and it was termed as UOI-0. Five UOIs were separated by AS16 and are named as UOI-1, UOI-2, UOI-3, UOI-4, and UOI-5. Meanwhile, PM_{10} samples collected on quartz filter were also extracted with water and measured with both IC columns. The same species (iodide, iodate, and UOIs) were detected using both columns. Quartz filters are regarded as the ideal sampling medium for organic aerosols due to its low trace contamination levels as well as to its relative inertness and ability to be baked at high temperature to remove trace organic contaminants. The sample detection found between cellulose nitrate filter and

quartz filter showed the UOI peaks were real instead of a filter artifact.

Table 3- 3 Unidentified organic iodine (UOI) in $PM_{2.5}$ during the MHC by IC-ICP-MS

Column	UOI	Range (pmol/m^3)	Median (pmol/m^3)	Average (pmol/m^3)
MHC				
G3268A [a]	UOI-0	1.54 – 814.47	89.08	168.68 ± 215.48 [b]
AS16 [c]	UOI-1	N.D.[d] – 3.71	0.85	1.06 ± 0.91
	UOI-2	N.D. – 1.40	0.47	0.61 ± 0.37
	UOI-3	N.D. – 1.31	0.61	0.65 ± 0.29
	UOI-4	1.28 – 15.93	6.78	6.28 ± 3.60
	UOI-5	N.D. – 1.66	0.92	0.97 ± 0.39
CEC				
G3268A	UOI-0	4.12. – 256.61	28.33	60.53 ± 61.19

a. samples on June 13 – 16, June 21 – 24, 27 – 28, July 1 – 4; b. standard deviation;

c. samples on June 17 – 20, 25 – 26, 29; d. not detectable.

The UOI concentrations are listed in Table 3-3. The results from the two columns were not comparable due to not only the number of peaks but also the level of UOIs. UOI-0 eluted by G3268A column was normally at a much higher concentration than any of the five UOIs found by AS16 column, accounting for 21.1% of TSI. ICP-MS was shown to be a sensitive detection method for organic iodine detection. However, the high temperature (> 6000K) of ICP makes the fragments unsuitable for structural identification. After the successful separation of iodine species, an electrospray ionization ion trap mass spectrometry (ESI-ITMS, Daltonics HCT-Plus, Bruker, Bremen, Germany) was coupled to the IC column trying to get the structural information of the UOI-0. However, no fragments were found in the mass spectra, indicating that the ESI is not an appropriate source for the ionization of UOI-0, or UOI-0 is a mixture of a molecular clusters of organically bound iodine which were individually not enriched enough for MS detection because of its lower sensitive detection than ICP-MS. With the separation using AS16, UOI-4 was the more abundant than other four UOIs with an median of 6.78 pmol m^{-3}. Different kinds of commercial soluble organic iodine standards were injected in an attempt to identify these compounds. The retention time of iodoacetic acid standard was similar to that of UOI-1 but no further proof was found to confirm this. Therefore, all of these peaks remain unidentified. Although UOIs were eluted in both columns, on average, 29.8 ± 31.8% and 84.9 ± 7.4% of TSI in $PM_{2.5}$ during the MHC were not eluted out with G3268A and AS16, respectively.

The successful application of IC-ICP-MS to soluble organic iodine speciation gives definitive proof of the existence of SOI, rather than only based on mass balance calculation. The unidentified peaks are most likely anionic organic iodine species, as they are efficiently separated by anion exchange resin which was initially developed for polarizable anion separation. Nevertheless, it is difficult to gain a better understanding of SOI in aerosols without obtaining any structural information. This should provide a clearer direction and motivation for further research of SOI.

3.2.2 Size fractionated aerosols during the MHC

Iodine concentration and speciation in the different stages of the Berner impactor size fractionated samples are presented in the Table 3-4.

Table 3- 4 Concentrations of iodine species in size fractionated samples during the MHC

Iodine species	Range ($pmol/m^3$)	Median ($pmol/m^3$)	Average ($pmol/m^3$)
Stage 1 (0.085 – 0.25 μm [a])			
Total soluble iodine (TSI)	5.17 – 271.70	59.30	79.54 ± 63.40 [b]
Total insoluble iodine (TII)	2.80 – 213.15	56.68	71.12 ± 63.94
Soluble organic Iodine (SOI)	5.17 – 248.77	58.14	76.11 ± 61.10
Iodide	N.D. [c] – 26.12	1.30	3.15 ± 4.98
Iodate	N.D. – 7.76	0.31	0.78 ± 1.46
Stage 2 (0.25 – 0.71 μm)			
Total soluble iodine (TSI)	9.07 – 428.40	64.00	81.93 ± 79.20
Total insoluble iodine (TII)	12.57 – 164.04	45.55	58.45 ± 43.49
Soluble organic Iodine (SOI)	8.20 – 377.94	60.90	77.72 ± 73.59
Iodide	N.D. – 46.99	1.89	4.12 ± 7.73
Iodate	N.D. – 3.47	0.32	0.46 ± 0.59
Stage 3 (0.71 – 2.0 μm)			
Total soluble iodine (TSI)	3.13 – 526.73	52.08	74.56 ± 91.65
Total insoluble iodine (TII)	11.39 – 101.12	38.58	56.18 ± 34.02

To be continued

Continued

Soluble organic Iodine (SOI)	1.42 – 504.51	48.91	74.56 ± 91.65
Iodide	N.D. – 55.57	1.69	4.30 ± 9.12
Iodate	N.D. – 2.93	0.31	0.59 ± 0.71
Stage 4 (2.0 – 5.9 μm)			
Total soluble iodine (TSI)	11.51 – 287.63	64.81	77.73 ± 62.88
Total insoluble iodine (TII)	18.79 – 80.36	42.88	46.02 ± 19.73
Soluble organic Iodine (SOI)	6.14 – 272.04	60.34	74.56 ± 91.65
Iodide	N.D. – 11.10	1.94	2.62 ± 2.25
Iodate	N.D. – 2.93	2.01	3.05 ± 2.94
Stage 5 (5.9 – 10.0 μm)			
Total soluble iodine (TSI)	5.10 – 260.54	51.28	71.48 ± 65.15
Total insoluble iodine (TII)	0.99 – 103.62	25.47	42.68 ± 36.77
Soluble organic Iodine (SOI)	3.41 – 242.75	44.64	66.58 ± 63.17
Iodide	N.D. – 19.91	1.92	3.44 ± 4.73
Iodate	N.D. – 15.11	1.10	1.75 ± 2.59

a. cutoff size; b. standard deviation; c. not detectable

The TSI levels (medians) in five stages were in the order of stage 4 ~ stage 2 > stage 1 > stage 3 ~ stage 5, although little difference was shown between them. Stage 1 – 3 collect aerosols sized lower than 2.0 μm, which suggests fine particle mode is important for TSI gathering in marine aerosols. The highest TII concentration (median, 56.68 pmol m^{-3}) was observed in the stage 1 with the smallest particle size range of 0.085 – 0.25 μm, more than two fold of that in the coarsest stage 5 with size range of 5.9 – 10 μm (median, 25.47 pmol m^{-3}). The TII concentration in the stage 1 was comparable to TSI, while lower TII levels were measured in other stages.

Inorganic iodine (iodide and iodate) was only a minor fraction of TSI. The percentages (medians) of inorganic iodine (sum of iodide and iodate) increased as the particle size increases in the order of 2.1%, 4.0%, 5.4%, 7.5%, and 6.7% from stage 1 to 5. In stage 1 – 3, iodide was the dominant inorganic species, with concentrations 4 – 6 times higher than iodate. However, comparable iodide and iodate concentrations were found in stage 4 and 5 with particle size ranges of 2.0 – 5.9 and 5.9 – 10 μm, respectively. This

indicates a higher iodate loading in coarse mode. Highest iodide and iodate were found in stage 4 (2.0 – 5.9 μm) with the medians of 1.94 pmol m^{-3} and 2.01 pmol m^{-3}, respectively. The iodate/iodide ratio was found in the 5 stages in the day and night samples (Figure 3-10). The median ratios during the day were slightly higher than at night especially in stage 4 (median 1.45 during the day and 0.36 at night, respectively). The statistical results show similar variation among the 5 stages during the day and the night samples. The ratios in stage 1 – 3 (fine particle size) were found to be consistent with that observed in $PM_{2.5}$ during the MHC and CEC with values (medians and averages) lower than 1, showing that the iodide was more abundant in the small size particles. However, in stage 4 and 5, more variable ratios were found during both day and night samples. The medians and averages of iodate/iodide ratio in stage 4 were observed to be the highest. Since iodide was extremely variable between the different stages, higher iodate/iodide ratio in coarse size particles implies the iodate formation and uptake happen mainly in coarse size range.

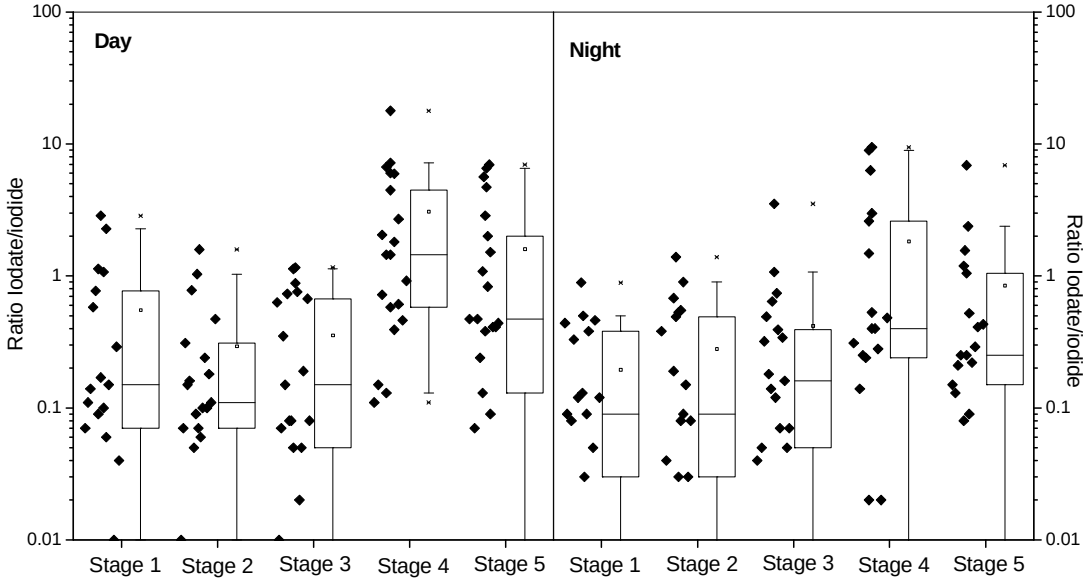

Figure 3- 10 Statistical chart of ratio of iodate/iodide in 5 stages of Berner impactor during day and night samples

SOI was the dominant iodine species of TSI in the size fractionated aerosol samples from Mace Head, ranging from 92.5 – 97.9% over all stages. This is consistent with the results from the $PM_{2.5}$ during the MHC, emphasizing the importance of SOI in particle phase iodine chemistry. The correlation between SOI and iodide was analyzed in day and night dataset as well as in different stages. Significant correlations between SOI and iodide were found in stage 2 and stage 3 while poor correlations were observed in other stages. In stage 2 (0.25 – 0.71μm), a significant diurnal difference was found that the regression coefficient (R^2) was 0.787 ($P < 0.0001$) in day samples but poor correlation ($R^2 = 0.131$) was found in the night samples. Their relation is likely to correspond with the influence of solar radiation. Moreover, when samples from the

sunny days were selected and an even better correlation was observed, with an R^2 of 0.823 ($P < 0.0001$). This verifies that solar radiation is an important factor for the relationship between SOI and iodide. It also strongly supports the hypothesis that iodide can be formed through the decomposition of SOI (Baker, 2005; Gilfedder et al., 2008). In stage 3 (0.71 – 2μm), significant correlations between SOI and iodide were observed both in day and night samples with the correlation coefficients (R^2) of 0.748 ($P < 0.0001$) and 0.703 ($P < 0.0001$), respectively. Obviously, processes operated during the night may affect the correlations in this size range. Nevertheless, samples collected on sunny days still have better correlation between the SOI fraction and iodide (R^2 = 0.820), suggesting solar radiation was an important factor for aerosol iodide estimation.

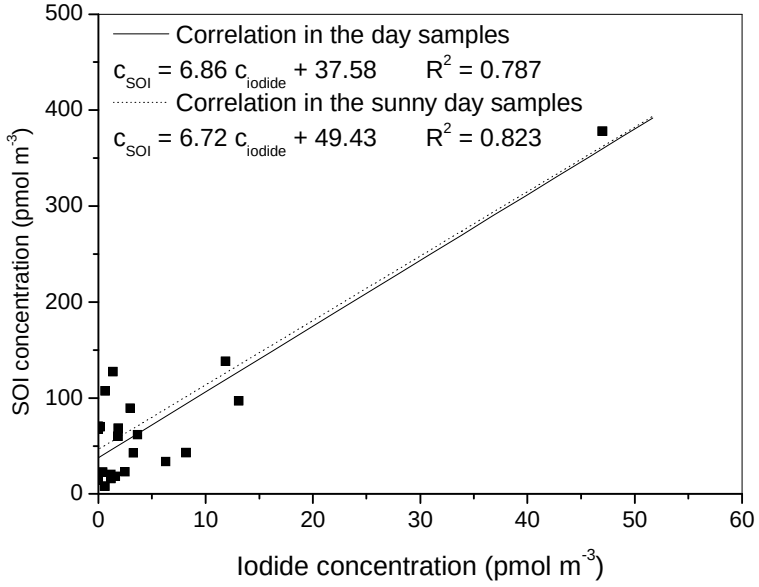

Figure 3- 11 Correlation between SOI and iodide in stage 2 of Berner impactor

The correlation coefficients found in stage 2 (day) and stage 3 (day and night) were higher than those in $PM_{2.5}$ ($R^2 > 0.5$). The stage 1 – 3 refer to the size range of 0.085 – 2.0 μm which is not exactly equal to the size range of $PM_{2.5}$ (< 2.5μm). The poor correlation in the range of 0.085 – 0.25 μm (stage 1) can also deteriorate the correlation.

The soluble iodine were measured by IC-ICP-MS with two IC columns (G3286A and AS16). Again, UOI-0 with large amount was eluted by G3286A and five UOIs (UOI-1 – UOI-5) were separated by AS16. The data of the UOIs are listed in Table 3-5. UOI-0 had the median concentrations of 39.74 – 49.32 pmol m^{-3} in the five stages, accounting for about 60% of TSI. As is discussed above, this large proportion of TSI may be related to a mixture of organic iodine species but more evidence is needed. UOIs measured by AS16 IC column were at much lower concentrations and not every peak was found in each chromatogram. UOI-4 was the most abundant among the UOIs and

was seen in most of the chromatograms. Its concentration ranged from 0.71 to 2.01 pmol m^{-3} (medians), which was similar to iodide and iodate levels. These organic iodine peaks are remain unidentified until now though different commercial standards have been tried.

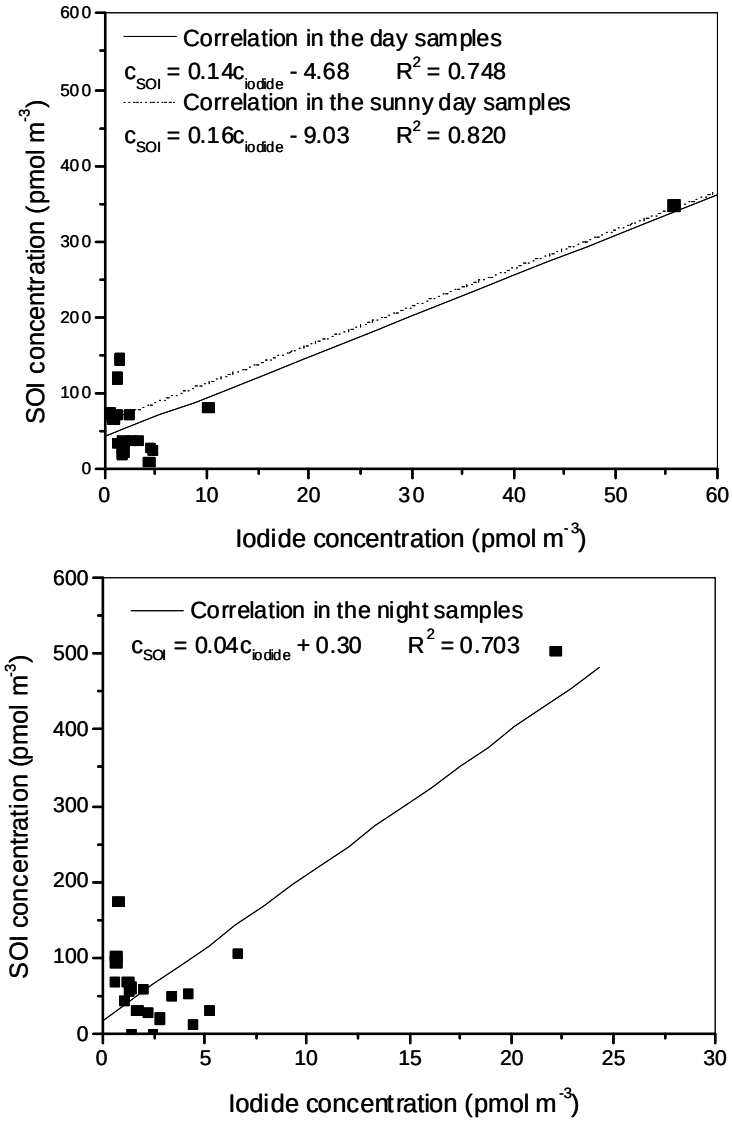

Figure 3- 12 Correlation between SOI and iodide in the sample stage 3 of Berner impactor

Although iodide, iodate and some UOIs were found in the chromatograms, a large part of SOI was not eluted out of both columns. On average, 37.0% and 86.3% of SOI in size fractionated aerosol samples from the MHC was not retained by G3268A and AS 16, respectively. In the future, other technique may be necessary to be applied in the further to the identification and quantification of organic iodine in particle phase.

Table 3- 5 Concentrations of UOIs in size fractionated samples in the MHC

Iodine species	Range ($pmol/m^3$)	Median ($pmol/m^3$)	Average ($pmol/m^3$)
Stage 1 (0.085 – 0.25 μm [a])			
UOI-0 [b]	1.57 – 146.81	39.74	51.14 ± 35.46 [d]
UOI-1 [c]	N.D. [e] – 1.66	0.16	0.33 ± 0.55
UOI-2 [c]	N.D. – 1.08	0.17	0.28 ± 0.31
UOI-3 [c]	N.D. – 0.23	0.17	0.15 ± 0.07
UOI-4 [c]	0.06– 4.02	0.71	1.22 ± 1.25
UOI-5 [c]	N.D. – 4.42	0.20	1.08 ± 1.87
Stage 2 (0.25 – 0.71 μm)			
UOI-0	7.46 – 136.64	41.49	50.69 ± 34.65
UOI-1	N.D. – 0.59	0.09	0.17 ± 0.18
UOI-2	N.D. – 0.37	0.11	0.13 ± 0.11
UOI-3	N.D. – 0.25	0.13	0.14 ± 0.06
UOI-4	0.14 – 3.67	1.07	1.22 ± 0.91
UOI-5	N.D. – 3.22	1.63	1.63 ± 2.25
Stage 3 (0.71 – 2.0 μm)			
UOI-0	16.77 – 131.26	42.40	49.52 ± 27.18
UOI-1	N.D. – 0.85	0.19	0.26 ± 0.24
UOI-2	N.D. – 0.51	0.17	0.20 ± 0.15
UOI-3	N.D. – 0.16	0.14	0.11 ± 0.05
UOI-4	0.19 – 2.84	1.23	1.44 ± 0.94
UOI-5	N.D. – 3.85	0.34	1.41 ± 2.12
Stage 4 (2.0 – 5.9 μm)			
UOI-0	10.94 – 130.43	49.32	53.95 ± 28.46
UOI-1	N.D. – 0.44	0.10	0.14 ± 0.12
UOI-2	N.D. – 0.15	0.09	0.08 ± 0.04

To be continued

Continued

UOI-3	N.D. – 0.21	0.08	0.11 ± 0.06
UOI-4	0.23 – 5.46	2.01	1.45 ± 1.45
UOI-5	N.D. – 0.15	0.12	0.12 ± 0.04
Stage 5 (5.9 – 10.0 μm)			
UOI-0	2.96 – 163.40	39.79	50.77 ± 36.99
UOI-1	N.D. – 0.30	0.17	0.18 ± 0.09
UOI-2	N.D. – 0.97	0.10	0.19 ± 0.26
UOI-3	N.D. – 0.15	0.09	0.09 ± 0.04
UOI-4	N.D. – 4.65	1.43	1.77 ± 1.30
UOI-5	N.D.	-	-

a. cutoff size; b. samples on June 13 – 16, June 21 – 24, 27 – 28, July 1 – 5 and measured by G3268A IC column; c. samples on June 17 – 20, 25 – 26, 29 and measured by AS 16 IC column; d. standard deviation; e. not detectable

Mass size distribution was made on the different iodine species. The data was normalized by the logarithm of impactor size ranges (i.e. by channel size; concentration/dlogDp), which can avoid effects caused by the uneven channel size width of the stages. Such transformation allows a more representative comparison between the impactor stages. As is shown in Figure 3-13 and Figure 3-14, medians are used to conduct the logarithmic normalization.

There were similar distributions of TSI and SOI with a bimodal distribution: one in the size range lower than 2.0 μm and the other in coarse particle range (5.9 – 10 μm). The size distribution of TII showed evident diurnal variation between the day and the night modes. More than 57% of the TII was found to reside in the fine particle size class (< 2.0 μm) in the night sample, which dominated in finest size range of 0.085 – 0.25μm compared to dominance in the size class of 0.71 – 2.0 μm during the day.

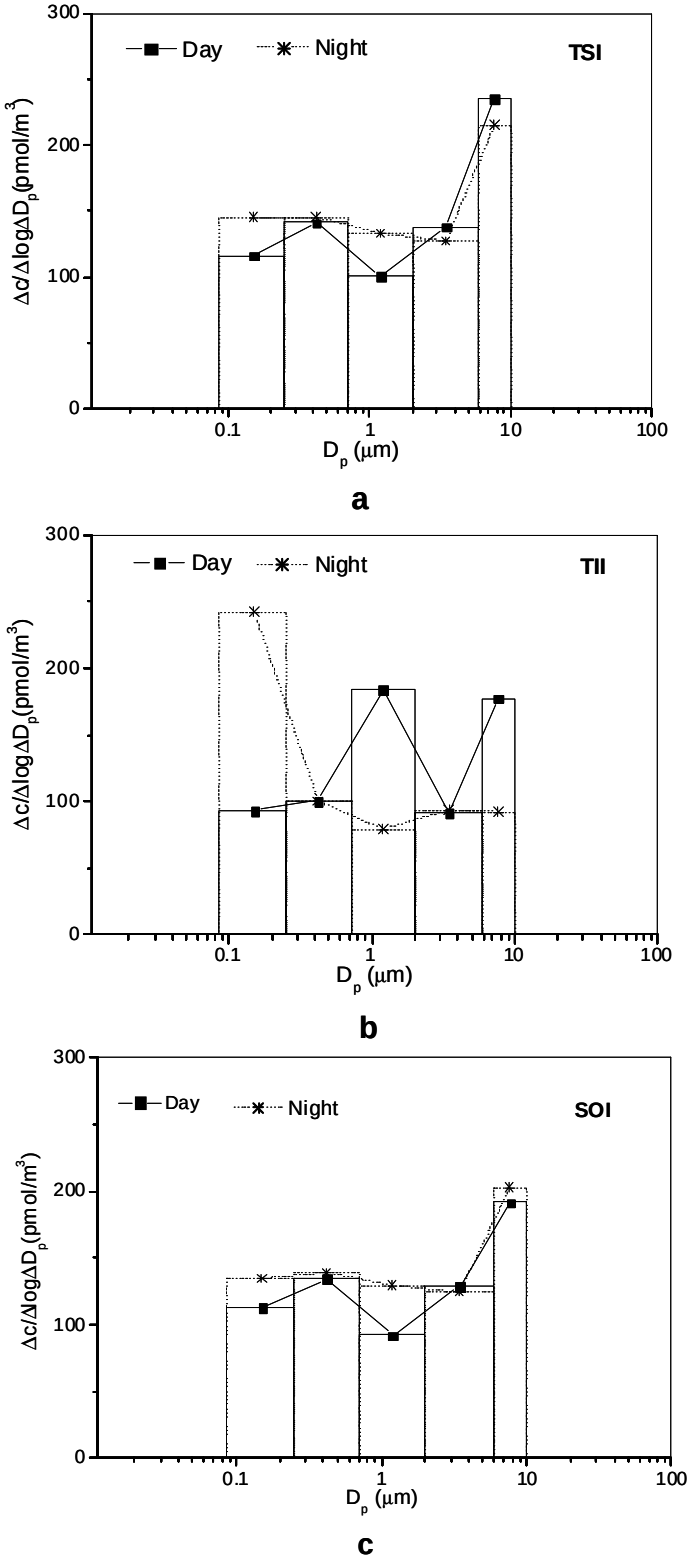

Figure 3- 13 Size distributions of TSI, TII, and SOI during the MHC: (a) TSI; (b) TII; (c) SOI

Iodide had a similar size distribution with TSI and SOI, with little difference between day and night. Iodate appeared to be concentrated in the coarse mode during both the day and night (both 70 % of iodate in the >2μm fraction) in agreement with previous data (Baker, 2005). It is also consistent with the interpretation of higher iodate/iodide

ratios found in coarse particles. As well the accumulation of iodate in the coarse size range in the day seems stronger than in the night, indicating more iodate was formed during day rather than at night.

Mass size distribution of UOI-0 was an accumulation structure. The concentration increased with the size increasing and dominated in the larger aerosol sizes. Then coarse mode seemed more important for UOI-0 than other species. No diurnal variation was found in the day and night distributions of UOI-0. The mass size distribution of UOI-4 displayed a bimodal structure: one in 0.71 – 2.0 μm and the other in > 5.9 μm. The distribution in coarse mode was less during the day compared to that at night. This may be due to the photolytic breakdown of organic iodine bond during the day.

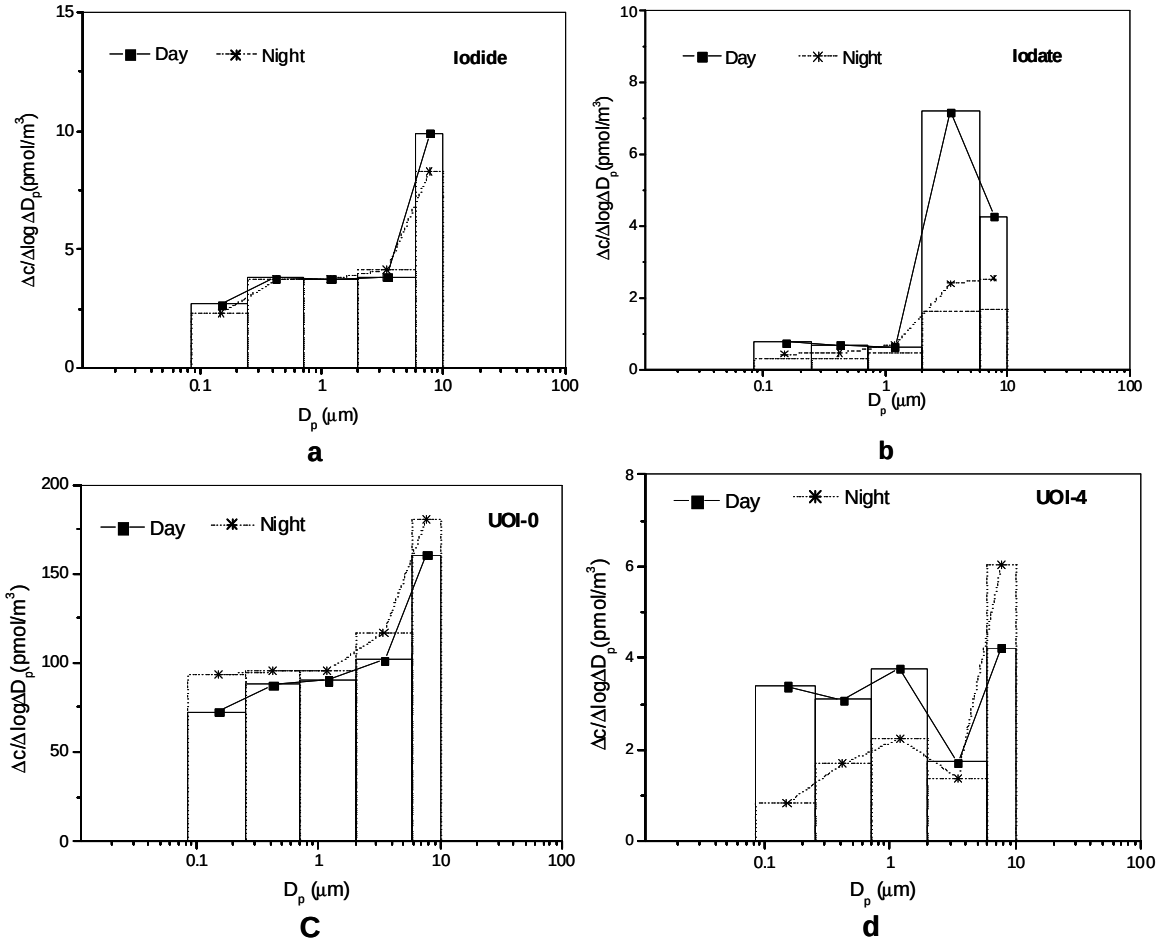

Figure 3- 14 Size distribution of iodide, iodate, UOI-0 and UOI-4 in the MHC: (a) Iodide; (b) Iodate; (c) UOI-0; (d) UOI-4.

3.2.3 Iodine in Rain and Aerosol duing MHC

The TSI concentrations found in the rainfall was variable on the different sampling days (18.11 – 47.24 nmol L^{-1}). TSI in the rainfall samples were not similar even though they were collected from the same days. As is shown in the marine aerosol samples, inorganic iodine (iodide and iodate) accounted for the minor part of TSI. Soluble organically bound iodine was also the major fraction in the rain samples from Mace Head station and the cottage (Table 3-6), accounting for 59.4 – 82.9% of TSI in the measured samples. However, SOI in rain consistently represented a lower proportion of TSI compared to the aerosol samples and generally had a larger proportion of iodate. In fact, in some of the rain samples iodate was at a similar, or slightly higher, concentration than iodide. This is consistent with inorganic iodine speciation measurements in rainfall from the North Sea region, analyzed by electrochemical methods (Campos et al., 1996), and rainfall from west England measured by photometry (Truesdale and Jones, 1996). This is further conformation that our speciation technique is accurately recording the iodide and iodate levels.

Table 3- 6 Concentrations of iodine species in the rainfall at Mace Head station and Mace Head cottage (nmol L^{-1}) (Gilfedder et al., 2008)

Sample location	Sample date	TSI	Iodide	Iodate	SOI
Mace Head station	17-18/06/06	19.69	2.99	3.45	13.24
Mace Head cottage	17-18/06/06	20.47	2.27	3.74	14.46
Mace Head station	19-20/06/06	24.41	4.96	3.74	15.71
Mace Head cottage	19-20/06/06	33.07	8.71	4.71	19.64
Mace Head station	26/06/06	37.01	6.81	4.27	25.93
Mace Head cottage	29/06/06	30.71	5.91	3.91	20.89
Mace Head station	08/07/06	47.24	6.38	1.72	39.14
Mace Head cottage	08/07/06	18.11	4.31	1.76	10.47

Interestingly, the largest unknown peak (UOI-4) observed in the aerosol chromatograms was also consistently found in the Mace Head rain chromatograms (Figure 2-16). Deposition fluxes in rain and aerosol are the major routes for removal of iodine from the marine atmosphere onto the Earth's surface (Baker et al., 2001). The similar chromatograms of both marine aerosols and rain samples give a more evident proof for the possible transferring between aerosol phase and precipitation. Not only rain but also snow has been measured to find large amount of organic iodine fraction as well as the unknowns peaks in IC chromatograms (Gilfedder et al., 2007b, 2007a; Gilfedder et al., 2008). Obviously, rain is one of the important sinks of soluble iodine in

the atmosphere due to the atmospheric wet deposition process. This is consistent with the finding that rain could influence on the variation of soluble iodine in aerosol samples.

3.3 Summary

Marine aerosol samples were collected from two sampling campaigns during June – July 2006: $PM_{2.5}$ from the MHC and CEC; Size fractionated aerosol samples (five stages, < 10 μm) from the MHC. TSI, TII, iodide, iodate and UOIs were measured by ICP-MS and IC-ICP-MS. The TSI and TII levels were at comparable levels in all the aerosol samples. The temporal variation of TSI was found to be related to nucleation events at Mace Head. In addition, the influences of airmass transport, tidal height as well as raining were observed to effect iodine concentrations in atmospheric aerosols. The speciation results showed that inorganic iodine (iodide and iodate) was the minor fraction of TSI at only 7.3% (median) in $PM_{2.5}$ from the MHC, 5.0% (median) in $PM_{2.5}$ from the CEC and 5.8% in size fractionated aerosol samples at Mace Head. More than 95% of the TSI was found to be SOI. Part of SOI was separated and eluted from the IC columns. The peaks were not sampling artifacts and must be polarizable compounds according to the IC separation mechanism; however, no identification has been achieved due to lack of structural information. Nevertheless, the importance of SOI was demonstrated and the participation of organic matter in iodine cycling is believed to be important in formation and uptake of particle iodine and also in the iodine chemistry in the MBL. The correlations between SOI and iodide in $PM_{2.5}$ ($R^2 > 0.5$, $P < 0.0001$) as well in size range of 0.25 – 0.71 μm and 0.71 – 2.0 μm ($R^2 > 0.7$, $P < 0.0001$) provide evidence for the close relation between both species. It also implies the formation of iodide through the decomposition of SOI under the affect of the environmental factors such as solar radiation (with better correlation during the sunny days).

Rainfall samples were also collected at Mace Head during the same period and measured by ICP-MS and IC-ICP-MS. Iodide and iodate were observed as the minor part while SOI was the major fraction of TSI in the rainfall. The same UOIs were detected both in aerosol and rainfall samples, implying the possible transferring between precipitation and aerosols.

4. Field Measurement during OOMPH Campaign

The importance of iodine chemistry in the MBL has been suggested in the past decades due to its participation on the ozone depletion events but also its contribution to new particle formation. Research in coastal area e.g. Mace Head, observed iodine was important for new particle formation process (O'Dowd et al., 2002b). Ocean covers more than 70% of the earth's surface. The iodine chemistry in the open ocean should not be neglected, however, and iodine speciation was reported by some researchers (Baker, 2004, , 2005; Read et al., 2008). Iodocarbons emitted from the marine macroalgae are still regarded as the reactive iodine precursors and can trigger the iodine cycling in the MBL. The data shown from the CEC, over the North Atlantic Ocean, have shown biological activity is related to iodine cycling. Therefore, the investigation of the iodine species in the gas phase and particle phase over the open ocean area is essential to further our knowledge of atmospheric iodine chemistry in the MBL.

Organics over the Ocean Modifying Particles in both Hemispheres (OOMPH) is a European Union financially supported research project to investigate the organic chemistry of the ocean and the MBL with a focus on organic vapors and their influence on particle nucleation processes. During its cruise campaign in south semisphere in 2007, the French scientific ship Marion Dufresne traveled a round trip between South Africa and South America. The campaign was split into two parts, hereafter called leg 1 and leg 2. The marine aerosol samples (by a Berner Impactor cascade sampler) were taken during the first leg crossing the South Atlantic Ocean from Cape Town, South Africa to Punta Arenas, Chile. This path crossed predominately the open ocean area which is good for characterization of particle phase iodine in open ocean aerosols. In addition, the influence from the open ocean as well as Antarctica can be estimated.

Iodine speciation was conducted in aerosol samples; TSI, iodide, iodate and UOI-0 in the different size ranges are presented here. The characteristics of different iodine fractions are studied.

4.1 Methodology

4.1.1 Sampling

The aerosol sampling was conducted place on the scientific vessel Marion Dufresne over the South Atlantic Ocean from Cape town, South Africa to Punta Arenas, Chile during January 19 – February 5, 2007. The Atlantic Ocean was crossed staying between 35°S and 45°S Latitude. The ship arrived at the coast of the South America then shifted south towards the Magellan Street. In this area, two phytoplankton blooms were

crossed (January 31 – February 2, 35°S – 45°S, 55°W)(Zorn et al., 2008). A Berner impactor cascade sampler (5 sampling stages with the size channels of 0.085 – 0.25 μm, 0.25 – 0.71μm, 0.71 – 2.0 μm, 2.0 – 5.9 μm and 5.9 – 10 μm.) was placed upwind on the upper-most deck of the ship to avoid the contamination from the ship emission plume. Cellulose nitrate filter (size: Φ_o=78 mm, Φ_i=40 mm, self-cut from the original filter Φ120 mm, Sartorius AG, Göttingen, Germany) was used for marine aerosol collection. The sampler was fixed to a flow of 4.5 m^3 h^{-1} during the sampling and the sampling period was 23.5 h for each set of samples (the last sample set taken on February 2 – 4, 2007 had duration of 47 h). After sampling, each loaded filter was parked in separate, sealed Poly-propylene vial (50 mL, GREINER BIO ONE, Frickenhausen, Germany) and stored under at -20℃ to avoid any contamination and loss of volatile compounds.

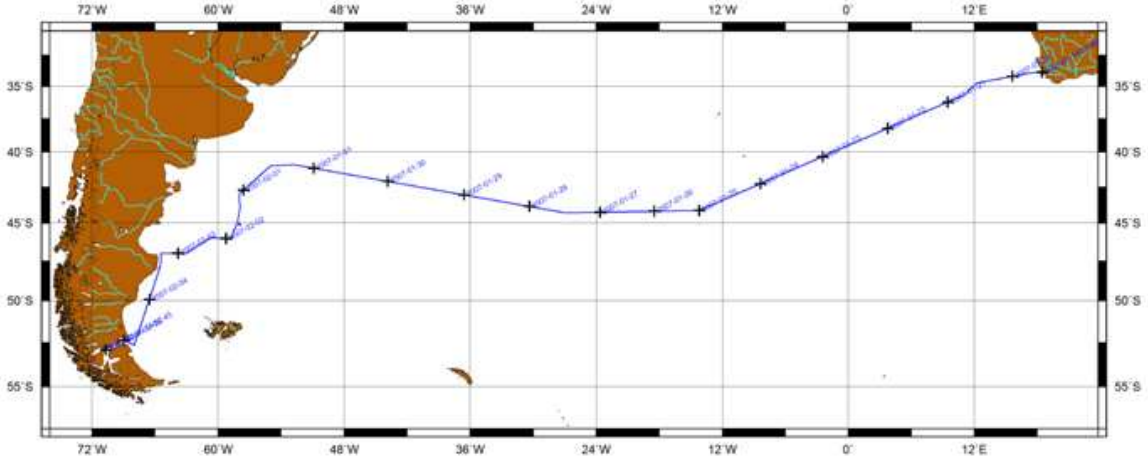

Figure 4- 1 Sketch map of the path of OOMPH campaign over South Atlantic Ocean during January – February 2007

4.1.2 Chemical Analysis

ICP-MS and IC-ICP-MS were used for TSI, iodide, iodate and UOIs measurements. The methods are discussed in detail in Chapter 2.

Firstly, all the samples were treated with an ultrasonic extraction using ultra pure water (Milli-Q, 18 MΩ). The extract was collected and then measured with a HP4500 quadrupole ICP-MS (Agilent, Waldbronn, Germany) to detect TSI. The detection limit of TSI was 0.1 μg L^{-1} in aqueous solution.

Secondly, iodide and iodate were separated and quantified with an online IC-ICP-MS system. A G3268A IC column was chosen as the chromatography column. 0.06 mol L^{-1} $(NH_4)_2CO_3$ eluent was used as the mobile phase with a flow of 1.0 mL min^{-1}. HP4500 ICP-MS was used as an element specific detector. Iodide and iodate were successfully separated and they were both quantified with an external calibration curve. The detection limits were 0.5 μg L^{-1} and 0.1 μg L^{-1} for iodide and iodate, respectively.

Soluble organic iodine (SOI) was calculated as the difference between total iodine and the inorganic iodine species. One unidentified organic iodine (UOI) peak distinctively occurred in the chromatograms for most of the samples, similar to that found during the MAP campaigns. This peak, which had the retention time of about 2.5 minutes, is also termed as also UOI-0 here to make the result comparison between the campaigns conveniently. This signal is not identified until now. The peak was quantified with the calibration curve of iodide because iodine atom is converted to I^+ in the plasma prior to quantification with mass spectrometer. Still part of the soluble iodine did not eluted out of the column during the measurement.

4.1.3 Additional Information

Meteorological data such as temperature, wind speed, wind direction, sea water temperature etc were collected simultaneously during the sampling period. Airmass back trajectory data are obtained by courtesy of H. Wernli from Max Plank Institute for Chemistry in Mainz, Germany.

4.2 Results and Discussion

4.2.1 Overview of Iodine Species

The concentrations of the iodine species including TSI, iodide, iodate, and UOI-0 are shown in Table 4-1.

Table 4- 1 Concentrations of iodine species in size fractionated samples in OOMPH campaign

Iodine species	Range ($pmol/m^3$)	Median ($pmol/m^3$)	Average ($pmol/m^3$)
Stage 1 (0.085 – 0.25 μm [a])			
Total soluble iodine (TSI)	14.26 – 133.48	56.46	57.00 ± 29.85 [b]
Soluble organic Iodine (SOI)	14.04 – 133.05	55.53	56.41 ± 29.69
Iodide	0.08 – 1.15	0.37	0.44 ± 0.36
Iodate	N.D. [c] – 1.11	0.03	0.15 ± 0.30
UOI-0	0.82 – 38.13	15.83	15.69 ± 9.87

To be continued

Continued

Stage 2 (0.25 – 0.71 μm)			
Total soluble iodine (TSI)	15.86 – 163.25	60.63	68.76 ± 41.36
Soluble organic Iodine (SOI)	15.74 – 162.99	60.37	68.21 ± 41.43
Iodide	0.08. – 1.89	0.20	0.45 ± 0.54
Iodate	0.02 – 0.68	0.05	0.10 ± 0.17
UOI-0	4.52 – 55.14	17.82	20.97 ± 14.84
Stage 3 (0.71 – 2.0 μm)			
Total soluble iodine (TSI)	9.16 – 90.08	35.14	42.30 ± 26.89
Soluble organic Iodine (SOI)	8.66 – 89.47	34.76	41.84 ± 26.78
Iodide	N.D. – 0.70	0.38	0.36 ± 0.22
Iodate	0.01 – 0.43	0.06	0.10 ± 0.12
UOI-0	2.27 – 27.64	8.34	10.77 ± 8.29
Stage 4 (2.0 – 5.9 μm)			
Total soluble iodine (TSI)	12.52 – 88.55	41.24	47.32 ± 25.39
Soluble organic Iodine (SOI)	11.63 – 86.19	39.84	44.86 ± 24.79
Iodide	0.08 – 1.16	0.57	0.59 ± 0.36
Iodate	0.07 – 4.52	1.92	1.88 ± 1.37
UOI-0	1.61 – 26.88	12.23	13.00 ± 7.64
Stage 5 (5.9 – 10.0 μm)			
Total soluble iodine (TSI)	14.76 – 118.91	42.42	47.83 ± 27.89
Soluble organic Iodine (SOI)	13.43 – 118.40	41.30	46.81 ± 27.83
Iodide	0.10 – 1.81	0.47	0.57 ± 0.48
Iodate	N.D. – 1.60	0.42	0.45 ± 0.40
UOI-0	3.73 – 37.98	12.16	14.28 ± 9.78

a. cutoff size; b. standard deviation; c. not detectable

The medians of TSI in stage 1 and 2 (~ 60 pmol m^{-3}) were found to be higher than those in stage 3 – 5 (~ 40 pmol m^{-3}). The TSI in stage 3 was the lowest level (median, 35.14 pmol m^{-3}). As is mentioned, the cutoff size range from stage 1 – 3 was 0.085 – 2.0 μm. During this campaign, 51.1 – 74.6% (median, 64.5%) of TSI was in the fine particle range (< 2.0 μm), indicating the TSI uptake mainly occurs in the fine particle range. It is consistent with that found during the MHC.

SOI was the most abundant soluble iodine fraction. The medians of SOI ranged from 34.76 pmol m^{-3} to 60.37 pmol m^{-3} in the 5 stages, accounting for from 87.6 % to 99.9% with a median of 98.6% in TSI.

Iodide and iodate were only minor iodine fractions in the samples. Most of the iodide and iodate concentrations were lower than 1 pmol m^{-3} except iodate in stage 4 (median 1.92 pmol m^{-3}). The iodate in stage 5 was the second highest with the median of 0.42 pmol m^{-3}. It is quite similar to the results from the MHC with higher iodate in stages 4 and 5, implying the formation and accumulation processes of iodate may relate highly to the size range larger than 2.0 μm. The medians of iodide concentration in the 5 stages were not much different, ranging from 0.20 to 0.57 pmol m^{-3}. Iodide accounted for 0 – 8.2 % in TSI with a median of 0.9%. The percentages of iodide were 1.4 % (median) and 1.6 % (median) in TSI in stage 4 and 5, higher than those in stages 1 – 3 (medians lower than 1.0% in TSI).

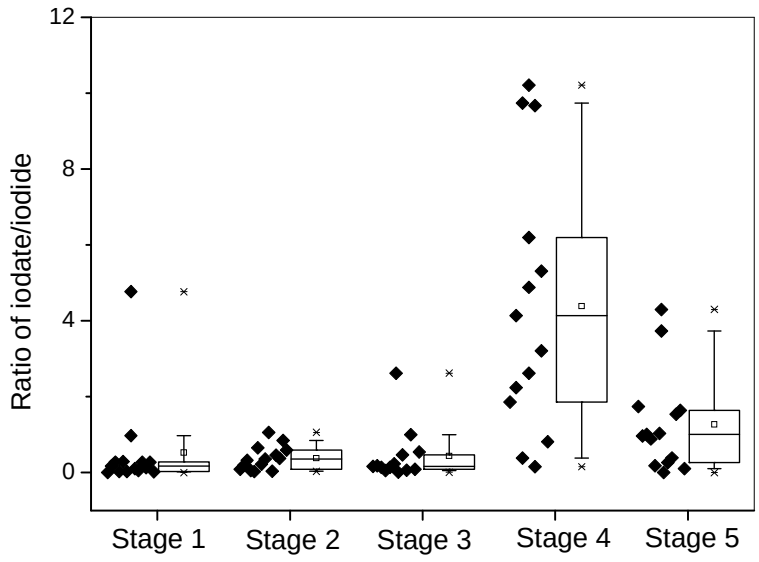

Figure 4- 2 Statistical chart of the ratio of iodate/iodide in 5 stages of Berner impactor

The ratios of iodate/iodide are shown in the Figure 4-2. The iodate/iodide ratios in stage 4 and 5 were more variable than in other stages. Stage 4 and stage 5 also had higher medians and averages of iodate/iodide ratios than in stages 1 – 3. The ratios in stages 1

– 3 were much lower than 1, in agreement with the corresponding ratios found in the same stages as well as in $PM_{2.5}$ during the MHC. Iodide obviously was more dominant inorganic iodine species found fine particle size range. However, the highest ratio (median, 3.68) was shown in stage 4. The iodate/iodide ratio of 0.98 was found in stage 5. This variation trend among the 5 stages is close to that observed at Mace Head using the same Berner impactor sampler. The ratios in stage 4 during the OOMPH campaign were higher than found at Mace Head. 11 of 14 samples (78.6%) had the ratio of iodate/iodide higher than 1 and 50% of the ratios were in the range from 2 – 6. The size range of 2.0 – 5.9 μm (stage 4) was found to be a very important diameter scope for iodate formation and accumulation in aerosols.

4.2.2 Spatial and Temporal Variations

The variations of TSI in fine aerosol, in coarse aerosol and in the five stages were presented during the sampling period during the OOMPH. The fine aerosol and coarse aerosols refer to the aerosols collected by stage 1 – 3 (size range 0.085 – 2.0 μm) and by stage 4 – 5 (2.0 – 10μm), respectively.

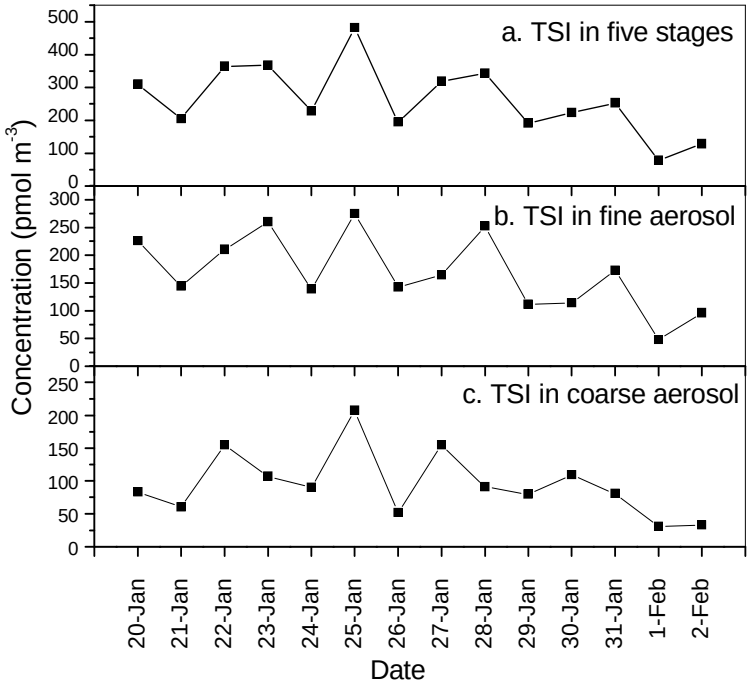

Figure 4- 3 Temporal variation of TSI during the OOMPH campaign: a. the sum of TSI in 5 stages; b. TSI in fine aerosol (sum of TSI in stage 1 – 3); c. TSI in fine aerosol (sum of TSI in stage 4 – 5)

The first and last samples in this dataset were collected along the South African coast and South American coast, respectively. The TSI concentration in the coastal South

Africa was higher than that in the coastal South America in both fine and coarse particles. Cape Town, the starting point of the campaign, is located in an ocean current upwelling region where more nutrients are brought up to the ocean surface causing macroalgae blooms in the inshore western coast of Africa. This enhanced the possibility of volatile iodine precursor emissions. In such cases, more iodine compounds might be produced and takes up into the particle phase. Contrarily, airmass back trajectories show the airmass mostly cross the terrestrial area along the Chilean coast which may be another reason for its lower iodine levels due to the little terrestrial iodine source. However, both coastal samples had lower TSI levels than those in the open oceanic coarse particle, indicating iodine sources contributed more to the fine particle in the coastal area. However, if macroalgae are regarded as the main source of iodine chemistry in the MBL, littoral zone should be a highly distributed area of macroalgae, a question raises why higher TSI was found in the open oceanic samples during the OOMPH. Unfortunately, only two samples were collected in the coastal zone, which make the interpretation difficult.

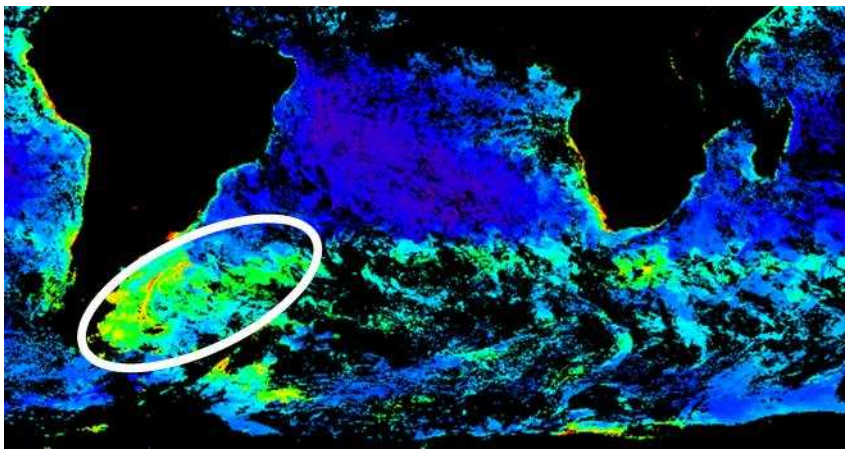

Figure 4- 4 Monthly average of oceanic chlorophyll in January of 2007 (http://oceancolor.gsfc.nasa.gov)

For TSI in open oceanic aerosols, the concentrations obtained in the first half leg (before January 29) were higher than those from the second half. It is interesting to note that blooms of oceanic phytoplankton occurred during the second period near the South American coast (Figure 4-5). If the oceanic biological activity is really correlated with the iodine emission in the open ocean, the results from the OOMPH seem not compatible. The airmass transport is found to be a possible source, which is suggested by the back trajectory analysis. During the OOMPH campaign, the cruise path was totally under the influence of westerlies in southern semisphere. If the transport was driven by the prevalent westerly wind, the airmass transported from the active biological bloom region may affect the iodine variation. There were several enhanced TSI values observed, which were measured on the samples taken on January 22 – 23, 25, 27 – 28, and 31. TSI on the January 25 and 27 – 28 were transported from the ice front sectors of the Antarctica, which is in accordance with the findings from the Antarctic coast with aerosol TSI (see Chapter 5) as well as iodine oxide in gas phase (Saiz-Lopez

et al., 2007). The airmass arrived the cruise on January 23 and 31 is found from the phytoplankton bloom area. Also, the airmass on both dates crossed the ocean instead of South America continent. This is likely to be the reason why the lower TSI levels measured on February 1 – 4. On January 22, the airmass came from the open ocean and iodine source was not clear yet.

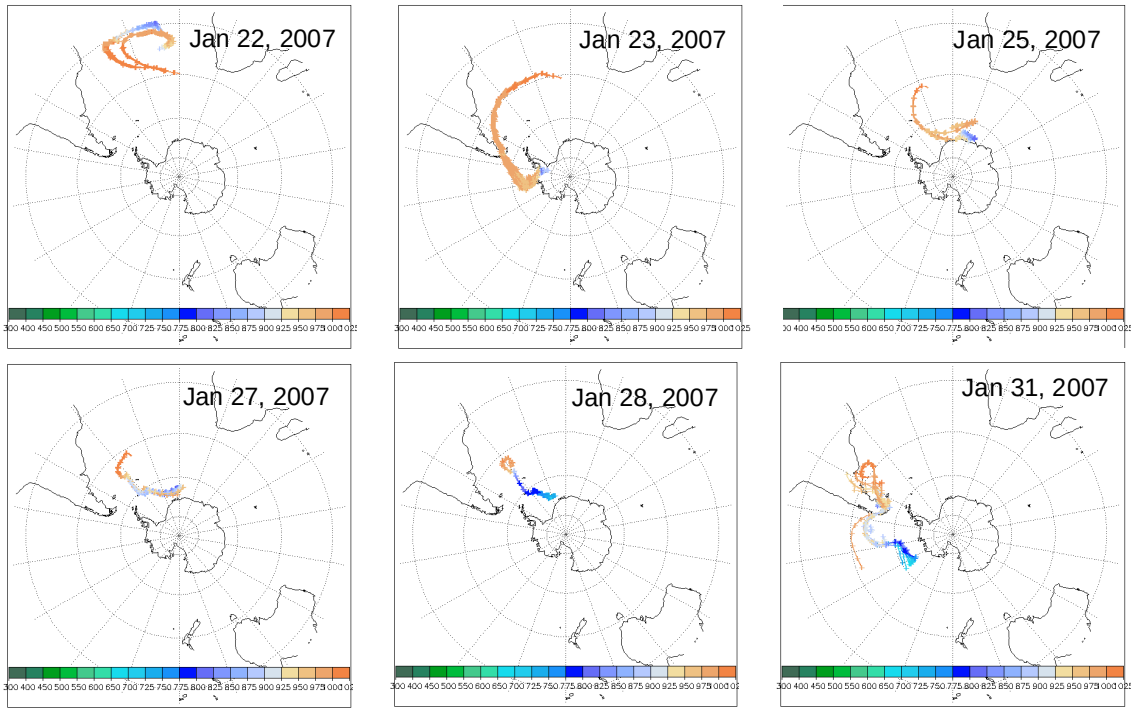

Figure 4- 5 Airmass back trajectories on the selected dates during the OOMPH campaign

According to the current understanding of iodine chemistry in the MBL, volatile iodine species such as I_2, CH_3I, CH_2I_2 etc are emitted from macroalgae. With exposure to UV radiation, iodine atom is formed by photolysis of volatile iodine species. The reaction with O_3, forming the iodine monoxide (IO) radical, is thought to be the major fate of iodine atoms. The iodine oxides may then self-nucleate and take up into aerosols (Carpenter et al., 2003). A recent research showed that most of the iodine should theorectically be taken up as HIO_3 (Pechtl et al., 2007). Recently, the existence of SOI in marine aerosols is widely reported. The most important consequence of SOI in aerosols is probably to increase the residence time of iodine within the particles (in particular by retarding iodine release to the gas phase) thus possibly decreasing ozone destruction. Increased residence time may also facilitate iodine transport out of the marine boundary layer into the free troposphere, and possibly even to the tropopause, by convective systems.

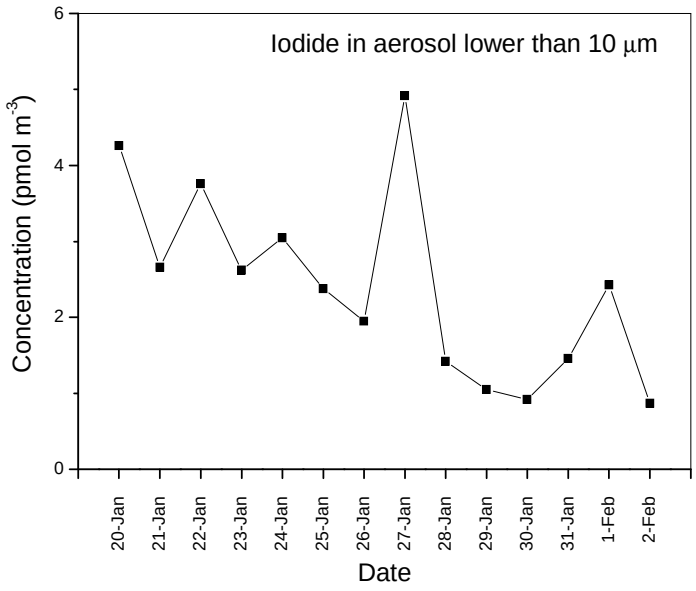

Figure 4- 6 Temporal variation of iodide in the aerosol sized lower than 10 μm

The iodide concentrations in different stages did not present a clear temporal variation. When the sum of iodide in the 5 stages was investigated, iodide showed a clear decreasing trend from January 20 until January 30. As is discussed above, airmass transport may play an important role in the iodine loading in the aerosols. In addition to the hypothesis that iodide formation mechanism is highly correlated with the SOI decomposition in the atmosphere, the longer residence time during transport increases the possibility of SOI decomposition with exposure of UV radiation. The variation of iodide adds evidence to the contribution of airmass transport to the particle phase iodine.

4.2.3 Soluble Organic Iodine

SOI was the most abundant iodine fraction in TSI from the size fractionated aerosol samples. The percentage of SOI in TSI ranged from 87.6 % to 99.9% with a median of 98.6%. The proportional contribution of SOI to TSI was extremely high in this case, even higher than observed during the CEC campaign over the North Atlantic Ocean (median 95.9% in $PM_{2.5}$). Nevertheless, the results from both ship campaigns displayed higher SOI percentages than that during the MHC (93.0% in $PM_{2.5}$ and 94.2% in size fractionated aerosol samples), suggesting that SOI may be more dominant in the open oceanic aerosols than in the inshore aerosols. The proportional contribution of SOI to TSI during the OOMPH was much higher than other work, although different techniques were applied in this work (Baker, 2005).

UOI-0 was eluted with a G3268A IC column and detected with a HP4500 ICP-MS. UOI-0 accounted for 1.4 – 42.4% (median, 28.8%) of TSI in all the samples, showing that UOI-0 is an abundant fraction in aerosols. The temporal variation of UOI-0 was similar to that of TSI. However, the peak shown in the chromatogram remains unidentified.

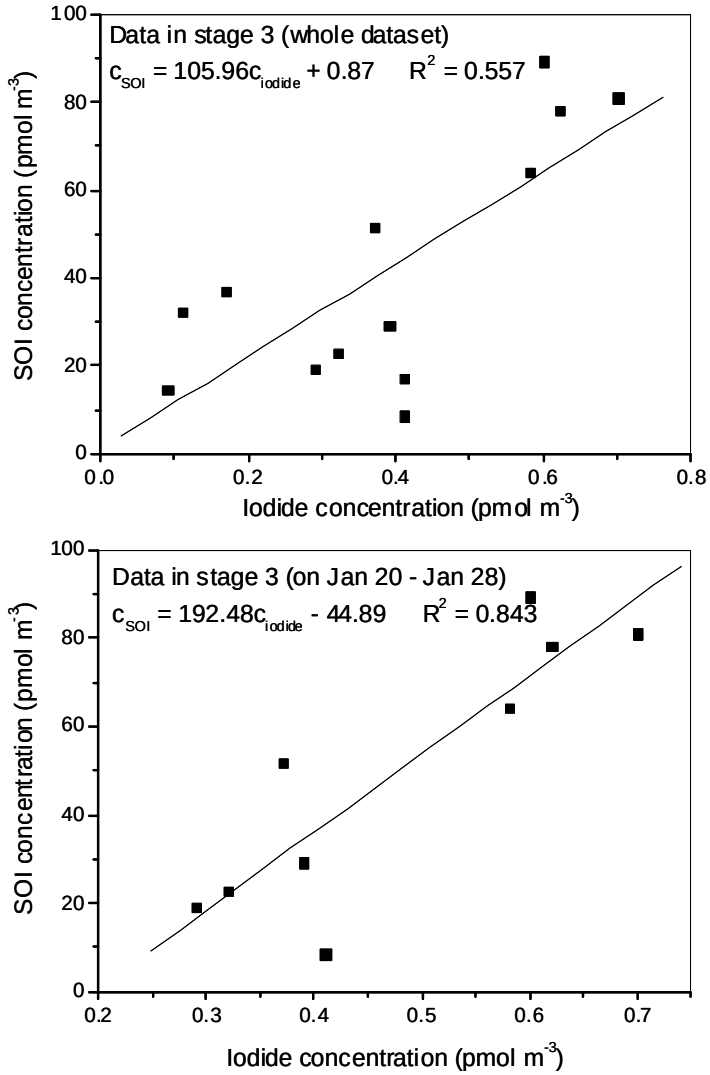

Figure 4- 7 Correlation between iodide and the SOI in stage 3 of Berner impactor during the OOMPH

Similarly to that discussed in Chapter 3, significant correlations were observed between iodide and SOI in marine aerosols. A significant correlation was found only in stage 3 between iodide and SOI. The correlation coefficient (R^2) was 0.557 ($P < 0.005$) which is close to the correlations found in $PM_{2.5}$ during the MHC but lower than the correlations found in stage 3 during the CEC (day, $R^2 = 0.748$; night, $R^2 = 0.703$). The marine aerosol samples taken during the OOMPH campaign were from the different areas over the South Atlantic Ocean compared to all from Mace Head. The moving path changed the sampling environments, which had more uncertainties and may negatively

effect the correlation. During the MHC, significant correlation have been reported in day samples in stage 2 with the R^2 of 0.787 but poor correlation was shown here in the stage 2 (R^2 = 0.017). Although the day samples in stage 2 had higher correlation coefficient, poor correlation was also reported in the night samples during the MHC. The sampling hours of the samples taken from the OOMPH were normally 23.5 h and no day and night samples were differentiated. Furthermore, if the complicated changes of sampling environment in an onboard campaign are taken into account, it is easier to cause the non-correlation in stage 2.

The correlation between SOI and iodide in stage 3 during the first part of the sampling period (January 20 – 28) is also analyzed. The correlation coefficient was found to be 0.843 ($P < 0.005$), more significant than that of the whole dataset. This implies the sources of SOI and iodide are highly related during the first part of the OOMPH. As is discussed above, the local sources of iodine seemed weak and airmass transport from the phytoplankton area and ice front sector of Antarctica is likely to be the important source of iodine in marine aerosols. The interpretation is supported by the decreasing iodide variation during the sampling period and a stronger correlation between SOI and iodide. Again, SOI is suggested to be essential for iodine chemistry in the MBL due not only to high proportional contribution but also its active participation in iodine cycling processes.

4.2.4 Size Distribution of Iodine Species

Size distributions of different iodine fractions in aerosols are shown in Figure 4-8, calculated by the normalization of logarithm of mass concentration against the particle size. The size distributions of TSI, SOI and iodate were similar to those observed during the MHC. TSI and SOI both had bimodal distributions with one peak in fine range (0.25 – 0.71 μm) and the other in coarse range (5.9 – 10 μm). Iodate was highly enriched in the coarse particle size range higher than 2.0 μm. The mass size distributions of TSI, SOI and iodate are consistent with those observed in the inshore marine aerosols at Mace Head.

UOI-0 also had a similar size distributions to TSI and SOI, but it was different from that found during the MHC. It was an accumulation-like distribution with continuously increasing distribution with the size increasing during the MHC. The percentage of UOI-0 in TSI was much higher during the MHC (median, 63.4%) than that during the OOMPH (median, 28.8%). If UOI-0 is a mixture of several organic iodine compounds, the difference between inshore environment and open oceanic environment may cause the different contribution and uptake of UOI in aerosols and make size distribution different.

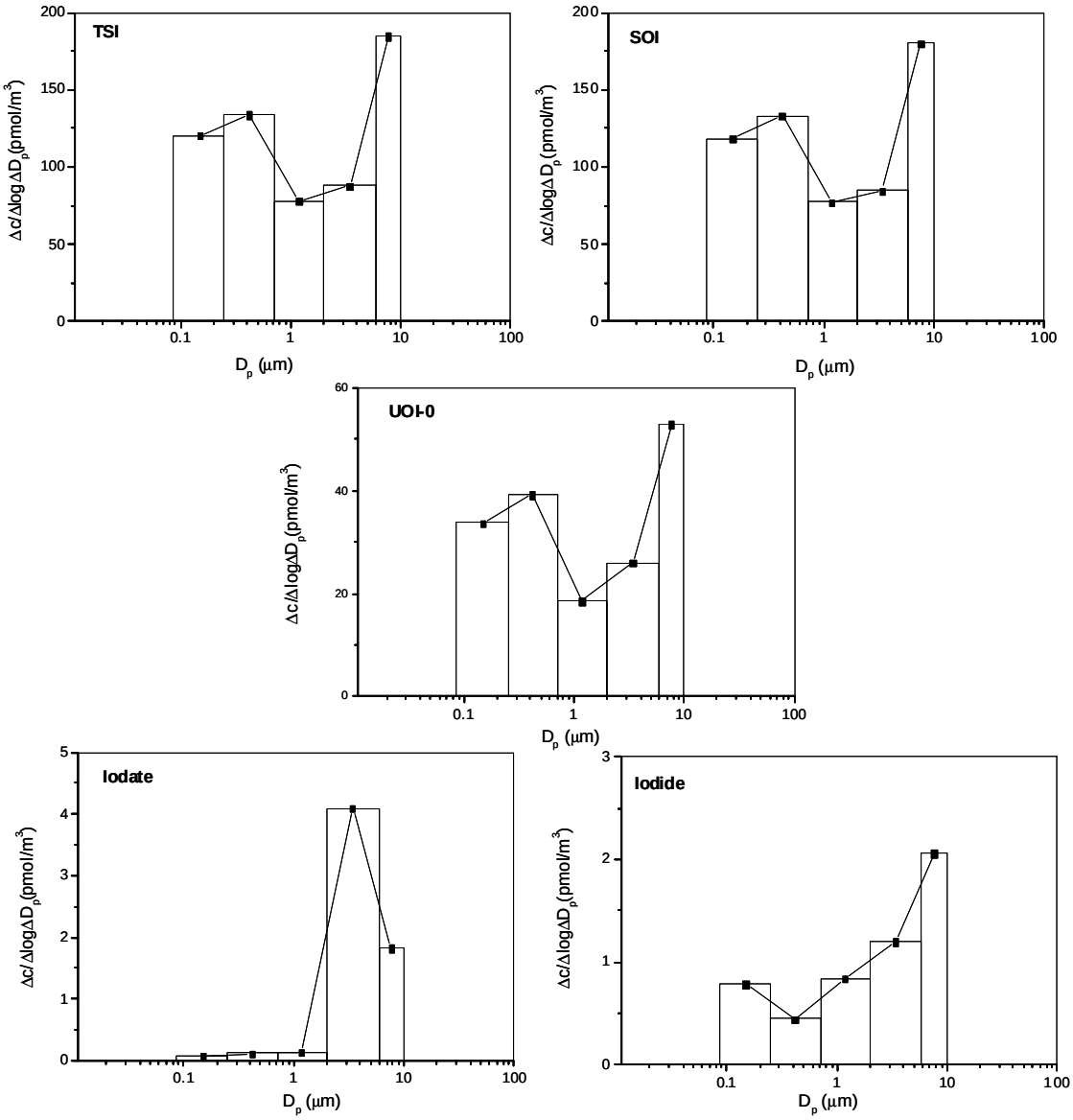

Figure 4- 8 Size distributions of TSI, SOI, UOI-0, iodate and iodide during the OOMPH

The iodide size distribution was also different from that in the MHC. The first peak was found in the finest stage of 0.085 – 0.25 μm instead of in the 0.71 – 2.0 μm as observed during the MHC. In the size range from 0.25 – 10 μm, iodide concentrated incrementally with the size was increased.

4.3 Summary

Size fractionated aerosol samples were collected by a 5-stage cascade sampler on the scientific ship Marion Dufresne over the South Atlantic Ocean during January – February 2007. TSI, iodide, iodate and UOI were measured by ICP-MS and IC-ICP-MS. The TSI levels were lower than those from the MHC in the five stages but

similar size distribution were found during both campaigns. Iodide and iodate were less abundant (medians 0.9% and 0.3%, respectively) compared to SOI (median 98.6%). The concentrations of iodide and iodate were lower than those measured in the inshore marine aerosols from the MHC. UOI-0 was again found in the IC chromatograms, but with a lower abundance in the open oceanic aerosols. Similar SOI and iodate distributions were observed as those from the MHC, although different patterns were found for iodide and UOI-0.

The spatial variation did not correlate with biological activity (algae bloom) in the oceanic area. The estimation of aerosol iodine source suggests the airmass transported from the phytoplankton and Antarctic ice front sector was the possible important source of aerosol iodine. The significant correlation between SOI and iodide (R^2 = 0.843) during first part of cruise path proves the close relation between the formation process of iodide and SOI. The formation of SOI and the role of organic matters in iodine chemistry are not clear in the open ocean and the mechanisms are needed to be studied in future research.

5. Iodine Speciation in Marine Aerosols along a Round-trip Cruise from Shanghai, China to Prydz Bay, Antarctica

Iodine chemistry plays an important role in the marine boundary layer (MBL) by altering the rate of the tropospheric ozone depletion and by forming new particles (O'Dowd et al., 2002b; Read et al., 2008). To understand the global effect of iodine chemistry, the observation of iodine species on a global scale is necessary, especially on the polar regions where ozone depletion events (ODEs) have frequently been reported (Saiz-Lopez et al., 2007; Schonhardt et al., 2008). Polar regions, namely Arctic and Antarctic, are geographically remote but have a significant impact on the global atmosphere (Landsberger et al., 2001; Calvert and Lindberg, 2004; Saiz-Lopez et al., 2007; Simpson et al., 2007). Currently iodine chemistry in gas phase in polar region has received intensive interests by field observations and model simulations (Friess et al., 2001; Saiz-Lopez et al., 2007; Saiz-Lopez and Boxe, 2008; Schonhardt et al., 2008), but iodine speciation in the particle phase has not yet been reported.

Iodine speciation data in Total Suspended Particles (TSP) samples collected on the Chinese Ice breaker *Xue Long* duringa 30,000 km round-trip cruise path over the Western Pacific Ocean, Eastern and Southern Indian Ocean, and Prydz Bay, coastal Antarctic during the 23th China Antarctic Campaign (Nobember 2005 – March 2006) are presented. Iodide, iodate and UOI were simultaneously determined by IC-ICP-MS. To the best of our knowledge, this study covers largest geographical extent to date and is the first report of iodine speciation in the polar region.

5.1 Methodology

5.1.1 Sampling

During the *Xue Long* expedition, a total of 57 particulate samples were collected from November 2005 to March 2006 between the China Sea (Western Pacific Ocean), the Eastern and Southern Indian Ocean, and Prydz Bay (28.5°N-69.4°S, 70.5-122.8°E; Figure 5-1). A high volume TSP sampler was placed upwind on the upper-most deck of the ship. Particles were collected by drawing air through a cellulose fiber filter (Whatman 41, Maidstone, UK, 20×25cm) at a flow rate of ～1.0 m^3 min^{-1}. During the cruise the sample duration was 24 hours. At the coastal Antarctic location the duration was set at 72 hours due to possible low iodine concentrations. After sampling, the filters were packed in separate, sealed plastic bags and stored frozen below -20℃.

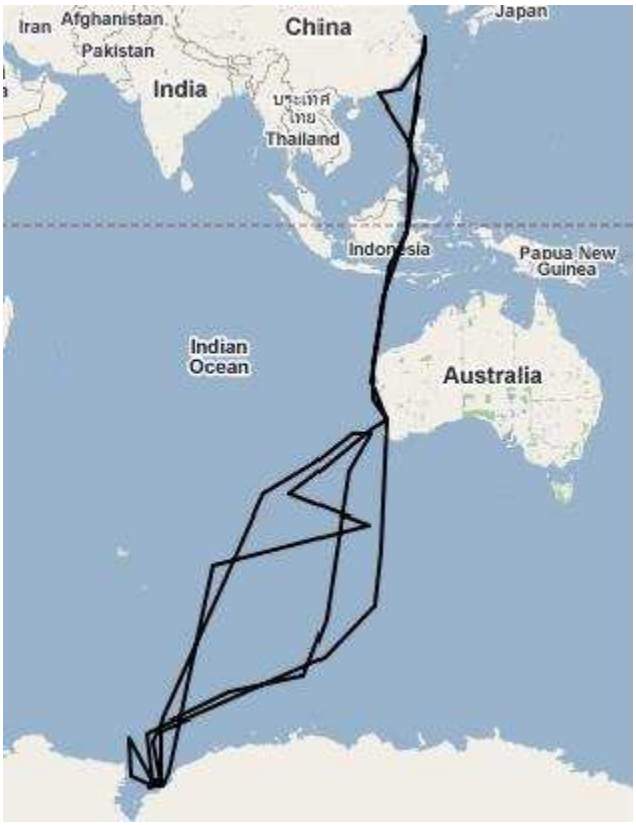

Figure 5- 1 Sketch map of cruise from Shanghai, China to Prydz Bay, Antarctica

5.1.2 Chemical Analysis

A part of filter (5 cm × 5 cm) was cut from every sampled filter and extracted in water by an ultrasonic assisted extraction for 20 minutes. TSI was measured with a HP4500 ICP-MS (Agilent, Waldbronn, Germany). The detection limit for TSI was 0.1 μg L^{-1} in aqueous solution calculated from the standard deviations of blank samples (n = 7, 3s criterion). Iodide and iodate were separated and quantified with an IC-ICP-MS system with a G3268A IC column (Agilent, Waldbronn, Germany). 0.06 mol/L $(NH_4)_2CO_3$ was used as the mobile phase with a flow rate of 1.0 mL min^{-1}. The HP4500 ICP-MS was used as a detector to scan Isotope ^{127}I. Using this method, iodide and iodate were successfully separated and they were quantified by the external calibration curves. The detection limits were 0.5 μg L^{-1} for iodide and 0.1 μg $L^{-1}$for iodate (expressed as I), respectively, with the injection of 20 μL. The relative standard deviations for iodide and iodate at the 5 μg L^{-1} were 1.74% and 3.03% (n=7), respectively. Soluble organic iodine (SOI) was calculated as the difference of total iodine and the inorganic iodine species (SOI = TSI – Iodide – Iodate). Unidentified organic iodine species were frequently observed in the chromatograms. One unidentified organic iodine signal was observed in most of the chromatograms in addition to iodide and iodate. This signal must result from an anionic compound as it is efficiently separated by the anion exchange column. Some commercial organic iodine compounds including iodo-acetic acid,

iodo-propionic acid, etc were run for comparison, but no similar retention time was found, and the signal remains unidentified. The retention time (about 2.5 minutes) was similar to the UOI-0 found in the chromatograms of the samples from other campaigns (MAP and OOMPH). Therefore, it is also termed UOI-0 here. The unknown signal was quantified with the iodide calibration curve as the iodine atom is converted to I^+ in the plasma prior to quantification with the mass spectrometer. Nevertheless, on average 42.6% of TSI was not eluted from the IC column.

5.1.3 Meteorological data

Meteorological data were also obtained from the scientific vessel during the cruise and included temperature, pressure, wind degree, wind direction etc. Airmass back trajectory were calculated using HYSPLIT model (FNL data set) from NOAA Air Resources Laboratory. Monthly global distributions of chlorophyll were downloaded from MODIS web, NASA (http://modis.gsfc.nasa.gov/).

5.2 Results and Discussion

5.2.1 Concentration of Iodine Species

The concentrations of total soluble iodine (TSI), iodate, iodide and soluble organic iodine (SOI) varied considerably over the cruise (Table 5-1).

Table 5- 1 Concentrations of iodine species during the cruise campaign (n = 57)

Iodine species	Range(pmol/m^3)	Median (pmol/m^3)	Average(pmol/m^3)
Total Soluble Iodine(TSI)	1.17-28.22	6.51	9.41±7.04 [b]
Soluble Organic Iodine (SOI)	0.78-17.84	4.50	5.98±4.30
Iodide	N.D.[a]-15.67	1.49	2.81±3.43
Iodate	N.D.-4.72	0.28	0.62±0.94
Unidentified Organic Iodine (UOI)	N.D. 15.64	1.21	2.06±2.47

a. N.D.= not detectable; b. standard deviation

The TSI concentration ranged from 1.17 to 28.22 pmol/m^3 with a median of 6.51 pmol m^{-3}, which was much lower than the TSI levels found during the MHC, CEC and

OOMPH. The relative contribution of inorganic iodine (iodide and iodate) was variable, ranging from 0.0% to 87.5%. The median values for iodide and iodate were 1.49 pmol m^{-3} and 0.28 pmol m^{-3}, respectively, accounting for 5.1% (median) and 22.8% (median) of TSI. The percentage of inorganic iodine was more abundant than the results from Mace Head, the South and North Atlantic Oceans. In those aerosol samples, the inorganic iodine was found to be almost all lower than 10% of TSI. The ratio of iodate/iodide ratio ranged from 0 to 3.49 with a median of 0.21, which was comparable to the $PM_{2.5}$ data during the MHC and indicates iodide is the most dominant inorganic iodine species in marine aerosols. This is in accord with the findings of former researches (Baker, 2004; Gilfedder et al., 2008). The iodate/iodide ratio did not differ significantly between coastal and oceanic samples (0.19 and 0.22, respectively).

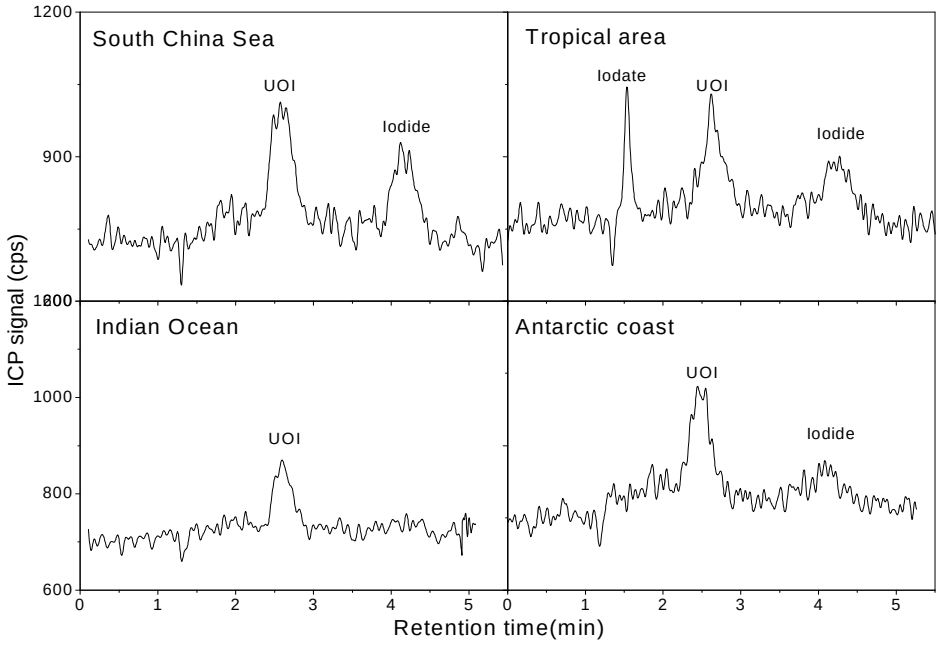

Figure 5- 2 The widely spread of UOI in different sampling area

SOI ranged from 12.5% to 100% with a median of 72.1%. This indicates that SOI was the most dominant iodine fraction in the particles over the entire 30,000 km transect. UOI-0 was responsible for up to 38.3% of SOI, with a median of 1.21 pmol m^{-3}, which is comparable with the average of iodide concentration. There are very few reports on the concentration of the different iodine species in the marine boundary layer. In comparison with the previous data observed over the Atlantic Ocean (Baker, 2004, , 2005), the concentrations of iodide and iodate were similar. Interestingly, the UOI-0 was present in most of the samples in several areas including the South China Sea, tropical area, Indian Ocean as well as the Antarctic coast (Figure 5-2). Its presence prove again the existence and the relevance of anionic organic iodine, which was recently found in the rain and snow samples collected in the continent boundary layer

and aerosols from Mace Head, Ireland (Gilfedder et al., 2007a, 2007b; Gilfedder et al., 2008), indicating that anionic organic iodine is globally ubiquitous. To obtain more detailed information on this species an investigation into the chemical structure of UOI is needed.

5.2.2 Spatial Variation of Iodine Species

The variation (concentration and relative contribution) of soluble iodine and its species were found to correlate with the different geographic locations. To investigate the spatial variation, the sampling regions were separated into coast (denoted as "C") and open ocean (denoted as "O") and classified into several subgroups as: C1, Chinese coast; C2, Southeast Asia where islands spread; C3, Australian coast; C4, Antarctic coast. O1, South China Sea; O2, the ocean between Southeast Asia and Australia; O3, the ocean between Australia and Antarctica. In general, the levels of TSI in the coastal regions were higher than over the open ocean except C4, which was locates on the Antarctic coast and had the lowest concentration at 3.22 pmol m^{-3}. The levels of TSI in the coastal regions decreased by an order: C1, C2, C3, C4, indicating a decreasing trend from North hemisphere to South hemisphere.

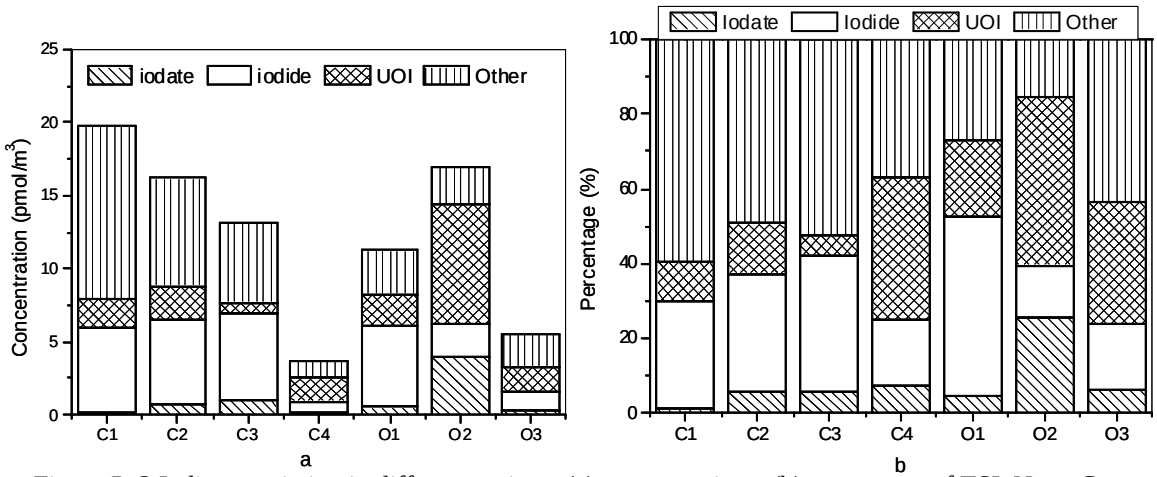

Figure 5- 3 Iodine speciation in different regions. (a) concentrations; (b) percentage of TSI. Note: C, costal area; O, open ocean. C1, China coast (n=5); C2, Southeast Asia (n=9); C3, the Australian coast (n=5); C4, the Antarctic coast (n=17); O1, the South China Sea (n=2); O2, the ocean between Southeast Asia and Australia (n=3); O3, the part of the Indian Ocean between Australia and Antarctica (n=16).

The variations in iodide, iodate and SOI were also similar to TSI. The ratios of iodate to iodide (IO_3^-/I^-) were highly variable, however, for most of cases, the ratios were in general lower than 1.0; except several outliers in C4, O2 and O3. This is in agreement with the previous findings in the Atlantic Ocean [*Baker et al., 2004*], indicating that higher levels of iodide than iodate in the marine boundary is a common phenomenon. For SOI, the highest fraction of UOI-0 was observed in C4, O2 and O3, with were 34.3%, 35.4% and 30.5% of SOI, respectively. In addition to iodide, iodate and UOI-0,

there was substantial amount of iodine not eluted out of the IC column during the measurements, e.g., it contributed 62.1%, 40.9%, 50.1% and 38.9% of the SOI in C1, C2, C3 and O3, respectively. The relative abundances of iodine species in different regions are summarized in Figure 5-3. The causes for the variation in iodine speciation and concentrations can be assumed to be connected to the flux of iodine from the oceans and cycling processes in the atmosphere.

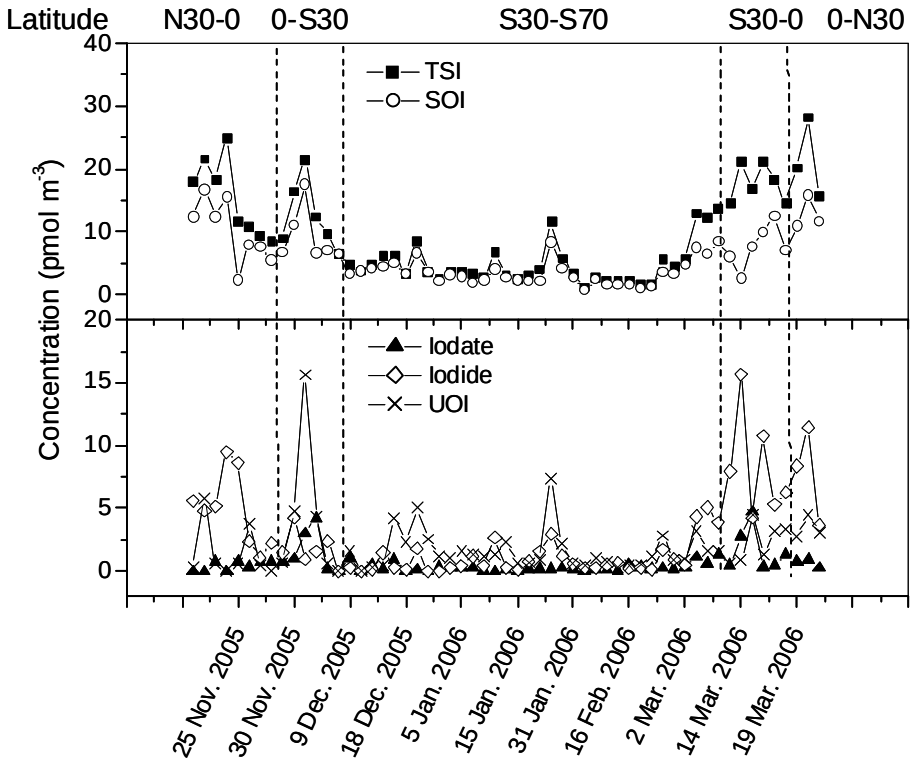

Figure 5- 4 Temporal and spatial variations of the different iodine species

The temporal variations in the iodine fraction concentrations are shown in the Figure 5-4. The locations with relatively higher TSI and SOI levels were located between latitude 30°N and 30°S. Tropical regions are well known to have relative higher abundance of algae blooms (Sparrow and Heimann, 2007), which in principle can release significant amounts of iodine precursors (e.g. I_2 and volatile organic iodine species) (O'Dowd and Hoffmann, 2005). Higher chlorophyll concentrations were observed along the cruise path in these tropical and subtropical coastal regions. The levels of TSI, iodide, iodate and UOI-0 were notably enhanced along the northwest coast of Australia; where there is may be the significant source of volatile organic iodine species due to highly productive ocean current upwelling. Biological activities such as macroalgae bloom can possibly contribute to the iodine precursor emissions. Temporal variations of TSI, SOI and iodide were also observed between the tropical area and the Australian coast. The concentrations of TSI and SOI were lower in December 2005 rather than in March 2006. This may be due to the seasonal variations in the halogen flux into the marine boundary layer (Carpenter et al., 1999; Carpenter et

al., 2000). Unfortunately, there are few reports on the seasonal concentrations of volatile organic iodine in this region. The concentrations of TSI, SOI, iodide and iodate were all found to be considerably lower during the sampling period in the Antarctica

5.2.3 Iodine and the Airmass Transport

The TSI levels were also found to be linked with the origin and direction of airmass transport. When the samples collected in the regions between Australia and Antarctica were derived from western airmass (previous 48 hours) the level of TSI was lower, indicating less soluble iodine were formed (or taken up into the particle phase) in the open India Ocean. Along the Antarctic coast (C4), the TSI concentrations increased when the previous 48 hours airmass had passed over ice front sector (in the east vicinity of Prydz Bay) instead of from Antarctic mainland.

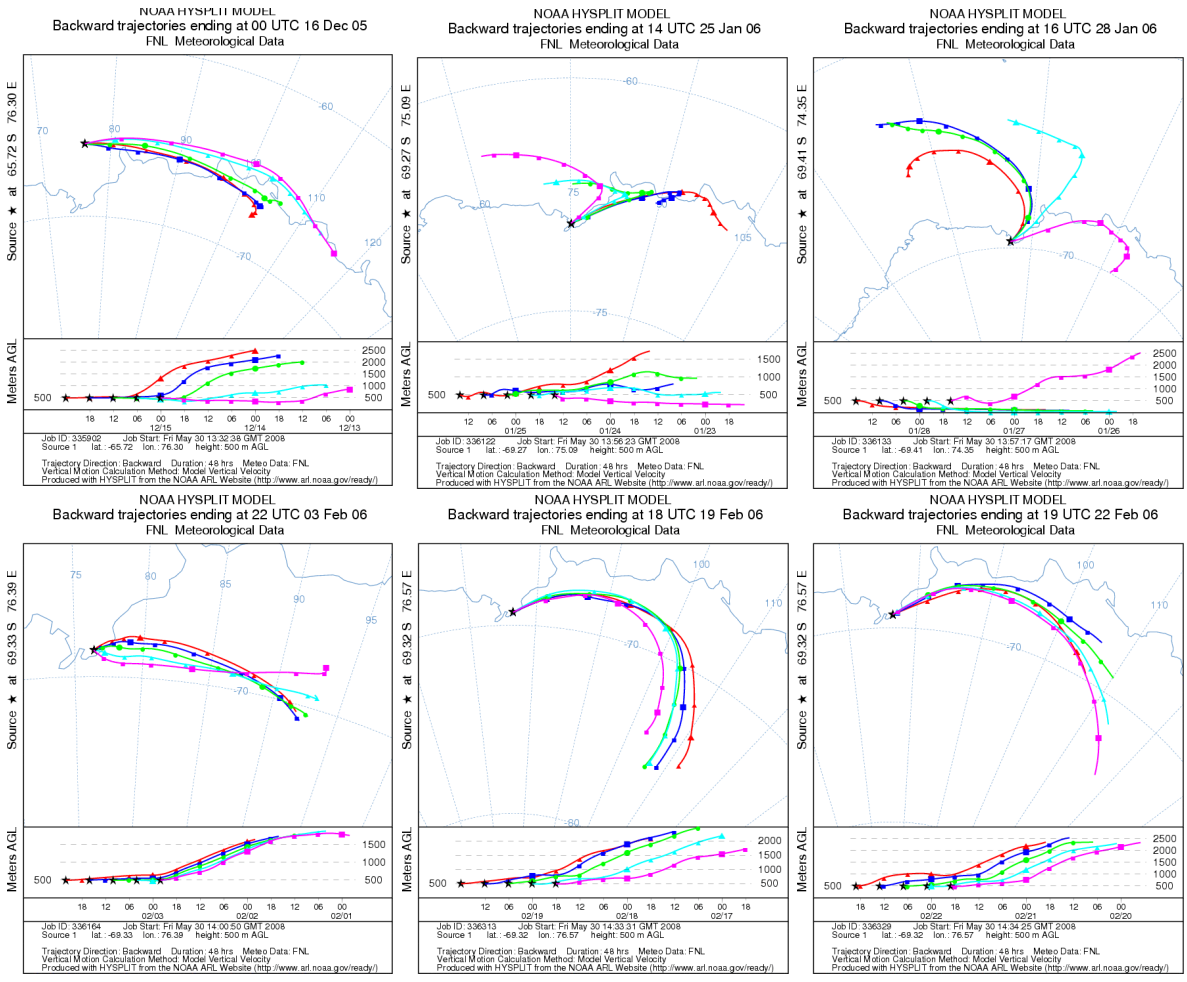

Figure 5- 5 Actual airmass back trajectories on the selected dates

In the Figure 5-5, the upper and lower three graphs display the airmass back trajectories for the highest and lowest TSI samples, respectively. The TSI levels were highly correlated with the airmass transport in the Antarctic coast. Although iodine in the

aerosol phase have not been reported to date, this finding is in accordance with the observations of IO and BrO in gas phases in coastal Antarctica (Halley Station), where airmass transport from the ice front sector increases the mixing ratios of IO and BrO (Saiz-Lopez et al., 2007). Recently a potential mechanism proposed that marine algae colonizing under the sea-ice and emit iodine precursors, which escape through brine channels into atmosphere(Saiz-Lopez and Boxe, 2008). The iodine speciation in marine aerosols in this study thus provides evidence to support this hypothesis.

5.2.4 Correlation between SOI and Iodide

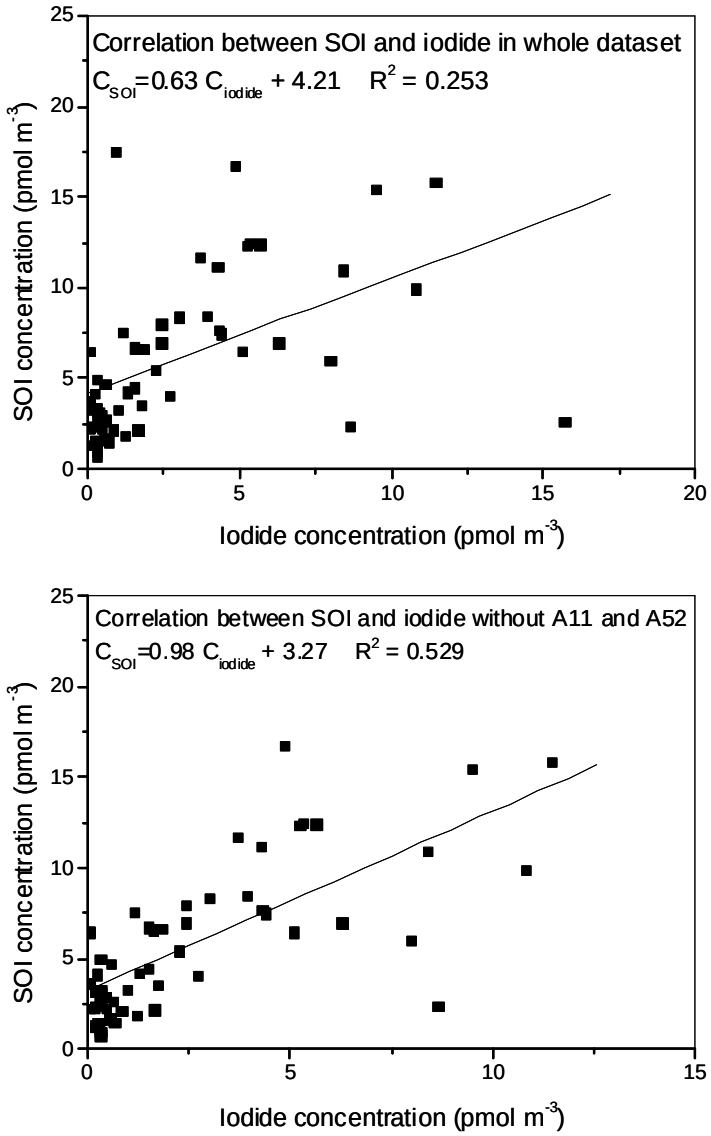

Figure 5- 6 Correlation between SOI and iodide in TSP samples

The chemical mechanisms involved in the iodine cycle are still poorly understood (O'Dowd and Hoffmann, 2005). One of the primary unknowns is whether the particle phase organic iodine components play an important role in the conversion of different iodine species, especially the formation of iodide. The relationship between iodide and

SOI was thus analyzed (Figure 5-6). The results suggested that the correlation between SOI and iodide in the whole dataset was poor but significant with the coefficient R^2 of 0.253 ($P<0.0001$). However, with the absence of two samples (A11 and A52) collected near Northwest Australia the correlation was then more significant with an coefficient R^2 of 0.529 ($P<0.05$). Although the different sizes of aerosols were collected in these several campaigns around the world, the correlations between SOI and iodide can always be found, indicating the SOI and iodide are closely related to each other in their formation processes, cycling etc. This strongly supports a recent hypothesis that iodide may be produced through the decomposition of SOI in the atmosphere (Pechtl et al., 2007; Gilfedder et al., 2008). However, the exact mechanism involved in this process is still unknown and expected to be investigated in the future.

5.3 Summary

Iodine speciation in marine aerosols is still poorly understood. During the 23th China Antarctic Campaign (November 2005 – March 2006) total suspended particle (TSP) samples were collected on the Chinese Ice braker *Xue Long* along a 30,000 km round-trip cruise path over the West Pacific Ocean, the East and South Indian Ocean, and Prydz Bay, the coastal Antarctica. Soluble iodine speciation was measured using IC-ICP-MS. The results revealed that organically bound iodine is the most abundant species, accounting for approximately 70% of TSI on average. An anionic organic iodine signal, namely UOI-0, is present in almost all of samples and is responsible for 22.1% of TSI. The signal is also shown in the chromatograms of the aerosols in different area around the world, indicating a global distribution of this signal. The abundances of inorganic iodine including iodide and iodate were less than 30% of TSI. The median value of iodide is 1.49 pmol m^{-3}, which is more than four-fold higher than that of iodate (median, 0.28 pmol m^{-3}). The level of TSI considerably varied with respect to the spatial distribution. High levels of iodine were observed in the region between latitude 30°N and 30°S, especially along Chinese coast and near northwestern Australia. The elevated TSI concentrations over the tropical ocean may be ascribed to potentially high flux of halocarbon due to macroalgae blooms initiated by upwelling current. In the coastal Antarctica, the observation of iodine species in aerosols is firstly reported in the Antarctic area. TSI is found to be correlated with the airmass transport. Enhanced levels of TSI were measured with the airmass transport from the ice front sector of the Antarctica, while lower TSI was found in the aerosols mainly contributed by the Antarctic continental airmass.

6. Summary and Outlook

Iodine is an essential element for all mammals and widely distributed in different all spheres, including the biosphere, the atmosphere and the geosphere (Edmonds and Morita, 1998). Iodine cycling in the MBL is suggested to play important roles in tropospheric ozone depletion as well as in new particle formation (O'Dowd and Hoffmann, 2005). This thesis concentrates on the method development for iodine speciation measurements in marine aerosols, field observations on aerosol iodine, and their implication for iodine cycling in the MBL.

6.1 Method Development for Iodine Measurement

ICP-MS is shown to be a sensitive, accurate and reliable technique for iodine measurements in the marine aerosol samples. The limits of detection (LODs) were both 0.1 μg L^{-1} for total iodine measurements in aerosol water extracts and aerosol TMAH extracts, which is sensitive enough for iodine measurement in the marine aerosol samples. Reproducibilites and recoveries were all within the requirement for iodine measurements in the ambient atmosphere. Quantification by external calibration and isotope dilution analysis were achieved successfully and no significant difference was found between the two methods.

Hyphenation techniques using ICP-MS as an iodine specific detector were also found to be fast, sensitive and accurate for soluble iodine speciation. IC and GE were both coupled to ICP-MS for soluble iodine speciation. Inorganic iodine species, iodide and iodate, were separated successfully and determined by ICP-MS. For the G3268A anion exchange column, the LODs for iodide and iodate were 0.5 μg L^{-1} and 0.1 μg L^{-1}, respectively; for AS16 anion exchange column, the LODs were both 0.03 μg L^{-1} for iodide and iodate. The LODs of GE-ICP-MS were both 0.5 μg L^{-1} for iodide and iodate. Reproducibilites and recoveries of the hyphenation techniques were satisfactory for soluble iodine speciation. In addition, unidentified signals (UOIs) were observed in the chromatograms of IC-ICP-MS with both columns and in the electropherograms of GE-ICP-MS. These species are believed to be polar anionic SOI in the marine aerosol, which are suitable for being retained by anion exchange column.

6.2 Global Distribution of Aerosol Iodine

The results from the four campaigns in this work have shown that iodine is ubiquitous in marine aerosols on a global scale. The sampling area included the West Irish coast, the North and South Atlantic Ocean, the West Pacific Ocean, the East and South Indian Ocean, and coastal Antarctica. Soluble iodine was detectable in all locations, in the

order of Mace Head > South Atlantic Ocean > North Atlantic Ocean >> West Pacific Ocean > Indian Ocean ≈ Antarctic coast. In general, the TSI variations were found to be correlated with biogenic activities (macro and micro algae blooms), showing a significant contribution from marine algae. Wet deposition played an important role in the TSI variation at Mace Head, which is suggested to be explained by the possible transfer of iodine species between aerosol particles and rainfall. Correlations were observed between new particle formation (nucleation) and the TSI concentration enhancement. In the South Atlantic Ocean and in costal Antarctica, TSI was highly correlated with the airmass history, showing higher TSI concentrations when the airmass were transported from the phytoplankton bloom area as well as from the ice front sector of coastal Antarctica, implying that the effects of airmass transport should not be neglected. The iodine contribution from the ice front sector in the coastal Antarctica indicates that an unknown mechanism may occur at the surface of the polar sea-ice, which was also suggested by iodine monoxide measurement in Antarctica (Saiz-Lopez et al., 2007; Saiz-Lopez and Boxe, 2008). The TII concentrations during the MHC was lower than the TSI, while comparable TII and TSI levels were measured during the CEC. It is likely that the open ocean may be a more important source for insoluble iodine in marine aerosols.

Soluble inorganic iodine was found to be only a minor iodine fraction in marine aerosols compared to SOI. Iodide concentrations were higher than iodate concentration in the fine particle mode (< 2.0 or 2.5 μm). This is accordance to the previous studies (Baker, 2005; Chen, 2005). Based on the results of the size fractionated samples, iodide was distributed evenly in the 5 stages, whilst iodate was enriched mainly in the coarse mode (size range: 2.0 – 10 μm), in particular in the range 2.0 – 5.9 μm. Consistent results were observed in both MHC and OOMPH campaigns.

6.3 Significance of Organic Iodine in Iodine Chemistry

SOI was the most abundant iodine fraction in the aerosols sampled during this work. The relatively contribution of SOI to TSI accounted for more than 90% at Mace Head, the North and South Atlantic Ocean as well as more than 70% during the cruise campaign from East Asia to Antarctica. In addition to the calculated SOI fraction (i.e. TSI – inorganic species), unidentified organic species (UOIs) were also measured by IC-ICP-MS and GE-ICP-MS, providing direct evidence of SOI in the aerosol particles. These UOIs should be polar anionic iodine species due to the ionic polarity separation in the IC columns.

Significant correlations were observed between SOI and iodide, implying a potential relationship between photochemical SOI decomposition and iodide formation. Such reactions have been reported to occur in the inshore seawater environment (Wong and Cheng, 2001).

$$DOM - I + h\nu \rightarrow DOM + I^{-} \qquad \text{(Reaction 6- 1)}$$

The iodinated marine gels or colloids and their decomposition products were observed globally in submicron aerosols (Leck and Bigg, 2005; Bigg, 2007; Leck and Bigg, 2008). These gels are transferred into the atmosphere by bubble bursting and observed by microscopy at particle size less than 50 nm sizes, implying that Reaction 6-1 may potentially occur in marine aerosols. The results from particle size ranges of 0.25 – 0.71 μm and 0.71 – 2.0 μm both presented better correlation between SOI and iodide during the day samples at Mace Head, especially showing most significant correlations during sunny days (Section 3.2.1). This further suggests the possibility of the SOI decomposition occurring in marine aerosols.

However, the abundant and widespread SOI in marine aerosols is not compatible with the current understanding of iodine chemistry in the MBL. The importance of organic matter participating in the iodine cycling is suggested in this work.

6.4 Outlook

6.4.1 Development of New Methods for Iodine Measurements

To date various techniques are applied to the measurements of iodine in the gas phase, particle phase, and aqueous phase (e.g. ICP-MS, NAA, DOAS, BBCRDS etc.) (Hou et al., 2000; Chen, 2005; Saiz-Lopez et al., 2006a). However, analytical challenges remain for iodine measurements especially for atmospheric iodine investigations.

Firstly, gaseous iodine measurements are vital for better understanding of the pathways of gaseous iodine reactions and for clarifying the gas-to-particle uptake process. Iodine oxides such as IO, OIO and elemental iodine (I_2) are mainly measured by DOAS in the field observations. One of the drawbacks of DOAS measurements is that it does not capture iodine emissions on small scales, for example inter tidal zones, averaging levels over a light path of at least a few km. Other techniques such as LIF (laser induced fluorescence) and CRDS (cavity ring-down spectroscopy) were introduced for IO and I_2 measurement recently and both appear to be suitable for measurement of IO on a small scale e.g. from coastal intertidal regions (Saiz-Lopez et al., 2006a; Wada et al., 2007; Whalley et al., 2007). In addition, HOI is thought to be a reactive iodine species which may be responsible for the reaction with organic matter to form organic iodine. According to a modeling study, HOI was suggested as the dominant tropospheric iodine-containing species at altitudes below 8 km (Davis et al., 1996) but the determination of HOI is still an analytical challenge due to its reactivity in the atmosphere. Interhalogens such as ICl and IBr are believe to significantly increase the gaseous halogen reservoir and suitable techniques are seldom reported (Vogt, 1999).

Recently the denuder technique for differentiation of ICl, IBr and I_2 are also reported as a promising technique for field reactive halogen observation (Huang and Hoffmann, 2008). The state of the science of gaseous iodine species measurements shows that more reliable techniques are necessary in the future.

Although more research focus has been given to aerosol iodine measurements, field observations are still limited (Baker et al., 2000; Baker et al., 2001; Baker, 2004, , 2005; Chen, 2006; Gilfedder et al., 2008). Iodide and iodate can be measured by many different techniques so far. New challenge arises for organic iodine measurement: both soluble and insoluble iodine. Anion exchange chromatography coupled to ICP-MS was shown to be possible for soluble organic iodine measurements (Gilfedder et al., 2008). Also, SOI signals appeared in the electropherograms from GE-ICP-MS (section 2.5.2) and chromatograms of Reverse Phase Liquid Chromatography (RPLC) -ICP-MS (Figure 6-1). A preliminary work was conducted by coupling of a RPLC and a high resolution ICP-MS (Element2, Thermo, Bremen, Germany). This method for organic iodine separation and quantification seems promising as RP column is thought to be universal for organic compound separation. Thus more improvement for the compatibility between RPLC and ICP-MS should be made for this method in the future (Lai et al., 2007). The mentioned organic iodine signals found in the newly developed methods are still not identified until now. In addition to SOI, insoluble iodine is seldom analyzed and no speciation work had been done (Chen, 2005). Therefore, novel techniques are expected to be used for soluble and insoluble iodine measurement in the future.

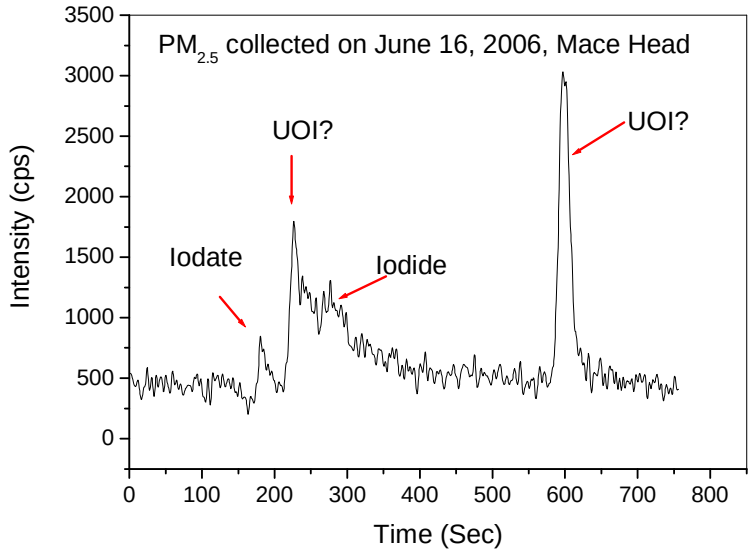

Figure 6- 1 Chromatograms of $PM_{2.5}$ marine aerosol measured by RP-HPLC-ICP-MS

In recent years, Aerosol Mass Spectrometry (AMS) has been applied to investigate

aerosol formation from iodine containing emission in laboratory chambers, in which several particulate iodine species such as IO^+, HIO^+, IO_2^+, HIO_2^+, HIO_3^+, IO_5^+, I_2O^+ and $I_2O_3^+$ have been detected (Jimenez et al., 2003). However, no field measurement for iodine in aerosols has been reported by this technique to date. Online measuring method is always ideal for monitoring actual products during the atmospheric reactions and for mechanism investigation. However detection limits may be problematic for aerosol iodine measurement.

6.4.2 Mechanism Investigation on Iodine Chemistry

Iodine precursors driven nucleation events have been observed at Mace Head (O'Dowd et al., 2002a). However, the nucleation events driven by iodine chemistry in the coastal areas are not always observed, despite rather extensive macro algae beds at other coastal sites such as Cape Grim, Tasmania, Australia (Cainey et al., 2007). The question arises whether iodine driven nucleation provides a source of particles of global importance. The global flux of iodine driven nucleation events is vital to estimate the impact of iodine chemistry on climate change on a global scale.

More investigations are needed on the release mechanisms of iodine precursors such as I_2 and volatile organic iodine. I_2 is regarded as the main iodine precursor in the MBL iodine cycle (McFiggans et al., 2004) but the release mechanisms are still not fully understood especially in the open ocean(O'Dowd and Hoffmann, 2005; O'Dowd and De Leeuw, 2007). Whether the pathways of I_2 release into the atmosphere is exclusively and directly connected with the biological processes or also consist of an abiotic process at the air-sea interface is currently not known (O'Dowd and Hoffmann, 2005). The significantly lower biogenic emissions over the open ocean when compared with the coastal ozone imply the mechanism diversity of volatile iodine release in the open ocean (O'Dowd and De Leeuw, 2007). The ice front sector in coastal Antarctica is also thought to be an area with large iodine flux and a new hypothesis of volatile iodine release in the sea-ice brine was proposed (Saiz-Lopez et al., 2007; Saiz-Lopez and Boxe, 2008). Further works should be designed to evaluate the release mechanisms of iodine precursors based on both lab experiments and field observations. Their roles in open ocean particle production are valuable for further exploration.

The relatively abundant SOI measured in the marine aerosols was recently emphasized by several studies (Baker, 2005; Gilfedder et al., 2008). The sources of SOI as well as the formation mechanisms are still open questions. Reaction between HOI and organic matter in gas phase is taken as the most possible mechanism for organic iodine formation and subsequently taken up into the particle phase.

$$Org - H + HOI \rightarrow Org - I + H_2O \qquad \text{(Reaction 6- 2)}$$

Also, by analogy with the known reactivity of dissolved organic iodine in seawater, the decay of SOI provides a route for the formation of aerosol iodide (Baker, 2005; Gilfedder et al., 2008). Nevertheless, there is little data gathered to date to evaluate formation mechanisms of SOI and their exact roles in aerosols. Identification and quantification of organic iodine is necessary and new modeling should be conducted, which will improve the current understanding of iodine chemistry.

Reference

Allan, B.J., Planc, J.M., Mcfiggans, G., 2001. Observations of OIO in the remote marine boundary layer. Geophysical Research Letters 28, 1945-1948.

Baker, A.R., 2004. Inorganic iodine speciation in tropical Atlantic aerosol. Geophysical Research Letters 31, L23S02.

Baker, A.R., 2005. Marine aerosol iodine chemistry: The importance of soluble organic iodine. Environmental Chemistry 2, 295-298.

Baker, A.R., Thompson, D., Campos, M.L.A.M., Parry, S.J., Jickells, T.D., 2000. Iodine concentration and availability in atmospheric aerosol. Atmospheric Environment 34, 4331-4336.

Baker, A.R., Tunnicliffe, C., Jickells, T.D., 2001. Iodine speciation and deposition fluxes from the marine atmosphere. Journal of Geophysical Research 106, 28743-28749.

Bassford, M.R., Nickless, G., Simmonds, P.G., Lewis, A.C., Pilling, M.J., Evans, M.J., 1999. The concurrent observation of methyl iodide and dimethyl sulphide in marine air; implications for sources of atmospheric methyl iodide. Atmospheric Environment 33, 2373-2383.

Berner, A., Lurzer, C., 1980. Mass Size Distributions of Traffic Aerosols at Vienna. Journal of Physical Chemistry 84, 2079-2083.

Bigg, E.K., 2007. Sources, nature and influence on climate of marine airborne particles. Environmental Chemistry 4, 155-161.

Bolin, B., 1959. Note on the Exchange of Iodine between the Atmosphere, Land and Sea. International Journal of Air Pollution 2, 127-131.

Brauer, F.P., Rieck, H.G., Jr., Hooper, R.L., 1974. Particulate and gaseous atmospheric iodine concentrations. IAEA, IAEA-SM-181/6, CONF-731110, 20 p., Vienna.

Bruchert, W., Helfrich, A., Zinn, N., Klimach, T., Breckheimer, M., Chen, H.W., Lai, S.C., Hoffmann, T., Bettmer, J., 2007. Gel electrophoresis coupled to inductively coupled plasma-mass spectrometry using species-specific isotope dilution for iodide and iodate determination in aerosols. Analytical Chemistry 79, 1714-1719.

Cainey, J.M., Keywood, M., Grose, M.R., Krummel, P., Galbally, I.E., Johnston, P., Gillett, R.W., Meyer, M., Fraser, P., Steele, P., Harvey, M., Kreher, K., Stein, T., Ibrahim, O., Ristovski, Z.D., Johnson, G., Fletcher, C.A., Bigg, E.K., Gras, J.L., 2007. Precursors to Particles (P2P) at Cape Grim 2006: campaign overview. Environmental Chemistry 4, 143-150.

Calvert, J.G., Lindberg, S.E., 2004. Potential influence of iodine-containing compounds on the chemistry of the troposphere in the polar spring. I. Ozone depletion. Atmospheric Environment 38, 5087-5104.

Campos, M., Nightingale, P.D., Jickells, T.D., 1996. A comparison of methyl iodide emissions from seawater and wet depositional fluxes of iodine over the southern North Sea. Tellus Series B-Chemical and Physical Meteorology 48, 106-114.

Carpenter, L.J., 2003. Iodine in the Marine Boundary Layer. Chemical Review 103, 4953-4962.

Carpenter, L.J., Hebestreit, K., Platt, U., Liss, P.S., 2001. Coastal zone production of IO precursors: a 2-dimensional study. Atmos. Chem. Phys. 1, 9-18.

Carpenter, L.J., Lewis, A.C., 2002. Ocean-atmosphere exchange of reactive halocarbons and hydrocarbons. Recent Research Developments in Geophysics 4, 45-56.

Carpenter, L.J., Liss, P.S., Penkett, S.A., 2003. Marine organohalogens in the atmosphere over the Atlantic and Southern oceans. Journal of Geophysical Research (Amospheres) 108, ACH 1/1 - ACH 1/13.

Carpenter, L.J., Malin, G., Kuepper, F., Liss, P.S., 2000. Novel biogenic iodine-containing trihalomethanes and other short-lived halocarbons in the coastal East Atlantic. Global Biogeochem. Cycles 14, 1191-1204.

Carpenter, L.J., Sturges, W.T., Penkett, S.A., Liss, P.S., Alicke, B., Hebestreit, K., Platt, U., 1999. Short-lived alkyl iodides and bromides at Mace Head, Ireland: links to biogenic sources and halogen oxide production. Journal of Geophysical Research (Atmospheres) 104, 1679-1689.

Chance, R., Malin, G., Jickells, T., Baker, A.R., 2007. Reduction of iodate to iodide by cold water diatom cultures. Marine Chemistry 105, 169-180.

Chen, H., 2005. Development of analytical methodologies for iodine species in gaseous and particulate phases of the coastal atmosphere. University of Mainz.

Chen, H., Brandt, R., Bandur, R., Hoffmann, T., 2006. Characterization of iodine species in the marine aerosol: to understand theirs roles in the particle formation processes. Frontiers of Chemistry in China 1, 119-129.

Collen, J., Ekdahl, A., Abrahamsson, K., Pedersen, M., 1994. The Involvement of Hydrogen-Peroxide in the Production of Volatile Halogenated Compounds by Meristiella-Gelidium. Phytochemistry 36, 1197-1202.

Davis, D., Crawford, J., Liu, S., McKeen, S., Bandy, A., Thornton, D., Rowland, F., Blake, D., 1996. Potential impact of iodine on tropospheric levels of ozone and other critical oxidants. Journal of Geophysical Research-Atmospheres 101, 2135-2147.

Duce, R.A., Hoffman, E.J., 1976. Chemical Fractionation at Air-Sea Interface. Annual Review of Earth and Planetary Sciences 4, 187-228.

Duce, R.A., Winchest.Jw, Vannahl, T.W., 1965. Iodine Bromine and Chlorine in Hawaiian Marine Atmosphere. Journal of Geophysical Research 70, 1775-&.

Edmonds, J.S., Morita, M., 1998. The determination of iodine species in environmental and biological samples (Technical report). Pure and Applied Chemistry 70, 1567-1584.

Flanagan, R.J., Geever, M., O'Dowd, C.D., 2005. Direct measurements of new-particle fluxes in the coastal environment. Environmental Chemistry 2, 256-259.

Friess, U., Wagner, T., Pundt, I., Pfeilsticker, K., Platt, U., 2001. Spectroscopic measurements of tropospheric iodine oxide at Neumayer Station, Antarctica. Geophysical Research Letters 28, 1941-1944.

Gaebler, H.E., Heumann, K.G., 1993. Determination of particulate iodine in aerosols from different regions by size fractionating impactor sampling and IDMS. Int. J. Environ. Anal. Chem. 50, 129-146.

Garland, J.A., Curtis, H., 1981. Emission of iodine from the sea surface in the presence of ozone. J. Geophys. Res. 86, 3183-3196.

Gilfedder, B.S., 2007. Observations of iodine speciation and cycling in the hydrosphere. PhD thesis in University of Heiderberg.

Gilfedder, B.S., Lai, S.C., Petri, M., Biester, H., Hoffmann, T., 2008. Iodine speciation in rain, snow and aerosols and possible transfer of organically bound iodine species from aerosol to droplet phases. Atmospheric Chemistry and Physics Discussions 8, 7977-8008.

Gilfedder, B.S., Petri, M., Biester, H., 2007a. Iodine and bromine speciation in snow and the effect of orographically induced precipitation. Atmospheric Chemistry and Physics 7, 2661-2669.

Gilfedder, B.S., Petri, M., Biester, H., 2007b. Iodine speciation in rain and snow: Implications for the atmospheric iodine sink. Journal of Geophysical Research-Atmospheres 112.

Heumann, K.G., Gallus, S.M., Rälinger, G., Vogl, J., 1998. Accurate determination of element species by on-line coupling of chromatographic system with ICP-MS using isotope dilution technique. Spectrochimica Acta Part B 53, 273-287.

Hinds, W.C., 1999. Aerosol Technology.

Hoffmann, T., O'Dowd, C.D., Seinfeld, J.H., 2001. Iodine oxide homogeneous nucleation: An explanation for coastal new particle production. Geophysical Research Letters 28, 1949-1952.

Hoffmann, T., Warnke, J., 2007. Organic Aerosols. In: Koppmann, R. (Ed.). Volitale Organic Compounds in the Atmosphere. Blackwell, Oxford, pp. 342-387.

Holmes, N.S., Adams, J.W., Crowley, J.N., 2001. Uptake and reaction of HOI and on frozen and dry IONO2 NaCl/NaBr surfaces and H2SO4. Phys. Chem. Chem. Phys. 3, 1679-1687.

Hou, X., Dahlgaard, H., Rietz, B., U.Jacobsen, S.P.Nielsen, 2000. Pre-separation neutron activation analysis of seawater urine and milk for iodide and iodate. Journal of Radioanalytical and Nuclear Chemistry 244, 87-91.

Hou, X., Dahlgaard, H., Rietz, B., U.Jacobsen, S.P.Nielsen, A.Aarkrog, 1999. Determination of Chemical Species of Iodine in Seawater by Radiochemical Neutron ActivationAnalysis Combined with Ion-Exchange Preseparation. Anal. Chem. 71, 2745-2750.

Huang, R.J., Hoffmann, T., 2008. Determination of highly reactive halogen species in the remote marine boundary layer. Post in European Geosciences Union General Assembly 2008, Vienna, Austria.

Huang, S., Arimoto, R., Rahn, K.A., 2001. Sources and source variations for aerosol at Mace Head, Ireland. Atmospheric Environment 35, 1421-1437.

Jenkin, M.E., 1992. The photochemistry of iodine-containing compounds in the marine boundary layer. Environ. and Energy Rep. AEA EE-0405; AEA Harwell Lab.; Oxfordshire, England.

Jimenez, J.L., III, D.R.C., Bahreini, R., Zhuang, H., Varutbangkul, V., Flagan, R.C., Seinfeld, J.H., O'Dowd, C., Hoffmann, T., 2003. New particle formation from photooxidation of diiodomethane. Journal of Geophysical Research 108, 4318.

Klick, S., Abrahamsson, K., 1992. Biogenic Volatile Iodated Hydrocarbons in the Ocean. Journal of Geophysical Research-Oceans 97, 12683-12687.

Kolb, C.E., 2002. Iodine's air of importance. Nature 417, 597-598.

Kupper, F.C., Carpenter, L.J., McFiggans, G.B., Palmer, C.J., Waite, T.J., Boneberg, E.M., Woitsch, S., Weiller, M., Abela, R., Grolimund, D., Potin, P., Butler, A., Luther, G.W., Kroneck, P.M.H., Meyer-Klaucke, W., Feiters, M.C., 2008. Iodide accumulation provides kelp with an inorganic antioxidant impacting atmospheric chemistry. Proc. Natl. Acad. Sci. U. S. A. 105, 6954-6958.

Küpper, F.C., Müller, D.G., Peters, A.F., Kloareg, B., Phillppe, P., 2002. Oligoalginate recognition and oxidative burst play a key role in natural and induced resistance of sporophytes of laminariales. J. Chem. Ecol 28, 2057-2081.

Lai, S.C., Warnke, J., Thiermann, R., Hoffmann, T., 2007. Determination of iodate and iodide in marine aerosols by HPLC-ICP-MS. 11th Workshop on Progress in Analytical Methodologies for Trace Metal Speciation, Munster.

Landsberger, S., Basunia, M.S., Iskander, F., 2001. Halogen determination in Arctic aerosols by neutron activation analysis with Compton suppression methods. Journal of Radioanalytical and Nuclear Chemistry 249, 303-305.

Laturnus, F., Giese, B., Wiencke, C., Adams, F.C., 2000. Low-molecular-weight organoiodine and organobromine compounds released by polar macroalgae – The influence of abiotic factors. Fresenius J Anal Chem 368.

Leck, C., Bigg, E.K., 2005. Source and evolution of the marine aerosol - A new perspective. Geophysical Research Letters 32.

Leck, C., Bigg, E.K., 2008. Comparison of sources and nature of the tropical aerosol with the summer high Arctic aerosol. Tellus Series B-Chemical and Physical Meteorology 60, 118-126.

Liss, P.S., Slater, P.G., 1974. Flux of Gases across Air-Sea Interface. Nature 247, 181-184.

Loo, B.W., Cork, C.P., 1988. Development of High-Efficiency Virtual Impactors. Aerosol Science and Technology 9, 167-176.

Lovelock, J.E., 1975. Natural halocarbons in the air and in the sea. Nature 256, 193-194.

Marple, V.A., Olson, B.A., Rubow, K.L., 2001. Inertial, Gravitational, Centrifugal, and Thermal Collection Techniques. In: Baron, P.A., Willeke, K. (Eds.). Aerosol Measurement - Principles, Techiques, and Applications. John Wiley & Sons, pp. 229-260.

McFiggans, G., 2005. Marine aerosols and iodine emissions. Nature 433, E13-E13.

McFiggans, G., Coe, H., Burgess, R., Allan, J., Cubison, M., Alfarra, M.R., Saunders, R., Saiz-Lopez, A., Plane, J.M.C., Wevill, D.J., Carpenter, L.J., Rickard, A.R., Monks, P.S., 2004. Direct evidence for coastal iodine particles from Laminaria macroalgae - linkage to emissions of molecular iodine. Atmospheric Chemistry and Physics 4, 701-713.

McFiggans, G., Plane, J.M.C., Allan, B.J., Carpenter, L.J., Coe, H., O'Dowd, C., 2000. A modeling study of iodine chemistry in the marine boundary layer. Journal of Geophysical Research-Atmospheres 105, 14371-14385.

Michalke, B., Schramel, P., 1999. Iodine speciation in biological samples by capillary electrophoresis - inductively coupled plasma mass spectrometry. Electrophoresis 20, 2547-2553.

Misra, A., Marshall, P., 1998. Computational investigations of iodine oxides. J. Phys. Chem. A 102, 9056-6060.

Miyake, Y., Tsunogai, S., 1963. Evaporation of iodine from the ocean. J. Geophys. Res. 68, 3989-3993.

Moore, R.M., 2003. Marine Source of Volatile Organohalogens. The Handbook of Environmental Chemistry, Vol.3, Part P. Springer-Verlag, Berlin, pp. 85-101.

Moore, R.M., Tokarczyk, R., 1993. Volatile Biogenic Halocarbons in the Northwest Atlantic. Global Biogeochemical Cycles 7, 195-210.

Moore, R.M., Webb, M., Tokarczyk, R., Wever, R., 1996. Bromoperoxidase and iodoperoxidase enzymes and production of halogenated methanes in marine diatom cultures. Journal of Geophysical Research-Oceans 101, 20899-20908.

Moore, R.M., Zafiriou, O.C., 1994. Photochemical Production of Methyl-Iodide in Seawater. Journal of Geophysical Research-Atmospheres 99, 16415-16420.

Moyers, J.L., Duce, R.A., 1972. Gaseous and particulate iodine in the marine atmosphere. J. Geophys. Res. 77, 5229-5238.

Moyers, J.L., Duce, R.A., Zoller, W.H., 1970. Gaseous Iodine and Bromine in Marine Atmosphere. Transactions-American Geophysical Union 51, 323-&.

Mtolera, M.S.P., Collen, J., Pedersen, M., Ekdahl, A., Abrahamsson, K., Semesi, A.K., 1996. Stress-induced production of volatile halogenated organic compounds in Eucheuma denticulatum (Rhodophyta) caused by elevated pH and high light intensities. European Journal of Phycology 31, 89-95.

Muller, G., 2003. Sense or no-sense of the sum parameter for water soluble "adsorbable organic halogens" (AOX) and "absorbed organic halogens" (AOX-S18) for the assessment of organohalogens in sludges and sediments. Chemosphere 52, 371-379.

Muramatsu, Y., Wedepohl, K.H., 1998. The distribution of iodine in the earth's crust. Chemical Geology 147, 201-216.

Murphy, D.M., Thomson, D.S., Middlebrook, A.M., 1997. Bromine, iodine, and chlorine in single aerosol particles at Cape Grim. Geophysical Research Letters 24, 3197-3200.

O'Dowd, C.D., De Leeuw, G., 2007. Marine aerosol production: a review of the current knowledge. Philosophical Transactions of the Royal Society a-Mathematical Physical and Engineering Sciences 365, 1753-1774.

O'Dowd, C.D., Hämeri, K., Mäkelä, J.M., Pirjola, L., Kulmala, M., al., e., 2002a. A dedicated study of New Particle Formation and Fate in the Coastal Enviroment (PARFORCE): Overview of objectives and achievements. Journal of Geophysical Research 107, 8108.

O'Dowd, C.D., Hoffmann, T., 2005. Coastal new particle formation: A review of the current state-of-the-art. Environmental Chemistry 2, 245-255.

O'Dowd, C.D., Jimenez, J.l., Bahreini, R., Flagan, R.C., Seinfeld, J.H., Hämeri, K., Pirjola, L., Kulmala, M., Jenning, S.G., Hoffmann, T., 2002b. Marine aerosol formation from biogenic iodine emissions. Nature 417, 632-634.

Palmer, C.J., Anders, T.L., Carpenter, L.J., Kupper, F.C., McFiggans, G.B., 2005. Iodine and halocarbon response of Laminaria digitata to oxidative stress and links to atmospheric new particle production. Environmental Chemistry 2, 282-290.

Pechtl, S., Schmitz, G., von Glasow, R., 2007. Modelling iodide-iodate speciation in atmospheric aerosol: Contributions of inorganic and organic iodine chemistry. Atmospheric Chemistry and Physics 7, 1381-1393.

Phillips, L.F., 1991. Co2 Transport at the Air-Sea Interface - Effect of Coupling of Heat and Matter Fluxes. Geophysical Research Letters 18, 1221-1224.

Rädlinger, G., Heumann, K.G., 1998. Iodine Determination in Food Samples Using Inductively Coupled Plasma Isotope Dilution Mass Spectrometry. Anal. Chem. 70, 2221-2224.

Rahn, K.A., Borys, R.D., Duce, R.A., 1977. Determination of Inorganic and Organic Components of Gaseous Chlorine, Bromine, and Iodine in The Atmosphere. WMO [Publ.] (Air Pollut. Meas. Tech.), Part-II. 460, 172-1728.

Read, K.A., Mahajan, A.S., Carpenter, L.J., Evans, M.J., Faria, B.V.E., Heard, D.E., Hopkins, J.R., Lee, J.D., Moller, S.J., Lewis, A.C., Mendes, L., McQuaid, J.B., Oetjen, H., Saiz-Lopez, A., Pilling, M.J., Plane, J.M.C., 2008. Extensive halogen-mediated ozone destruction over the tropical Atlantic Ocean. Nature 453, 1232-1235.

Richter, U., Wallace, D.W.R., 2004. Production of methyl iodide in the tropical Atlantic Ocean. Geophysical Research Letters 31.

Rosinski, J.P., F, 1966. Terpene-Iodine Compounds as Ice Nuclei. Journal of Applied Meteorology 5, 119-123.

Saionz, P., Bookalam, J., Miller, R.A., 2006. Separation of periodate, iodate and iodide on a C-18 stationary phase. Dependence of the retention on the temperature and solvent composition. Monitoring of an oxidative cleavage reaction. Chromatographia 64, 635-640.

Saiz-Lopez, A., Boxe, C.S., 2008. A mechanism for biologically-induced iodine emissions from sea-ice. Atmospheric Chemistry and Physics Discussions 8, 2953-2976.

Saiz-Lopez, A., Mahajan, A.S., Salmon, R.A., Bauguitte, S.J.B., Jones, A.E., Roscoe, H.K., Plane, J.M.C., 2007. Boundary layer halogens in coastal Antarctica. Science 317, 348-351.

Saiz-Lopez, A., Plane, J.M.C., 2004. Novel iodine chemistry in the marine boundary layer. Geophysical

Research Letters 31, L04112.

Saiz-Lopez, A., Plane, J.M.C., McFiggans, G., Williams, P.I., Ball, S.M., Bitter, M., Jones, R.L., Hongwei, C., Hoffmann, T., 2006a. Modelling molecular iodine emissions in a coastal marine environment: the link to new particle formation. Atmospheric Chemistry and Physics 6, 883-895.

Saiz-Lopez, A., Saunders, R.W., Joseph, D.M., Ashworth, S.H., Plane, J.M.C., 2004. Absolute absorption cross-section and photolysis rate of I2. Atmos. Chem. Phys. 4, 1443-1450.

Saiz-Lopez, A., Shillito, J.A., Coe, H., Plane, J.M.C., 2006b. Measurements and modelling of I-2, IO, OIO, BrO and NO3 in the mid-latitude marine boundary layer. Atmospheric Chemistry and Physics 6, 1513-1528.

Saunders, R.W., Plane, J.M.C., 2005. Formation pathways and composition of iodine oxide ultra-fine particles. Environmental Chemistry 2, 299-303.

Schall, C., Heumann, K.G., 1993. GC determination of volatile organoiodine and organobromine compounds in Arctic seawater and air samples. Fresenius J. Anal. Chem. 346, 717-722.

Schonhardt, A., Richter, A., Wittrock, F., Kirk, H., Oetjen, H., Roscoe, H.K., Burrows, J.P., 2008. Observations of iodine monoxide columns from satellite. Atmospheric Chemistry and Physics 8, 637-653.

Sellegri, K., Loon, Y.J., Jennings, S.G., O'Dowd, C.D., Pirjola, L., Cautenet, S., Chen, H.W., Hoffmann, T., 2005. Quantification of coastal new ultra-fine particles formation from in situ and chamber measurements during the BIOFLUX campaign. Environmental Chemistry 2, 260-270.

Seto, F.Y.B., Duce, R.A., 1971. Laboratory Study of Iodine Enrichment on Atmospheric Sea Salt Particles. Transactions-American Geophysical Union 52, 256-&.

Simpson, W.R., von Glasow, R., Riedel, K., Anderson, P., Ariya, P., Bottenheim, J., Burrows, J., Carpenter, L.J., Friess, U., Goodsite, M.E., Heard, D., Hutterli, M., Jacobi, H.W., Kaleschke, L., Neff, B., Plane, J., Platt, U., Richter, A., Roscoe, H., Sander, R., Shepson, P., Sodeau, J., Steffen, A., Wagner, T., Wolff, E., 2007. Halogens and their role in polar boundary-layer ozone depletion. Atmospheric Chemistry and Physics 7, 4375-4418.

Singh, H.B., Salas, L.J., Stiles, R.E., 1983. Methyl halides in and over the eastern Pacific (40 N-32 S). J. Geophys. Res. 88, 3684-3690.

Sparrow, L., Heimann, K., 2007. The influence of nutrients and temperature on the global distribution of algal blooms.

Sturges, W.T., Barrie, L.A., 1988. Chlorine, Bromine and Iodine in Arctic Aerosols. Atmospheric Environment 22, 1179-1194.

Stutz, J., Hebestreit, K., Alicke, B., Platt, U., 1999. Comparison of model calculations with recent field data. J. Atmos. Chem. 34, 65-85.

Stutz, J., Pikelnaya, O., Hurlock, S.C., Trick, S., Pechtl, S., von Glasow, R., 2007. Daytime OIO in the gulf of Maine. Geophysical Research Letters 34.

Theiler, R., Cook, J.C., Hager, L.P., 1978. Halohydrocarbon Synthesis by Bromoperoxidase. Science 202, 1094-1096.

Thompson, A.M., Zafiriou, O.C., 1983. Air-sea fluxes of transient atmospheric species. J. Geophys. Res. 88, 6696-6708.

Tian, R.C., Nicolas, E., 1995. Iodine Speciation in the Northwestern Mediterranean-Sea - Method and Vertical Profile. Marine Chemistry 48, 151-156.

Truesdale, V.W., 1978. Iodine in Inshore and Off-Shore Marine Waters. Marine Chemistry 6, 1-13.

Truesdale, V.W., Jones, S.D., 1996. The variation of iodate and total iodine in some UK rainwaters during 1980-1981. Journal of Hydrology 179, 67-86.

Truesdale, V.W., Luther, G.W., Canosamas, C., 1995. Molecular-Iodine Reduction in Seawater - an Improved Rate-Equation Considering Organic-Compounds. Marine Chemistry 48, 143-150.

Tsunogai, S., 1971. Iodine in the deep water of the ocean. Deep-Sea Res. 18, 913-919.

Ullman, W.J., G.W., L., G.J., d.L., J.R.W., W., 1990. Iodine chemistry in deep anoxic basins and overlying waters of the Mediterranean Sea. Marine Chemistry 31, 153-170.

Vakeva, M., Hameri, K., Aalto, P.P., 2002. Hygroscopic properties of nucleation mode and Aitken mode particles during nucleation bursts and in background air. Journal of Geophysical Research-Atmospheres 107.

Vogt, R., 1999. Iodine Compounds in the Atmosphere. The Handbook of Environmental Chemistry Vol. 4 Part E. Springer-Verlag, Berlin Heidelberg, pp. 114-128.

Vogt, R., Sander, R., Glasow, R.v., Crutzen, P.J., 1999. Iodine Chemistry and its Role in Halogen Activation and Ozone Loss in the Marine Boundary Layer: A Model Study. Journal of Atmospheric Chemistry 32, 375–395.

von Glasow, R., Crutzen, P.J., 2003. Tropospheric halogen chemistry. . In: D., H.H., Turekian, K.K. (Eds.). Treatise on Geochemistry. Elsevier, pp. 21-63.

von Glasow, R., Crutzen, P.J., 2007. Tropospheric halogen chemistry. . In: D., H.H., Turekian, K.K. (Eds.). Treatise on Geochemistry. Elsevier, pp. 21-63.

von Glasow, R., Sander, R., Bott, A., Crutzen, P.J., 2002. Modeling halogen chemistry in the marine boundary layer - 1. Cloud-free MBL. Journal of Geophysical Research-Atmospheres 107.

Wada, R., Beames, J.M., Orr-Ewing, A.J., 2007. Measurement of IO radical concentrations in the marine boundary layer using a cavity ring-down spectrometer. Journal of Atmospheric Chemistry 58, 69-87.

Waite, T.J., Truesdale, V.W., 2003. Iodate reduction by Ioschrysis galbana is relatively insensitive to de-activation of nitrate reductase activity - are phytoplankton really responsible for iodate reduction in seawater? Marine Chemistry 81, 137-148.

Watson, J.G., Chow, J.C., 2001. Ambient air sampling. In: Baron, P.A., Willeke, K. (Eds.). Aerosol Measurement - Principles, Techniques and Applications. John Wiley & Sons, pp. 821-844.

Wever, R., Tromp, M.G.M., Krenn, B.E., Marjani, A., Van Tol, M., 1991. Brominating activity of the seaweed ascophyllum nodosum: impact on the biosphere. Environ Sci. Technol. 25, 446-449.

Whalley, L.K., Furneaux, K.L., Gravestock, T., Atkinson, H.M., Bale, C.S.E., Ingham, T., Bloss, W.J., Heard, D.E., 2007. Detection of iodine monoxide radicals in the marine boundary layer using laser induced fluorescence spectroscopy. Journal of Atmospheric Chemistry 58, 19-39.

Williams, J., Gros, V., Atlas, E., Maciejczyk, K., Batsaikhan, A., Scholer, H.F., Forster, C., Quack, B., Yassaa, N., Sander, R., Van Dingenen, R., 2007. Possible evidence for a connection between methyl iodide emissions and Saharan dust. Journal of Geophysical Research-Atmospheres 112.

Wimschneider, A., Heumann, K.G., 1995. Iodine speciation in size fractionated atmospheric particles by isotope dilution mass spectrometry. Fresenius J. Anal. Chem. 353, 191-196.

Winchest, J.W., Duce, R.A., 1967. Global Distribution of Iodine Bromine and Chlorine in Marine Aerosols. Naturwissenschaften 54, 110-&.

Wong, G.T.F., 1991. The Marine Geochemistry of Iodine. Reviews in Aquatic Sciences 4, 45-73.

Wong, G.T.F., Cheng, X.H., 1998. Dissolved organic iodine in marine waters: Determination, occurrence and analytical implications. Marine Chemistry 59, 271-281.

Wong, G.T.F., Cheng, X.H., 2001. The formation of iodide in inshore waters from the photochemical decomposition of dissolved organic iodine. Marine Chemistry 74, 53-64.

Wuilloud, R.G., Altamirano, J.C., 2005. Speciation of Halogen Compounds. In: Cornelis, R. (Ed.). Handbook of Elemental Speciation. John Wiley & Sons, Chichester, England, pp. 564-597.

Yang, H.X., Liu, W., Li, B., Zhang, H.J., Liu, X.D., Chen, D.Y., 2007. Speciation analysis for iodine in groundwater using high performance liquid chromatography-inductively coupled plasma-mass spectrometry (HPLC-ICP-MS). Geostandards and Geoanalytical Research 31, 345-351.

Yokouchi, Y., Mukai, H., Yamamoto, H., Otsuki, A., Saitoh, C., Nojiri, Y., 1997. Distribution of methyl iodide, bromoform and dibromomethane over the ocean (east and southeast Asian Seas and the western Pacific). J. Geophys. Res. 102, 8805-8809.

Zorn, S.R., Drewnick, F., Schott, M., Hoffmann, T., Borrmann, S., 2008. Characterization of the South Atlantic marine boundary layer aerosol using an Aerodyne Aerosol Mass Spectrometer. Atmos. Chem. Phys. Discuss. 8, 4831-4876.

Appendix

Chlorophyll Data (from Modis website, modis.gsfc.nasa.gov/)

November 2005

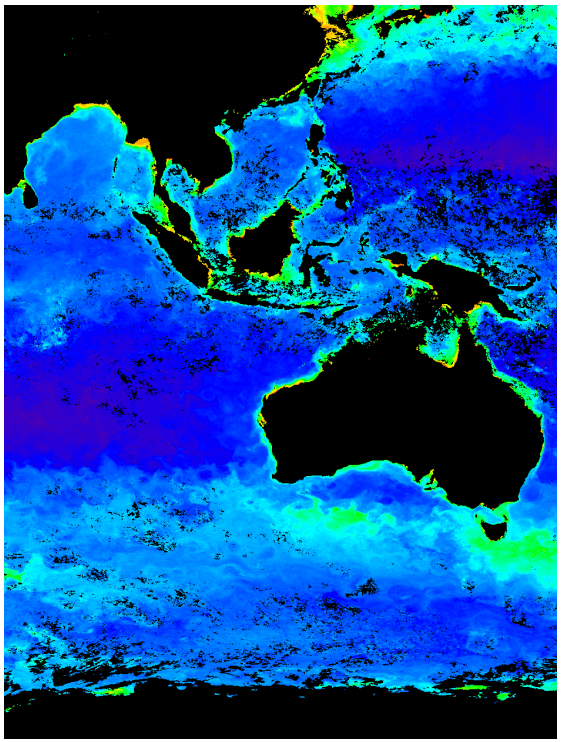

December 2005

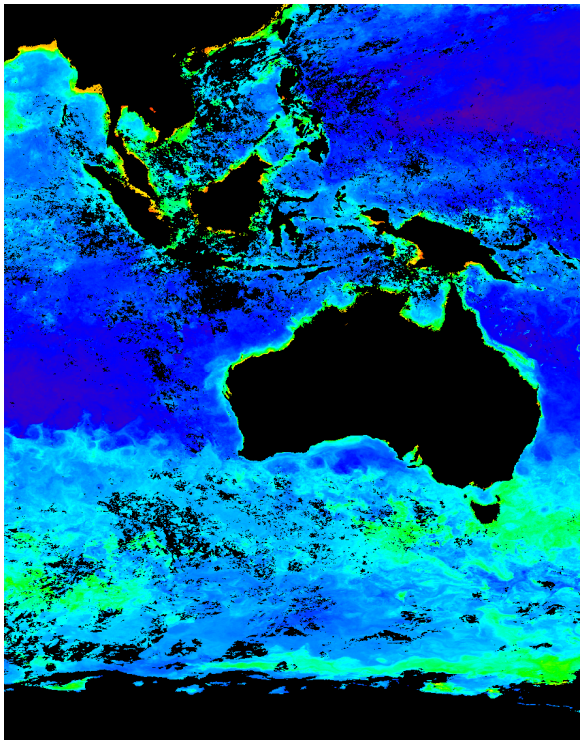

January 2006

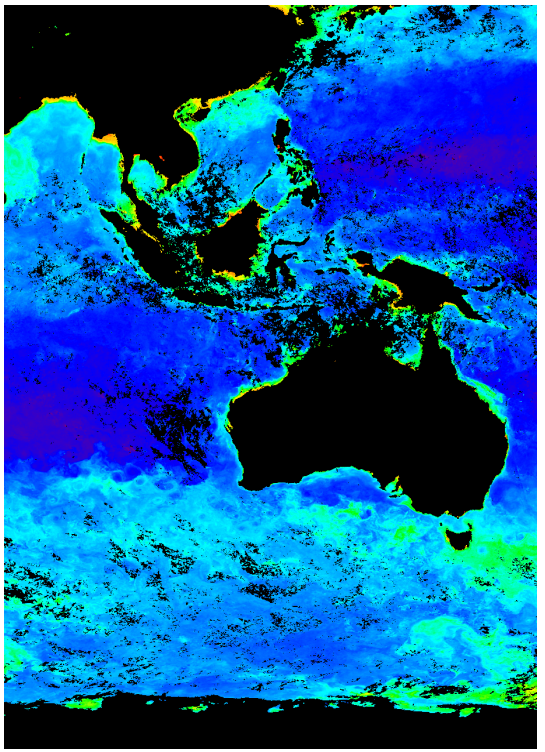

Chlorophyll Data (from Modis website, modis.gsfc.nasa.gov/)

February 2006

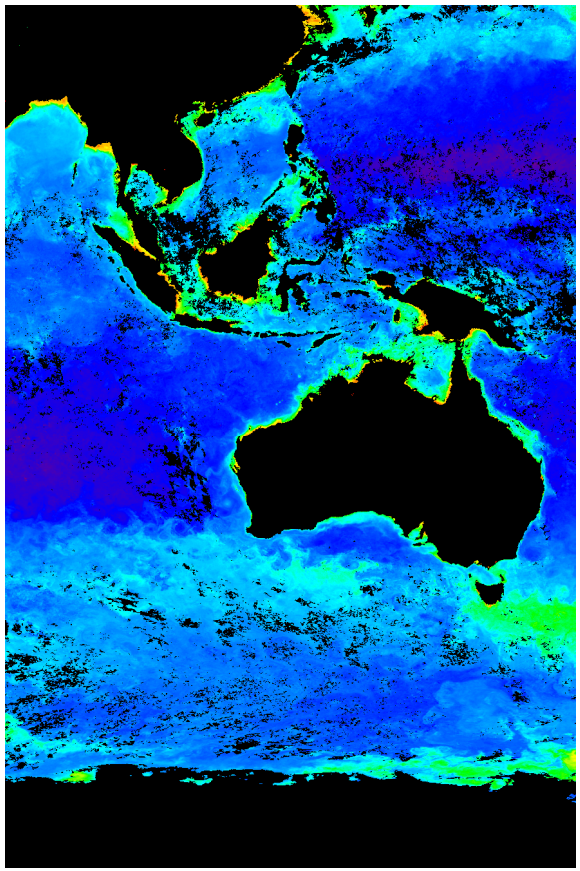

March 2006

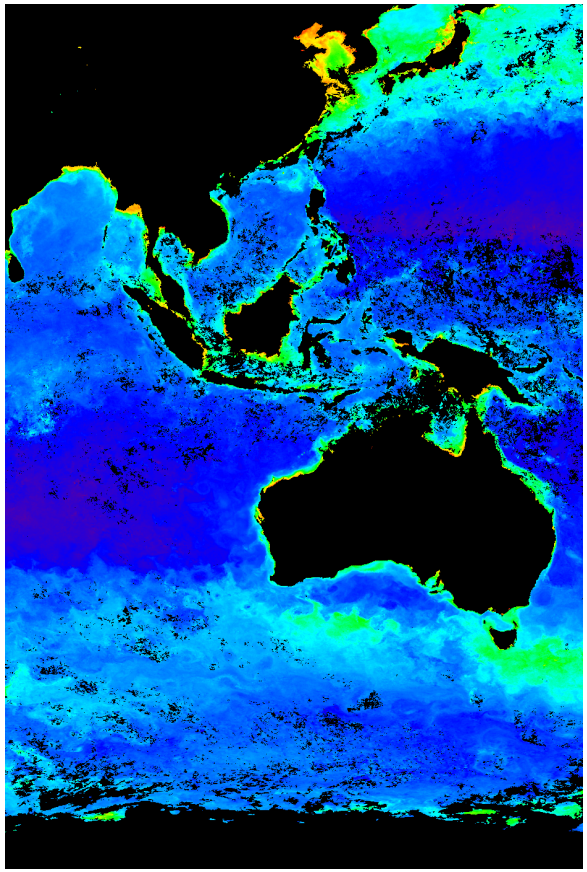

Chlorophyll Data (from Modis website, modis.gsfc.nasa.gov/)

June 2006

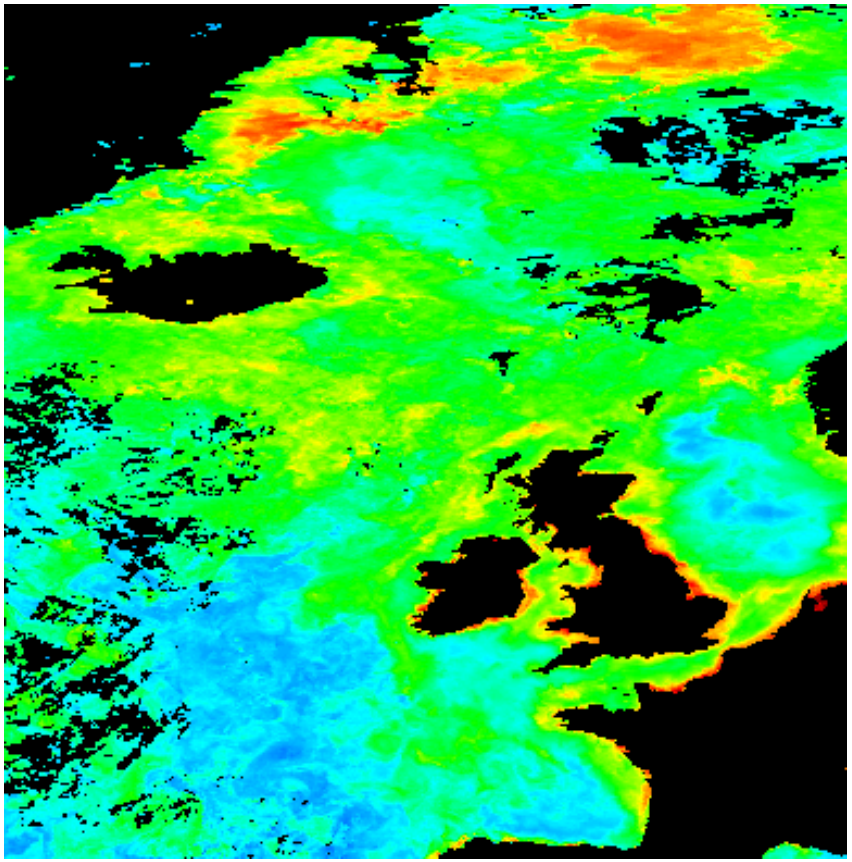

July 2006

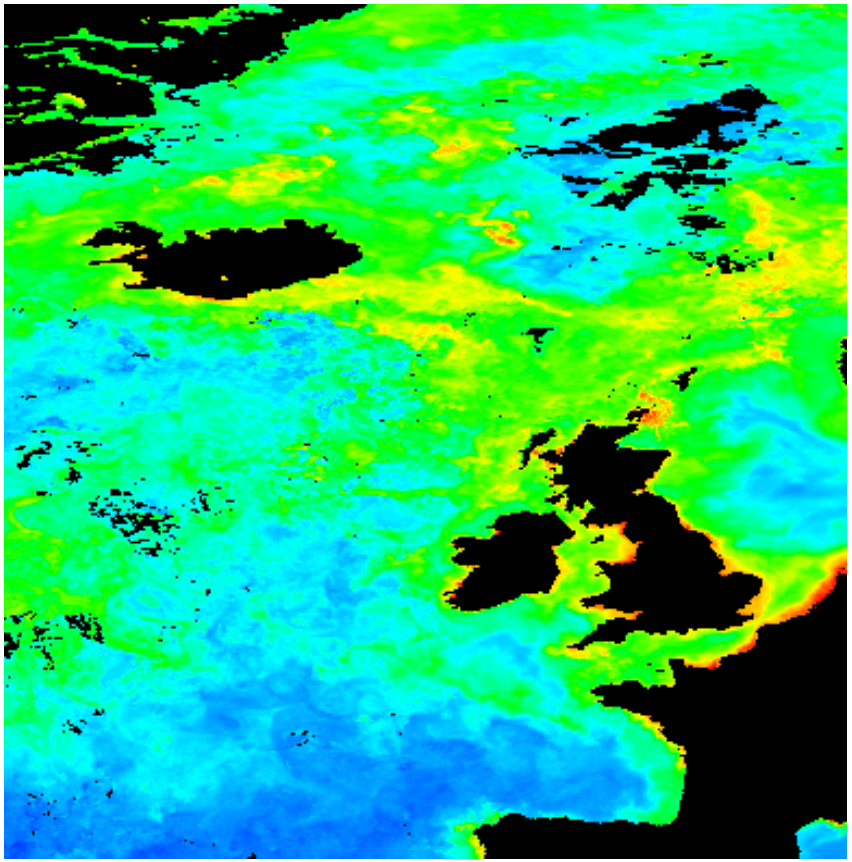

Chlorophyll Data (from the fluorometer on the Celtic Explorer)

CEC Leg 1

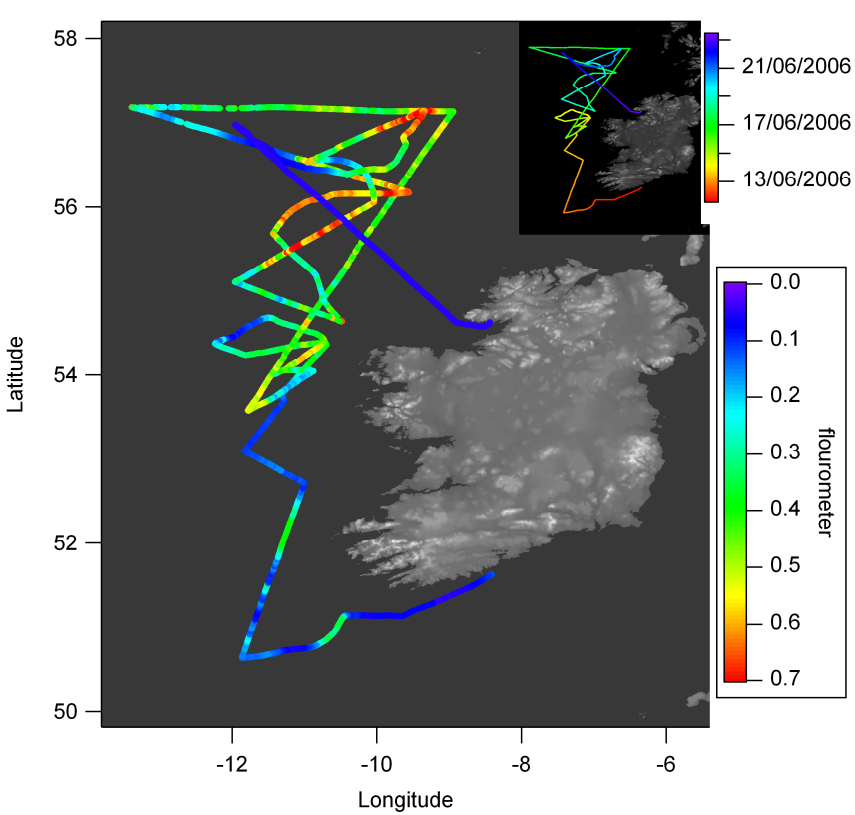

CEC Leg 2

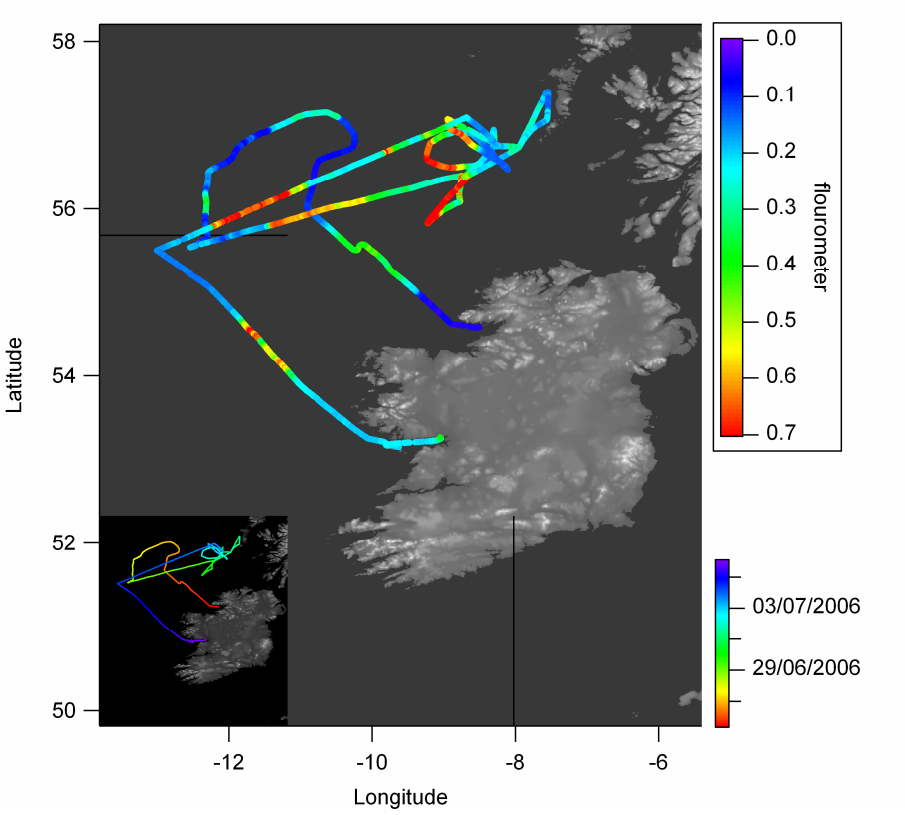

Abbreviation Index

AMS	Aerosol Mass Spectrometry
BBCRDS	Broadband Cavity Ring-Down Spectroscopy
CE	Capillary Electrophoresis
CEC	Celtic Explorer ship Campaign
CPC	Condensation Particle Counter
DOAS	Differential Optical Absorption Spectroscopy
DOM	Dissolved Organic Matter
ESI-ITMS	Electrospray Ionization Ion Trap Mass Spectrometry
FRM	Federal Reference Method
GC	Gas Chromatography
GE	Gel Electrophoresis
HPLC	High Performance Liquid Chromatography
IC	Ion Chromatography
ICP-MS	Inductively Coupled Plasma – Mass Spectrometry
IDA	Isotope Dilution Analysis
IDMA	Isotope Dilution Mass Spectrometry
LA	Laser Ablation
LOD	Limit of Detection
MAP	Marine Aerosol Production from natural sources
MBL	Marine Boundary Layer
MHARS	Mace Head Atmospheric Research Station
MHC	Mace Head Campaign
MS	Mass Spectrometry
NAA	Neutron Activation Analysis
N.D.	not detectable
ODEs	Ozone Depletion Events
OOMPH	Organics over the Ocean Modifying Particles in both Hemispheres

PEEK	Polyetheretherketone
PM_{10}	Particulate Matter with aerodynamic diameter smaller than 10 µm
$PM_{2.5}$	Particulate Matter with aerodynamic diameter smaller than 2.5 µm
RF	Radiofrequency
RPLC	Reversed Phase Liquid Chromatography
SOI	Soluble Organic Iodine
SSM	Sea Surface Microlayer
TII	Total Insoluble Iodine
TMAH	Tetra-Methyl-Ammonium-Hydroxide
TSI	Total Soluble Iodine
TSP	Total Suspended Particle
UOI	Unidentified Organic Iodine
VFC	Volumetric Flow Controller
VOI	Volatile Organic Iodine